J. Fluid Mech. (2025), *vol.* 1024, A41, doi:10.1017/jfm.2025.10821

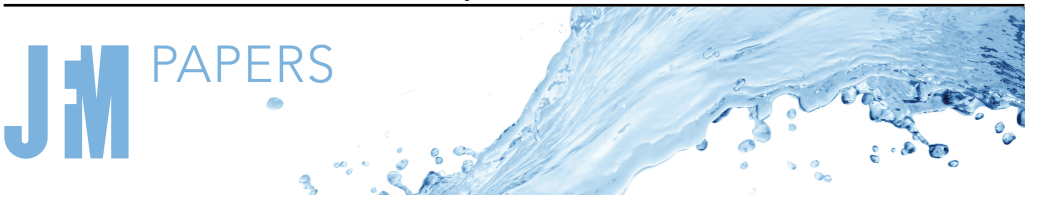

Far field asymptotics of nematic flows around a small spherical particle

Dmitry Golovaty[1] **and Nung Kwan Yip**[2]

[1]Department of Mathematics, The University of Akron, Akron, OH 44325, USA

[2]Department of Mathematics, Purdue University, West Lafayette, IN 47907, USA

Corresponding author: Nung Kwan Yip, yipn@purdue.edu

(Received 21 October 2024; revised 30 April 2025; accepted 28 September 2025)

In this paper, we consider the flow of a nematic liquid crystal in the domain exterior to a small spherical particle. We work within the framework of the $\boldsymbol{Q}$-tensor model, taking into account the orientational elasticity of the medium. Under a suitable regime of physical parameters, the governing equations can be reduced to a system of linear partial differential equations. Our focus is on precise far-field asymptotics of the flow velocity with an emphasis on its anisotropic behaviour. We are able to analytically characterize the flow pattern and compare it with that of the classical isotropic Stokes flow. The expression for velocity away from the particle can be computed numerically or symbolically.

Key words: liquid crystals, variational methods, general fluid mechanics

1. Introduction

This paper analyses the flow pattern around a small spherical particle immersed in a nematic liquid crystalline environment. Although a similar phenomenon in a classical isotropic fluid has been well-studied (Acheson 1990, Chapter 7), the understanding in the case of this complex fluid is far from complete, despite the fact that it is of utmost importance in many physical and biological systems (Stark 2001; Spagnolie 2015).

A typical nematic liquid crystal consists of molecules that possess a degree of orientational order but no positional order, so that this medium can be thought of as an anisotropic Newtonian fluid with additional elastic properties. Hence, in order to understand the flow field around a particle, one needs to analyse the behaviour of solutions to a coupled system of partial differential equations that describes both flow and orientational elasticity.

© The Author(s), 2025. Published by Cambridge University Press. This is an Open Access article, distributed under the terms of the Creative Commons Attribution licence (https://creativecommons.org/licenses/by/4.0/), which permits unrestricted re-use, distribution and reproduction, provided the original article is properly cited.

https://doi.org/10.1017/jfm.2025.10821 Published online by Cambridge University Press

In a broader context, we are interested in multiparticle systems such as colloidal suspensions of both passive and active particles in complex media (Muševič 2017; Smalyukh 2018). The overall behaviour of these systems certainly depends on the particle–fluid and particle–particle interactions. As a typical initial step, one would consider a dilute system in which particles are distributed away from each other in an attempt to understand far-field interactions between these particles. We refer to Batchelor & Green (1972), Guazzelli & Morris (2012) and Russel, Saville & Schowalter (1992) for extending approaches for modelling flows around a single particle to flows in a multiparticle system.

As a starting point, one needs to investigate the case of a single particle in a host medium and determine the far-field asymptotics of the corresponding flow patterns. Here, these asymptotics should also include the far-field orientational information about the liquid crystal. In our work, we concentrate on the parameter regime in which we are able to obtain explicit asymptotics, in the same spirit as those known for the classical Stokes flow. Our work seems to be the first to give a precise characterization of the flow around a particle immersed in a nematic liquid crystal.

First, we briefly discuss prior work on liquid crystalline flows, both with and without particles. The theory of nematic flows has proceeded along two somewhat different, but related directions that rely on distinct continuum descriptions of the nematics. The first and most widely used approach, due to Ericksen (1961, 1987) and Leslie (1979, 1992), is based on the $\mathbb{S}^2$-valued nematic director n. The director is used to represent the local orientation of the nematic molecules and, along with the velocity $\boldsymbol{v}$ of the flow, it describes the local state of the nematic. The corresponding system of equations is derived by (*a*) assuming local balances of mass as well as linear and angular momenta and (*b*) specifying the energy dissipation density in the form that conforms with the second law of thermodynamics. As a result, the system of governing equations consists of a Navier–Stokes equation coupled with an equation for harmonic maps. The Ericksen–Leslie model has been a subject of numerous studies (Lin & Liu 1995, 2000; Liu & Walkington 2000; Du, Guo & Shen 2001; Walkington 2011).

Another approach relies on the Landau–de Gennes description of orientational elasticity which is designed to take into account certain symmetry properties of the orientational distribution of nematic molecules. The Landau–de Gennes variational theory replaces the nematic director n by a so-called $\boldsymbol{Q}$-tensor – a symmetric traceless 3×3 matrix – the eigenvectors of which encode orientational properties of the medium (De Gennes & Prost 1993). We refer to Sonnet & Virga (2012, Chapter 1) for the derivation of the $\boldsymbol{Q}$-tensor model from a molecular perspective.

An alternative to the $\boldsymbol{Q}$-tensor model – that can also be thought of as an extension of the Ericksen–Leslie model – was proposed by Ericksen in Ericksen (1991). This model is known as Ericksen's model for nematics with variable degree of orientation and it is based on the state variables (s, n), where n is the director and s is a scalar measuring the degree of local orientational order. We refer to Ball (2017*a*,*b*), Wang, Zhang & Zhang (2021) and Borthagaray & Walker (2021) for the overview of the mathematical theory of liquid crystals and simulation methods.

Regardless of the choice of state variables, the behaviour of a nematic in the absence of flow is captured by minimizing an underlying energy functional. This is given by the following:

$$\mathcal{F}_{OF}(n) = \int W(n, \nabla n)\, \mathrm{d}x, \quad \text{or} \quad \mathcal{F}_{LdG}(\boldsymbol{Q}) = \int \mathcal{E}_{LdG}(\boldsymbol{Q}, \nabla \boldsymbol{Q}), \tag{1.1}$$

within the Oseen–Frank director-based and the Landau–de Gennes $\boldsymbol{Q}$-tensor-based theories, respectively. In the most general setting, W takes the following form:

https://doi.org/10.1017/jfm.2025.10821 Published online by Cambridge University Press

$$W(n, \nabla n) = \frac{K_1}{2}(\nabla \cdot n)^2 + \frac{K_2}{2}\big(n \cdot (\nabla \times n)\big)^2 + \frac{K_3}{2}\big|n \wedge (\nabla \times n)\big|^2 + \frac{(K_2 + K_4)}{2}\big(\mathrm{tr}(\nabla n)^2 - (\nabla \cdot n)^2\big). \tag{1.2}$$

The analogous component in $\mathcal{E}_{LdG}(\boldsymbol{Q}, \nabla \boldsymbol{Q})$ is given by

$$\frac{L_1}{2}\partial_{x_k}\boldsymbol{Q}_{ij}\partial_{x_k}\boldsymbol{Q}_{ij} + \frac{L_2}{2}\partial_{x_j}\boldsymbol{Q}_{ij}\partial_{x_k}\boldsymbol{Q}_{ik} + \frac{L_3}{2}\partial_{x_k}\boldsymbol{Q}_{ij}\partial_{x_j}\boldsymbol{Q}_{ik} + \frac{L_4}{2}\boldsymbol{Q}_{mn}\partial_{x_m}\boldsymbol{Q}_{ij}\partial_{x_n}\boldsymbol{Q}_{ij}. \tag{1.3}$$

We refer to Ball (2017*b*) and Selinger (2018) for a general discussion on the elastic constants K_i and L_i and the relationship between the constants that appear in different models. Within the so called one-constant approximation, the elastic constants are chosen in such a way that (1.2) and (1.3) take the form $(K/2)\|\nabla n\|^2$ and $(L/2)\|\nabla \boldsymbol{Q}\|^2$. We will make this as a standing assumption in this paper. The full expression of $\mathcal{E}_{LdG}(\boldsymbol{Q}, \nabla \boldsymbol{Q})$ in this case is given by (2.2)–(2.3) in § 2.

When extended to describe nematic flow, the evolution of $\boldsymbol{Q}$ and the velocity $\boldsymbol{v}$ of the nematic is given by a coupled system of the Landau–de Gennes and Navier–Stokes equations and can be derived following the procedure outlined by Sonnet and Virga on the basis of the principle of minimum constrained dissipation (Sonnet & Virga 2001; Sonnet, Maffettone & Virga 2004; Sonnet & Virga 2012). This is captured by a dissipation functional $R(\boldsymbol{Q}; \boldsymbol{A}, \boldsymbol{Q})$ where $\boldsymbol{A}$ is the symmetric part of $\nabla \boldsymbol{v}$ and $\boldsymbol{Q}$ is an invariant version of $\partial_t \boldsymbol{Q}$ (see (2.10)–(2.12)). Another related but more popular model, due to Beris and Edwards (Beris & Edwards 1994), was obtained by making use of the concept of a Poisson bracket with dissipation. (In a later work, we will in fact show that the Beris–Edwards model is a specific example of the Sonnet–Virga formulation.) The Beris–Edwards model has been studied extensively in recent years, see for example, Abels, Dolzmann & Liu (2016), Wu, Xu & Zarnescu (2019) and Du, Hu & Wang (2020), just to name a few.

Particulate flows in a classical fluid is another widely studied subject, see Galdi (2002, 2011) for overview of relevant literature and mathematical theory. Motion of particles in a complex fluid, and in particular in a nematic host, has also attracted attention of many investigators, especially with the expanding interest in motion of immersed active particles (Lavrentovich 1998; Peng *et al.* 2016; Zhou *et al.* 2014, 2017). The experimental and modelling work in this field has so far outpaced the analysis effort (Ruhwandl & Terentjev 1996; Stark 2001; Stark & Ventzki 2001). The goal of the present paper is to make inroads into a rigorous understanding of a nematic flow around a single particle within the framework of a $\boldsymbol{Q}$-tensor-based model. We believe this choice is most appropriate for studying nematic flows (cf. Ravnik & Žumer 2009).

The details of the model are given in § 2. Here we highlight some key physically justifiable assumptions that we make in order to obtain precise asymptotics of the flow pattern. These assumptions allow us to reduce the overall dynamics to a linear system of partial differential equations describing an anisotropic Stokes flow with elastic contribution. We emphasize that the distinction with the standard isotropic Stokes flow is not only due to orientability of the medium (described by $\boldsymbol{Q}$) that makes the flow anisotropic, but also because the flow is coupled to the elastic properties of the medium (described by $\nabla \boldsymbol{Q}$).

Our principal assumptions are as follows. We set both Ericksen (Er) and Reynolds (Re) numbers to be small. This means that the dynamics is dominated by the elastic effects of the nematics and the flow is highly dissipative in the sense that inertial effects are negligible. As the result, our model becomes a partially decoupled system (2.32) in which $\boldsymbol{Q}$ satisfies an equation that does not involve $\boldsymbol{v}$. The solution of this equation can then be

https://doi.org/10.1017/jfm.2025.10821 Published online by Cambridge University Press

treated as a prescribed function which enters into an inhomogeneous linear Stokes-like equation describing the evolution of $\boldsymbol{v}$.

To obtain an explicit solution for $\boldsymbol{Q}$, we further take advantage of the small particle limit considered in Alama, Bronsard & Lamy (2016) which appears to be the first work to rigorously analyse the solution for $\boldsymbol{Q}$ in the exterior of a particle. In this regime, $\boldsymbol{Q}$ solves a Laplace equation. By imposing a weak homeotropic boundary condition of 'hedgehog type' on the surface of the particle, an exact analytical solution for $\boldsymbol{Q}$ can be produced. We refer to § 2.3 and § 2.4 for more a detailed description of the assumptions used in this paper.

With the above, our first key observation is that the equation for the velocity field $\boldsymbol{v}$ takes the following form (see (4.18)):

$$-\big(\Delta \boldsymbol{v} + \operatorname{div}\big[\mathcal{B}_\gamma[\nabla \boldsymbol{v}] + \mathcal{A}_\gamma(x) + \mathcal{C}_\gamma(x)\big]\big) + \nabla p = \mathcal{D}_\gamma(x), \tag{1.4}$$

where $\mathcal{A}_\gamma, \mathcal{B}_\gamma, \mathcal{C}_\gamma$ and $\mathcal{D}_\gamma$ are the extra contributions coming from the $\boldsymbol{Q}$-tensor field. Using the above equation, our main result is the precise characterization of the far-field asymptotics for $\boldsymbol{v}$ by computing its deviation from the classical Stokes flow $\boldsymbol{v}_0$ (see (5.28)),

$$\boldsymbol{v} \sim \boldsymbol{v}_0 + \overline{\varphi}_\gamma. \tag{1.5}$$

We are able to obtain an analytical expression for $\overline{\varphi}_\gamma$. This is stated in (5.30),

$$\overline{\varphi}_\gamma(x) = \mathcal{I}_\gamma(x) + \boldsymbol{E}(x)\mathcal{J}_\gamma + O\left(\frac{1}{|x|^2}\right), \tag{1.6}$$

where $\mathcal{I}_\gamma$ and $\mathcal{J}_\gamma$ are some explicit bulk and boundary integrals (5.31) and (5.32), and $\boldsymbol{E}$ is the Green's function (3.9) for the classical Stokes system. All the relevant quantities of $\overline{\varphi}_\gamma$ can be computed symbolically or numerically. In particular, we have that $\boldsymbol{v}$ retains the $(1/r)$-far field decay property as the classical Stokes flow.

Here we mention some earlier works in the problem of nematic flows around a particle. In Diogo (1983), flows of a nematic fluid are considered when $Er = \infty$ so that the nematic is essentially an isotropic fluid. Analysis is performed in Kneppe, Schneider & Schwesinger (1991), Heuer, Kneppe & Schneider (1992), Gómez-González & del Álamo (2013) and Kos & Ravnik (2018), but they consider the director n-model, where the director is taken to be uniform in space. Numerical simulations for the director model for similar parameter regimes (low Ericksen and Reynolds numbers) as in our work are discussed in Ruhwandl & Terentjev (1996) and Stark & Ventzki (2001). Simulations were also performed for intermediate parameter regimes in Fukuda *et al.* (2004). Our present work seems to be the first to incorporate a genuine $\boldsymbol{Q}$-tensor field which is an exact minimizer of the Landau–de Gennes energy with suitable boundary condition. Its effect on the far-field behaviour of the velocity field $\boldsymbol{v}$ has not been rigorously analysed prior to this work.

As a follow-up to this work, it would be interesting to consider a system of multiple particles in a nematic environment. Note that the interaction between particles in this case is mediated via the elastic forces in the nematic medium. These interactions have been considered from a purely energetic perspective analogous to electrostatic potential (see for example Kishita *et al.* (2010, 2011) and Izaki & Kimura (2013)). Complex variables techniques have been used in two-dimensions to compute the nematic fields between particles (Chandler & Spagnolie 2023, 2024*a*). There has also been a recent effort to understand defect structures around a particle (for example, Saturn ring or dipole

https://doi.org/10.1017/jfm.2025.10821 Published online by Cambridge University Press

configurations) in relation to the anchoring conditions on the surface and also external magnetic fields (Stark 1999; Alouges, Chambolle & Stantejsky 2021). See also Chandler & Spagnolie (2024*b*) for an overview from an energetic perspective in both the director and $\boldsymbol{Q}$-tensor models for bodies immersed in a nematic environment. However, these works consider static configurations only, with no associated flow present. We believe that our current contribution can provide information about the effects of the fluid flow away from a single particle. Our approach can then be generalized to understand the flow behaviour in systems of many particles immersed in a nematic medium.

The outline of this paper is as follows. In § 2, we provide a detailed description of our model and the relevant parameter regimes. In § 3, we recall the explicit solutions for a $\boldsymbol{Q}$-tensor and the classical Stokes flow in the exterior of a small particle that we use in subsequent sections. In § 4, we analyse the structure of our anisotropic Stokes system. Then, in § 5, we investigate the precise far-field asymptotic behaviour of the velocity flow, in particular its deviation from the isotropic Stokes flow. Finally, in § 6, we present numerical results. Given the generality of the model considered in this work, the analysis relies on some tedious but routine computations that we summarize in the Appendices A and B. In Appendix C, we provide validation of our numerical procedure by carrying it out for a Stokes flow in a bounded annular domain. The mathematical proof of the existence of the velocity field $\boldsymbol{v}$ is given in the Supplementary materials is available at https://doi.org/10.1017/jfm.2025.10821.

We conclude this section with the list of notations and conventions that will be used throughout the paper. We remind the reader that we work with the fields defined in $\mathbb{R}^3$.

(*a*) Given a vector $u = (u_1, u_2, u_3) \in \mathbb{R}^3$, we define $\widehat{u} := u/|u| = (u_1/|u|, u_2/|u|, u_3/|u|)$ to be the unit vector in the same direction as u (we will simplify the notation by dropping the hat, whenever there is no ambiguity).
Euclidean inner product between two vectors $u, v \in \mathbb{R}^3$ will be denoted by $u \cdot v$ and the symbols e_1, e_2 and e_3 will be used to represent the coordinate vectors in $\mathbb{R}^3$.

(*b*) A symbol such as $x = (x_1, x_2, x_3)^T$ will denote either a generic point or a dummy integration variable in $\mathbb{R}^3$. For convenience, we will also use

$$r := |x| = \sqrt{x_1^2 + x_2^2 + x_3^2}, \tag{1.7}$$

to denote the magnitude of x.

(*c*) The (three-dimensional (3-D)) volume integration element will be denoted by

$$\mathrm{d}x = \mathrm{d}x_1 \mathrm{d}x_2 \mathrm{d}x_3. \tag{1.8}$$

The (two-dimensional (2-D)) area integration element will be denoted by

$$\mathrm{d}\sigma_x, \quad \text{or simply} \quad \mathrm{d}\sigma \quad \text{(if the variable is clear from context)}. \tag{1.9}$$

The unit outward normal to the domain Ω occupied by the liquid crystal will be given by ν.

(*d*) For any pair of 3×3 matrices $\boldsymbol{B}, \boldsymbol{C} \in M^{3\times 3}$, their dot product will be defined via $\boldsymbol{B} \cdot \boldsymbol{C} = \mathrm{tr}\,(\boldsymbol{C}^T \boldsymbol{B})$ so that $|\boldsymbol{B}|^2 = \boldsymbol{B} \cdot \boldsymbol{B}$.

(*e*) The Einstein convention for repeated indices will be used whenever possible.

(*f*) For any matrix (or a second-order tensor) field $\boldsymbol{T} = (\boldsymbol{T}_{ij})_{1\le i,j\le 3}$, the symbol $\boldsymbol{T}_i$ will denote its ith row. The divergence div $\boldsymbol{T}$ is to be taken rowwise, i.e. $(\mathrm{div}\,\boldsymbol{T})_i := \mathrm{div}\,\boldsymbol{T}_i = \partial_{x_j} \boldsymbol{T}_{ij}$ for all i.

(*g*) Sometimes we find it advantageous to use the symbol $\langle \text{matrix}, \text{vector} \rangle$ and $\langle \text{vector}, \text{vector} \rangle$ to denote the matrix–vector multiplication and the dot product, respectively.

https://doi.org/10.1017/jfm.2025.10821 Published online by Cambridge University Press

The symbol ' :' will be used to denote a generic tensor contraction. It will be explicitly defined whenever necessary.

(*h*) The symbol $O(A)$ will refer to a quantity of order A in the sense that $|O(A)| \leq CA$ for some (positive) constant C. The notation $o(A)$ represents a quantity that is asymptotically small compared with A in the sense that $\lim(|o(A)|/A) = 0$ where the limit will be clear from the context. The expression $A \lesssim B$ means that $A \leq CB$ for a generic positive constant C that might change from one line to another.

2. Problem formulation

2.1. *A model for the dynamics of nematic liquid crystals*

Suppose that a nematic liquid crystal occupies a region Ω in $\mathbb{R}^3$ and let the $\boldsymbol{Q}$-tensor and the velocity field $\boldsymbol{v}$,

$$\boldsymbol{Q}: \Omega \to \mathcal{M} := \left\{\boldsymbol{Q} \in M^{3\times 3}(\mathbb{R}) : \boldsymbol{Q}^T = \boldsymbol{Q},\ \operatorname{tr}\boldsymbol{Q} = 0\right\}, \quad \boldsymbol{v}: \Omega \to \mathbb{R}^3, \tag{2.1}$$

describe the local state of the nematic. We introduce the Landau–de Gennes energy density and the corresponding energy functional as

$$\mathcal{E}_{LdG}(\nabla \boldsymbol{Q}, \boldsymbol{Q}) = \frac{L}{2}|\nabla \boldsymbol{Q}|^2 + f(\boldsymbol{Q}), \quad \mathcal{F}_{LdG}(\boldsymbol{Q}) = \int \mathcal{E}_{LdG}(\nabla \boldsymbol{Q}, \boldsymbol{Q})\, \mathrm{d}x. \tag{2.2}$$

The parameter L is the elastic constant of the liquid crystal. Note that as mentioned in the Introduction, this form of $\mathcal{E}_{LdG}(\nabla \boldsymbol{Q}, \boldsymbol{Q})$ makes use of the one-constant approximation of (1.3).

The nonlinear Landau–de Gennes potential f is given by

$$f(\boldsymbol{Q}) = -\frac{A}{2}\operatorname{tr}\boldsymbol{Q}^2 + \frac{B}{3}\operatorname{tr}\boldsymbol{Q}^3 + \frac{C}{4}\left(\operatorname{tr}\boldsymbol{Q}^2\right)^2, \tag{2.3}$$

with $A, C > 0$. The minimum of f over $\mathcal{M}$ is attained at the nematic states given by

$$s_*\left(n_* \otimes n_* - \frac{1}{3}\boldsymbol{I}\right), \quad \text{where } n_* \in \mathbb{S}^2 \text{ and } s_* = \begin{cases} -\dfrac{B + \sqrt{B^2 + 24AC}}{4C} & \text{for } B > 0, \\ \dfrac{-B + \sqrt{B^2 + 24AC}}{4C} & \text{for } B < 0. \end{cases} \tag{2.4}$$

Let

$$\boldsymbol{Q} = \dot{\boldsymbol{Q}} + \boldsymbol{Q}\boldsymbol{W} - \boldsymbol{W}\boldsymbol{Q}, \quad \boldsymbol{A} = \frac{1}{2}\left(\nabla \boldsymbol{v} + \nabla \boldsymbol{v}^T\right), \quad \boldsymbol{W} = \frac{1}{2}\left(\nabla \boldsymbol{v} - \nabla \boldsymbol{v}^T\right), \tag{2.5}$$

where $\dot{\boldsymbol{Q}}$ denotes the convective derivative

$$\dot{\boldsymbol{Q}} = \partial_t \boldsymbol{Q} + \boldsymbol{v} \cdot \nabla \boldsymbol{Q}. \tag{2.6}$$

The quantity $\boldsymbol{Q}$ is used instead of $\dot{\boldsymbol{Q}}$ because it is frame indifferent (Sonnet & Virga 2012, § 2.1.3, (2.87), § 4.1.3). Expressions such as $\boldsymbol{Q}\boldsymbol{W}$ and so forth refer to matrix multiplications. The 3×3-matrices $\boldsymbol{A}$ and $\boldsymbol{W}$ are, respectively, symmetric and skew-symmetric. From the form of $\boldsymbol{Q}$, we infer that it is also a symmetric, traceless matrix.

We consider the incompressible flow of the nematic in Ω described by the following system of equations:

https://doi.org/10.1017/jfm.2025.10821 Published online by Cambridge University Press

$$\begin{cases} \dfrac{\partial \mathcal{E}_{LdG}}{\partial \boldsymbol{Q}} - \operatorname{div}\left[\dfrac{\partial \mathcal{E}_{LdG}}{\partial \nabla \boldsymbol{Q}}\right] - \Lambda \boldsymbol{I} + \zeta_1 \boldsymbol{Q} + \zeta_2 \boldsymbol{A} + \frac{\zeta_3}{2}(\boldsymbol{A}\boldsymbol{Q} + \boldsymbol{Q}\boldsymbol{A}) + \zeta_9 (\boldsymbol{A} \cdot \boldsymbol{Q})\boldsymbol{Q} = 0, \\ \rho\, \dot{\boldsymbol{v}} + \operatorname{div}\left[p\boldsymbol{I} - \boldsymbol{T}^v_{SV} - \boldsymbol{T}^{el}\right] = 0, \\ \operatorname{div} \boldsymbol{v} = 0, \end{cases} \tag{2.7}$$

where

$$\frac{\partial \mathcal{E}_{LdG}}{\partial \boldsymbol{Q}} = -A\boldsymbol{Q} + B\left(\boldsymbol{Q}^2 - \frac{1}{3}|\boldsymbol{Q}|^2 \boldsymbol{I}\right) + C|\boldsymbol{Q}|^2 \boldsymbol{Q}, \tag{2.8}$$

$$\operatorname{div}\left[\frac{\partial \mathcal{E}_{LdG}}{\partial \nabla \boldsymbol{Q}}\right] = L \triangle \boldsymbol{Q}. \tag{2.9}$$

The parameter ρ denotes the density of the nematic and ζ_1 through ζ_{11} are the viscosity coefficients of the nematic with ζ_8 being the isotropic viscosity. The pressure p and the function Λ are the Lagrange multipliers corresponding, respectively, to the incompressibility and tracelessness constraints for $\boldsymbol{v}$ and $\boldsymbol{Q}$. (Note that there is no need for an explicit Lagrange multiplier for the symmetry condition $\boldsymbol{Q}^T = \boldsymbol{Q}$ as the individual terms in (2.7) that involve the velocity field are already symmetric.) The viscous and elastic stress tensors are

$$\begin{aligned} \boldsymbol{T}^v_{SV} = {} & \zeta_1(\boldsymbol{Q}\boldsymbol{Q} - \boldsymbol{Q}\boldsymbol{Q}) + \zeta_2\big(\boldsymbol{Q} + \boldsymbol{Q}\boldsymbol{A} - \boldsymbol{A}\boldsymbol{Q}\big) + \frac{\zeta_3}{2}\big(\boldsymbol{Q}\boldsymbol{Q} + \boldsymbol{Q}\boldsymbol{Q} + \boldsymbol{Q}^2\boldsymbol{A} - \boldsymbol{A}\boldsymbol{Q}^2\big) \\ & + \zeta_4(\boldsymbol{Q}\boldsymbol{A} + \boldsymbol{A}\boldsymbol{Q}) + \zeta_5\big(\boldsymbol{Q}^2\boldsymbol{A} + \boldsymbol{A}\boldsymbol{Q}^2\big) + \zeta_6(\boldsymbol{A} \cdot \boldsymbol{Q})\boldsymbol{Q} + \zeta_7|\boldsymbol{Q}|^2\boldsymbol{A} + \zeta_8\boldsymbol{A} \\ & + \zeta_9(\boldsymbol{Q} \cdot \boldsymbol{Q})\boldsymbol{Q} + \zeta_{10}\big((\boldsymbol{Q}^2 \cdot \boldsymbol{A})\boldsymbol{Q} + (\boldsymbol{Q} \cdot \boldsymbol{A})\boldsymbol{Q}^2\big) + \zeta_{11}|\boldsymbol{Q}|^2(\boldsymbol{A} \cdot \boldsymbol{Q})\boldsymbol{Q} \end{aligned} \tag{2.10}$$

and

$$\begin{aligned} \boldsymbol{T}^{el} &= -\frac{\partial \mathcal{E}_{LdG}}{\partial\big(\partial_j \boldsymbol{Q}_{mn}\big)}\big(\partial_i \boldsymbol{Q}_{mn}\big)\mathbf{e}_i \otimes \mathbf{e}_j = -L(\partial_j \boldsymbol{Q}_{mn})(\partial_i \boldsymbol{Q}_{mn})\mathbf{e}_i \otimes \mathbf{e}_j \\ &= -L\big(\partial_i \boldsymbol{Q} \cdot \partial_j \boldsymbol{Q}\big)\mathbf{e}_i \otimes \mathbf{e}_j \\ &=: -L\big(\nabla \boldsymbol{Q} \odot \nabla \boldsymbol{Q}\big), \end{aligned} \tag{2.11}$$

respectively, so that componentwise, we have $(\nabla \boldsymbol{Q} \odot \nabla \boldsymbol{Q})_{ij} = \partial_i \boldsymbol{Q} \cdot \partial_j \boldsymbol{Q}$.

The model (2.7) is established in Sonnet & Virga (2012, § 4.1.3), where a dissipation function $R = R(\boldsymbol{Q}; \boldsymbol{A}, \boldsymbol{Q})$ is introduced from which the viscous stress tensor (2.10) can be derived. In particular, the following general form of a dissipation function is proposed in Sonnet & Virga (2012, (4.23)):

$$\begin{aligned} R(\boldsymbol{Q}; \boldsymbol{A}, \boldsymbol{Q}) = {} & \frac{\zeta_1}{2}\boldsymbol{Q} \cdot \boldsymbol{Q} + \zeta_2 \boldsymbol{A} \cdot \boldsymbol{Q} + \zeta_3(\boldsymbol{Q}\boldsymbol{Q}) \cdot \boldsymbol{A} + \zeta_4 \boldsymbol{Q} \cdot \boldsymbol{A}^2 + \zeta_5 \boldsymbol{Q}^2 \cdot \boldsymbol{A}^2 + \frac{\zeta_6}{2}(\boldsymbol{Q} \cdot \boldsymbol{A})^2 \\ & + \frac{\zeta_7}{2}|\boldsymbol{A}|^2|\boldsymbol{Q}|^2 + \frac{\zeta_8}{2}|\boldsymbol{A}|^2 + \zeta_9(\boldsymbol{Q} \cdot \boldsymbol{Q})(\boldsymbol{A} \cdot \boldsymbol{Q}) + \zeta_{10}\big(\boldsymbol{Q}^2 \cdot \boldsymbol{A}\big)(\boldsymbol{Q} \cdot \boldsymbol{A}) \\ & + \frac{\zeta_{11}}{2}|\boldsymbol{Q}|^2(\boldsymbol{A} \cdot \boldsymbol{Q})^2. \end{aligned} \tag{2.12}$$

We remark that Sonnet & Virga (2012) considers only the terms involving ζ_1 to ζ_8 so that R is exactly quadratic in the rates $\boldsymbol{Q}$ and $\boldsymbol{A}$ and at most quadratic in $\boldsymbol{Q}$ but the idea can certainly be generalized. In particular, R can involve a linear combination of nineteen invariants of the tensor triple $(\boldsymbol{Q}, \boldsymbol{Q}, \boldsymbol{A})$ (Sonnet & Virga 2012, p. 223). A simpler version

https://doi.org/10.1017/jfm.2025.10821 Published online by Cambridge University Press

of (2.12), introduced in Qian & Sheng (1998), given by $\zeta_3 = \zeta_5 = \zeta_7 = 0$, also appears in Sonnet & Virga (2012, (4.25)). Here, we include the terms with coefficients ζ_9 to ζ_{11} because with these terms the model (2.7) subsumes the model in Beris & Edwards (1994), derived by Beris and Edward. In a forthcoming work, we will show that the Beris–Edward model is, in fact, a particular version of (2.7), corresponding to a specific choice of dissipation constants ζ_i, $i = 1, \ldots, 11$.

The above Sonnet–Virga model is derived using a variational framework together with the principle of minimum constrained dissipation (Sonnet & Virga 2012, § 2.2, (2.172), (2.178), (2.179)). Using R, we can rewrite (2.7) as (see also Sonnet & Virga (2012), (4.21) and (4.22))

$$\begin{cases} \dfrac{\partial \mathcal{E}_{LdG}}{\partial \boldsymbol{Q}} - \operatorname{div}\left[\dfrac{\partial \mathcal{E}_{LdG}}{\partial \nabla \boldsymbol{Q}}\right] - \Lambda \boldsymbol{I} + \dfrac{\partial R}{\partial \boldsymbol{Q}} = 0, \\ \rho\, \dot{\boldsymbol{v}} - \operatorname{div}[\boldsymbol{T}] = 0, \\ \operatorname{div} \boldsymbol{v} = 0, \end{cases} \tag{2.13}$$

where

$$\boldsymbol{T} = -p\boldsymbol{I} + \boldsymbol{T}^{v}_{SV} + \boldsymbol{T}^{\mathrm{el}} \tag{2.14}$$

with

$$\boldsymbol{T}^{v}_{SV} = \frac{\partial R}{\partial \boldsymbol{A}} + \boldsymbol{Q}\frac{\partial R}{\partial \boldsymbol{Q}} - \frac{\partial R}{\partial \boldsymbol{Q}}\boldsymbol{Q} \quad \text{and} \quad \boldsymbol{T}^{\mathrm{el}} = -\nabla \boldsymbol{Q} \odot \frac{\partial \mathcal{E}_{LdG}}{\partial (\nabla \boldsymbol{Q})}. \tag{2.15}$$

To complete the description of the model, we point out that the dissipation function R has to be non-negative. The set of conditions satisfied by $\boldsymbol{Q}$ and ζ_i, $i = 1, \ldots, 11$ to ensure that this property holds is too complicated to list here but some of these conditions can be found in Sonnet & Virga (2012, pp. 221–222). However, if R only has the terms associated with ζ_1, ζ_2 and ζ_8, i.e.

$$R(\boldsymbol{Q}; \boldsymbol{A}, \boldsymbol{Q}) = \frac{\zeta_1}{2}\boldsymbol{Q}\cdot\boldsymbol{Q} + \zeta_2 \boldsymbol{A}\cdot\boldsymbol{Q} + \frac{\zeta_8}{2}|\boldsymbol{A}|^2, \tag{2.16}$$

then R is non-negative if and only if

$$\zeta_1 > 0 \quad \text{and} \quad \zeta_2^2 \le \zeta_1 \zeta_8. \tag{2.17}$$

2.2. *Non-dimensionalization*

Suppose l is the characteristic length of the system and v is the characteristic velocity. With these, we introduce

$$\tilde{x} = \frac{x}{l}, \quad \tilde{\boldsymbol{v}} = \frac{\boldsymbol{v}}{v}, \quad \tilde{t} = \frac{vt}{L}, \quad \tilde{f}(\boldsymbol{Q}) = \frac{f(\boldsymbol{Q})}{C}, \quad \text{and} \quad \tilde{\mathcal{E}}_{LdG} = \frac{l^2}{L}\mathcal{E}_{LdG}, \tag{2.18}$$

so that

$$\partial_t = \frac{v}{l}\partial_{\tilde{t}}, \quad \partial_x = \frac{1}{l}\partial_{\tilde{x}}, \quad \boldsymbol{Q} = \tilde{\boldsymbol{Q}}, \quad \boldsymbol{A} = \frac{v}{l}\tilde{\boldsymbol{A}}, \quad \tilde{\boldsymbol{W}} = \frac{v}{l}\tilde{\boldsymbol{W}}, \quad \dot{\boldsymbol{Q}} = \frac{v}{l}\dot{\tilde{\boldsymbol{Q}}}, \quad \boldsymbol{Q} = \frac{v}{l}\tilde{\boldsymbol{Q}}, \tag{2.19}$$

$$\tilde{f}(\boldsymbol{Q}) = -\frac{A}{2C}\operatorname{tr}\boldsymbol{Q}^2 + \frac{B}{3C}\operatorname{tr}\boldsymbol{Q}^3 + \frac{1}{4}\left(\operatorname{tr}\boldsymbol{Q}^2\right)^2, \quad \text{and} \quad \tilde{\mathcal{E}}_{LdG}(\tilde{\boldsymbol{Q}}) = \frac{1}{2}|\tilde{\nabla}\tilde{Q}|^2 + \frac{Cl^2}{L}\tilde{f}(\tilde{\boldsymbol{Q}}). \tag{2.20}$$

https://doi.org/10.1017/jfm.2025.10821 Published online by Cambridge University Press

The forms of $\tilde{f}$ and $\tilde{\mathcal{E}}_{LdG}$ are consistent with the following change of variable relation for the Ginzburg–Landau functional:

$$\mathcal{F}_{LdG}(\boldsymbol{Q}) = \int \frac{L}{2}|\nabla \boldsymbol{Q}|^2 + f(\boldsymbol{Q})\,\mathrm{d}x = Ll \int \frac{1}{2}|\tilde{\nabla}\tilde{\boldsymbol{Q}}|^2 + \frac{Cl^2}{L}\tilde{f}(\tilde{\boldsymbol{Q}})\,\mathrm{d}\tilde{x} = Ll \int \tilde{\mathcal{E}}_{LdG}(\tilde{Q})\,\mathrm{d}\tilde{x}. \tag{2.21}$$

If we further introduce $\varepsilon = \frac{1}{l}\sqrt{(L/C)}$ as the ratio between the nematic correlation length $\sqrt{(L/C)}$ and the system length scale l, we can then write the energy density in the following non-dimensional form:

$$\tilde{\mathcal{E}}_{LdG}(\tilde{\nabla}\tilde{\boldsymbol{Q}}, \tilde{\boldsymbol{Q}}) = \frac{1}{2}|\tilde{\nabla}\tilde{Q}|^2 + \frac{1}{\varepsilon^2}\tilde{f}(\tilde{\boldsymbol{Q}}). \tag{2.22}$$

If $\varepsilon \ll 1$, then the potential function imposes a heavy penalty on deviations of $\boldsymbol{Q}$ from the nematic states (2.4).

The non-dimensional system of the governing equations (2.7) is then

$$\frac{\partial \tilde{\mathcal{E}}_{LdG}}{\partial \tilde{\boldsymbol{Q}}} - \widetilde{\mathrm{div}}\left[\frac{\partial \tilde{\mathcal{E}}_{LdG}}{\partial \tilde{\nabla}\tilde{\boldsymbol{Q}}}\right] - \tilde{\Lambda}\boldsymbol{I} + Er\left(\gamma_1\tilde{\boldsymbol{Q}} + \gamma_2\tilde{\boldsymbol{A}} + \frac{\gamma_3}{2}(\tilde{\boldsymbol{A}}\tilde{\boldsymbol{Q}} + \tilde{\boldsymbol{Q}}\tilde{\boldsymbol{A}}) + \gamma_9(\tilde{\boldsymbol{A}}\cdot\tilde{\boldsymbol{Q}})\tilde{\boldsymbol{Q}}\right) = 0, \tag{2.23}$$

$$Re\,\dot{\tilde{\boldsymbol{v}}} + \widetilde{\mathrm{div}}\left[\tilde{p}\boldsymbol{I} - \tilde{\boldsymbol{T}}^{v}_{SV} - \frac{1}{Er}\tilde{\boldsymbol{T}}^{el}\right] = 0, \tag{2.24}$$

$$\widetilde{\mathrm{div}}\,\tilde{\boldsymbol{v}} = 0, \tag{2.25}$$

where the non-dimensional viscous and elastic stress tensors are

$$\begin{aligned}\tilde{\boldsymbol{T}}^{v}_{SV} = {} & \gamma_1(\tilde{\boldsymbol{Q}}\tilde{\boldsymbol{Q}} - \tilde{\boldsymbol{Q}}\tilde{\boldsymbol{Q}}) + \gamma_2(\tilde{\boldsymbol{Q}} + \tilde{\boldsymbol{Q}}\tilde{\boldsymbol{A}} - \tilde{\boldsymbol{A}}\tilde{\boldsymbol{Q}}) + \frac{\gamma_3}{2}\left(\tilde{\boldsymbol{Q}}\tilde{\boldsymbol{Q}} + \tilde{\boldsymbol{Q}}\tilde{\boldsymbol{Q}} + \tilde{\boldsymbol{Q}}^2\tilde{\boldsymbol{A}} - \tilde{\boldsymbol{A}}\tilde{\boldsymbol{Q}}^2\right) \\ & + \gamma_4(\tilde{\boldsymbol{Q}}\tilde{\boldsymbol{A}} + \tilde{\boldsymbol{A}}\tilde{\boldsymbol{Q}}) + \gamma_5\left(\tilde{\boldsymbol{Q}}^2\tilde{\boldsymbol{A}} + \tilde{\boldsymbol{A}}\tilde{\boldsymbol{Q}}^2\right) + \gamma_6(\tilde{\boldsymbol{A}}\cdot\tilde{\boldsymbol{Q}})\boldsymbol{Q} + \gamma_7|\tilde{\boldsymbol{Q}}|^2\tilde{\boldsymbol{A}} + \tilde{\boldsymbol{A}} \\ & + \gamma_9(\tilde{\boldsymbol{Q}}\cdot\tilde{\boldsymbol{Q}})\tilde{\boldsymbol{Q}} + \gamma_{10}((\tilde{\boldsymbol{Q}}^2\cdot\tilde{\boldsymbol{A}})\tilde{\boldsymbol{Q}} + (\tilde{\boldsymbol{Q}}\cdot\tilde{\boldsymbol{A}})\tilde{\boldsymbol{Q}}^2) + \gamma_{11}|\tilde{\boldsymbol{Q}}|^2(\tilde{\boldsymbol{A}}\cdot\tilde{\boldsymbol{Q}})\tilde{\boldsymbol{Q}}\end{aligned} \tag{2.26}$$

and

$$\tilde{\boldsymbol{T}}^{el} = -\tilde{\nabla}\tilde{\boldsymbol{Q}} \odot \tilde{\nabla}\tilde{\boldsymbol{Q}}, \tag{2.27}$$

respectively. In the above, the non-dimensional groups

$$Er = \frac{\zeta_8 vl}{L} \quad \text{and} \quad Re = \frac{\rho vl}{\zeta_8} \tag{2.28}$$

are, respectively, the Ericksen and Reynolds numbers with

$$\gamma_i = \frac{\zeta_i}{\zeta_8},\ i = 1, \ldots, 7, 9, \ldots, 11. \tag{2.29}$$

We note that the constant Er gives the ratio between the viscous and elastic forces while Re gives the ratio between the inertial and viscous forces.

For the rest of the paper, we will refer to our non-dimensionalized system (2.23)–(2.25) but for simplicity omit the tildes in all the variables.

https://doi.org/10.1017/jfm.2025.10821 Published online by Cambridge University Press

2.3. *Decoupling of the governing equations*

In this section, we introduce physical regimes in which the far-field behaviour of $\boldsymbol{Q}$ and $\boldsymbol{v}$ can be explicitly characterized. In particular, we will assume that the Ericksen number is small so that – as we will see shortly – the equation for the $\boldsymbol{Q}$-tensor decouples from the equation for the velocity $\boldsymbol{v}$. To this end, observe that

$$\begin{aligned}\operatorname{div} \boldsymbol{T}^{el} &= -\operatorname{div}\left(\left(\partial_i \boldsymbol{Q}\cdot\partial_j \boldsymbol{Q}\right)\mathbf{e}_i\otimes\mathbf{e}_j\right) = -\partial_j\left(\partial_i \boldsymbol{Q}\cdot\partial_j \boldsymbol{Q}\right)\mathbf{e}_i\\ &= -\nabla\left(\frac{1}{2}|\nabla \boldsymbol{Q}|^2\right) - \left(\partial_i \boldsymbol{Q}\cdot\Delta \boldsymbol{Q}\right)\mathbf{e}_i,\end{aligned} \tag{2.30}$$

from which $\operatorname{div} \boldsymbol{T}^{el}$ can be eliminated. More precisely, using (2.23), we have

$$\partial_i \boldsymbol{Q}\cdot\Delta \boldsymbol{Q} = \frac{1}{\varepsilon^2}\frac{\partial f}{\partial \boldsymbol{Q}}\cdot\partial_i \boldsymbol{Q} + Er\left(\gamma_1 \boldsymbol{Q} + \gamma_2 \boldsymbol{A} + \frac{\gamma_3}{2}(\boldsymbol{A}\boldsymbol{Q}+\boldsymbol{Q}\boldsymbol{A}) + \gamma_9(\boldsymbol{A}\cdot\boldsymbol{Q})\boldsymbol{Q}\right)\cdot\partial_i \boldsymbol{Q}, \tag{2.31}$$

where the $\Lambda \boldsymbol{I}$ disappears as $\operatorname{tr} \boldsymbol{Q} = 0$: $\Lambda \boldsymbol{I}\cdot\partial_i Q = \Lambda\partial_i \operatorname{tr}\boldsymbol{Q} = 0$. Combining (2.30) and (2.31), we have

$$\begin{aligned}&\operatorname{div} \boldsymbol{T}^{el}\\ &= -\nabla\left(\frac{1}{2}|\nabla \boldsymbol{Q}|^2 + \frac{1}{\varepsilon^2}f(\boldsymbol{Q})\right) - Er\left(\gamma_1 \boldsymbol{Q} + \gamma_2 \boldsymbol{A} + \frac{\gamma_3}{2}(\boldsymbol{A}\boldsymbol{Q}+\boldsymbol{Q}\boldsymbol{A}) + \gamma_9(\boldsymbol{A}\cdot\boldsymbol{Q})\boldsymbol{Q}\right)\cdot\partial_i \boldsymbol{Q}\mathbf{e}_i\\ &= -\nabla\mathcal{E}_{LdG}(\boldsymbol{Q}) - Er\left(\gamma_1 \boldsymbol{Q} + \gamma_2 \boldsymbol{A} + \frac{\gamma_3}{2}(\boldsymbol{A}\boldsymbol{Q}+\boldsymbol{Q}\boldsymbol{A}) + \gamma_9(\boldsymbol{A}\cdot\boldsymbol{Q})\boldsymbol{Q}\right)\cdot\partial_i \boldsymbol{Q}\mathbf{e}_i.\end{aligned} \tag{2.32}$$

Hence

$$\begin{aligned}\operatorname{div}\left(-p\boldsymbol{I} + \boldsymbol{T}^v_{SV} + \frac{1}{Er}\boldsymbol{T}^{el}\right) &= \operatorname{div}\left(-p\boldsymbol{I} - \frac{1}{Er}\mathcal{E}_{LdG}(\boldsymbol{Q})\boldsymbol{I} + \boldsymbol{T}^v_{SV}\right)\\ &\quad - \left(\gamma_1 \boldsymbol{Q} + \gamma_2 \boldsymbol{A} + \frac{\gamma_3}{2}(\boldsymbol{A}\boldsymbol{Q}+\boldsymbol{Q}\boldsymbol{A}) + \gamma_9(\boldsymbol{A}\cdot\boldsymbol{Q})\boldsymbol{Q}\right)\cdot\partial_i \boldsymbol{Q}\mathbf{e}_i.\end{aligned} \tag{2.33}$$

By absorbing the gradient of the Landau–de Gennes energy density into the pressure field, our system (2.23)–(2.25) takes the following form:

$$\begin{cases}\dfrac{\partial\mathcal{E}_{LdG}}{\partial \boldsymbol{Q}} - \operatorname{div}\left[\dfrac{\partial\mathcal{E}_{LdG}}{\partial\nabla \boldsymbol{Q}}\right] - \Lambda \boldsymbol{I} + Er\left(\gamma_1 \boldsymbol{Q} + \gamma_2 \boldsymbol{A} + \dfrac{\gamma_3}{2}(\boldsymbol{A}\boldsymbol{Q}+\boldsymbol{Q}\boldsymbol{A}) + \gamma_9(\boldsymbol{A}\cdot\boldsymbol{Q})\boldsymbol{Q}\right) = 0,\\ Re\,\dot{\boldsymbol{v}} + \operatorname{div}\left[p\boldsymbol{I} - \boldsymbol{T}^v_{SV}\right] + \left(\gamma_1 \boldsymbol{Q} + \gamma_2 \boldsymbol{A} + \dfrac{\gamma_3}{2}(\boldsymbol{A}\boldsymbol{Q}+\boldsymbol{Q}\boldsymbol{A}) + \gamma_9(\boldsymbol{A}\cdot\boldsymbol{Q})\boldsymbol{Q}\right)\cdot\partial_i \boldsymbol{Q}\mathbf{e}_i = 0,\\ \operatorname{div}\boldsymbol{v} = 0.\end{cases} \tag{2.34}$$

With the above, we now consider a specific regime of the above system so that the far-field behaviour can be revealed explicitly. This is described as follows.

(*a*) The Ericksen number is small, i.e. $Er \to 0$, so that the elastic stress in the liquid crystal dominates the viscous stress. Formally, this leads to

$$\begin{cases}\dfrac{\partial\mathcal{E}_{LdG}}{\partial \boldsymbol{Q}} - \operatorname{div}\left[\dfrac{\partial\mathcal{E}_{LdG}}{\partial\nabla \boldsymbol{Q}}\right] = 0,\\ Re\,\dot{\boldsymbol{v}} + \operatorname{div}\left[p\boldsymbol{I} - \boldsymbol{T}^v_{SV}\right] + \left(\gamma_1 \boldsymbol{Q} + \gamma_2 \boldsymbol{A} + \dfrac{\gamma_3}{2}(\boldsymbol{A}\boldsymbol{Q}+\boldsymbol{Q}\boldsymbol{A}) + \gamma_9(\boldsymbol{A}\cdot\boldsymbol{Q})\boldsymbol{Q}\right)\cdot\partial_i \boldsymbol{Q}\mathbf{e}_i = 0,\\ \operatorname{div}\boldsymbol{v} = 0\end{cases} \tag{2.35}$$

https://doi.org/10.1017/jfm.2025.10821 Published online by Cambridge University Press

where there is no need for $\Lambda \boldsymbol{I}$ as the tracelessness condition for $\boldsymbol{Q}$ is already incorporated in (2.8). Note that the first equation is the Euler–Lagrange equation for the Landau–de Gennes energy and it is decoupled from the equation for the velocity. In other words, the tensor field $\boldsymbol{Q}$ serves as the inhomogeneous source term for the velocity field $\boldsymbol{v}$.

(*b*) The characteristic length of the problem is much smaller than the nematic correlation length, i.e. $\varepsilon \to \infty$ so that $(\partial \mathcal{E}_{LdG}/\partial \boldsymbol{Q}) = (1/\varepsilon^2)(\partial f(\boldsymbol{Q})/\partial \boldsymbol{Q}) \approx 0$. Hence, we are led to the following system:

$$\begin{cases} -\Delta \boldsymbol{Q} = 0, \\ Re\, \dot{\boldsymbol{v}} + \operatorname{div}\left[p\boldsymbol{I} - \boldsymbol{T}^v_{SV}\right] = -\left(\gamma_1 \boldsymbol{Q} + \gamma_2 \boldsymbol{A} + \dfrac{\gamma_3}{2}(\boldsymbol{A}\boldsymbol{Q} + \boldsymbol{Q}\boldsymbol{A}) + \gamma_9 (\boldsymbol{A}\cdot\boldsymbol{Q})\boldsymbol{Q}\right) \cdot \partial_i \boldsymbol{Q}\mathbf{e}_i, \\ \operatorname{div} \boldsymbol{v} = 0. \end{cases} \tag{2.36}$$

We remark that the non-negativity of the dissipation function is ensured if among others, the inequality (2.17) is satisfied. However, as $\boldsymbol{Q}$ is fixed or actually 'prescribed' by (2.36) in our asymptotic regime, these inequalities can simply be replaced by the condition that all the coefficients, γ_1 through γ_{11} are sufficiently small.

(*c*) The Reynolds number is small and the system has reached stationarity, i.e. $Re \to 0$ and $\partial_t \boldsymbol{Q} = \partial_t \boldsymbol{v} = 0$. Hence, the system (2.36) becomes

$$\begin{cases} -\Delta \boldsymbol{Q} = 0, \\ \operatorname{div}\left[p\boldsymbol{I} - \boldsymbol{T}^v_{SV}\right] = -\left(\gamma_1 \boldsymbol{Q} + \gamma_2 \boldsymbol{A} + \dfrac{\gamma_3}{2}(\boldsymbol{A}\boldsymbol{Q} + \boldsymbol{Q}\boldsymbol{A}) + \gamma_9 (\boldsymbol{A}\cdot\boldsymbol{Q})\boldsymbol{Q}\right) \cdot \partial_i \boldsymbol{Q}\mathbf{e}_i, \\ \operatorname{div} \boldsymbol{v} = 0. \end{cases} \tag{2.37}$$

Note that in this case, we have $\boldsymbol{Q} = \boldsymbol{v}\cdot\nabla \boldsymbol{Q} + \boldsymbol{Q}\boldsymbol{W} - \boldsymbol{W}\boldsymbol{Q}$. We record $\boldsymbol{T}^v_{SV}$ (2.26) here again for convenience,

$$\begin{aligned} \boldsymbol{T}^v_{SV} = {} & \gamma_1(\boldsymbol{Q}\boldsymbol{Q} - \boldsymbol{Q}\boldsymbol{Q}) + \gamma_2(\boldsymbol{Q} + \boldsymbol{Q}\boldsymbol{A} - \boldsymbol{A}\boldsymbol{Q}) + \frac{\gamma_3}{2}(\boldsymbol{Q}\boldsymbol{Q} + \boldsymbol{Q}\boldsymbol{Q} + \boldsymbol{Q}^2\boldsymbol{A} - \boldsymbol{A}\boldsymbol{Q}^2) \\ & + \gamma_4(\boldsymbol{Q}\boldsymbol{A} + \boldsymbol{A}\boldsymbol{Q}) + \gamma_5(\boldsymbol{Q}^2\boldsymbol{A} + \boldsymbol{A}\boldsymbol{Q}^2) + \gamma_6(\boldsymbol{A}\cdot\boldsymbol{Q})\boldsymbol{Q} + \gamma_7|\boldsymbol{Q}|^2\boldsymbol{A} + \boldsymbol{A} \\ & + \gamma_9(\boldsymbol{Q}\cdot\boldsymbol{Q})\boldsymbol{Q} + \gamma_{10}\big((\boldsymbol{Q}^2\cdot\boldsymbol{A})\boldsymbol{Q} + (\boldsymbol{Q}\cdot\boldsymbol{A})\boldsymbol{Q}^2\big) + \gamma_{11}|\boldsymbol{Q}|^2(\boldsymbol{A}\cdot\boldsymbol{Q})\boldsymbol{Q}. \end{aligned} \tag{2.38}$$

REMARK 1. *Here we provide some typical values of the parameters to justify the above assumptions. Using the values from Ravnik & Žumer (2009) and Ruhwandl & Terentjev (1995), we have*

$$\eta_8 \sim 10^{-1}\, Pa\, s, \quad L \sim 10^{-11}\, N \quad \text{and} \quad C \sim 10^6\, J\, m^{-3}. \tag{2.39}$$

Hence, for $Er \ll 1$, we would need $vl \ll 10^{-10}\, m^2\, s^{-1}$. This can be satisfied if $l \ll 10^{-6}\, m$ and $v \ll 10^{-4}\, m\, s^{-1}$. With these, we have $Re \sim 10^{-9} \ll 1$. For $\varepsilon \gg 1$, we need $l \ll \sqrt{L/C} \sim 10^{-8}\, m$ leading to $l \ll 10\, nm$.

Note that the requirement that the particle size $l \ll 10\, nm$ seems quite restrictive. This choice is mainly due to mathematical reasons as this assumption allows us to use an explicit formula for $\boldsymbol{Q}$ to facilitate our analysis. We expect both our approach and our results to remain valid for particles of larger sizes (see Remark 3 in § 3.1).

To conclude, the current paper analyses the stationary system (2.37) in the domain exterior to a particle. We are particularly interested in the far-field behaviour of the flow.

https://doi.org/10.1017/jfm.2025.10821 Published online by Cambridge University Press

To complete the description of the system, we need to incorporate boundary conditions for $\boldsymbol{v}$ and $\boldsymbol{Q}$ which are discussed next.

2.4. *Boundary conditions*

We will solve the system (2.37) in the exterior domain $\Omega = \mathbb{R}^3 \setminus \boldsymbol{B}_a(0)$ in a moving frame. The following boundary conditions will be imposed for $\boldsymbol{Q}$ and $\boldsymbol{v}$:

$$\boldsymbol{Q} \longrightarrow \boldsymbol{Q}_*, \quad \boldsymbol{v} \longrightarrow \boldsymbol{v}_* \quad \text{as } |x| \longrightarrow \infty, \tag{2.40}$$

$$\text{on } \partial\Omega: \quad \begin{cases} \dfrac{1}{w}\dfrac{\partial \boldsymbol{Q}}{\partial \nu} = \boldsymbol{Q}_b - \boldsymbol{Q}, \\ \boldsymbol{v} = \boldsymbol{v}_b. \end{cases} \tag{2.41}$$

In the above, $\boldsymbol{Q}_*$, $\boldsymbol{v}_*$ are the far-field states for $\boldsymbol{Q}$ and $\boldsymbol{v}$, $\boldsymbol{Q}_b$ is some $\mathcal{M}$-valued function defined on $\partial \boldsymbol{B}_a(0)$ and ν is the outward unit normal to $\partial\Omega$ (or inward to $\boldsymbol{B}_a(0)$). The number w represents the anchoring strength.

Note that the Robin boundary condition for $\boldsymbol{Q}$ in (2.41) is associated with the following surface anchoring energy:

$$\mathcal{F}_s(\boldsymbol{Q}) = \frac{w}{2}\int_{\partial\Omega} |\boldsymbol{Q} - \boldsymbol{Q}_b|^2 \, \mathrm{d}\sigma. \tag{2.42}$$

We refer to Willman *et al.* (2007) for a discussion of surface anchoring phenomena. Recalling (2.2), the combined total energy of the system for the liquid crystal part is then given by

$$\mathcal{E}(\boldsymbol{Q}) = \mathcal{F}_{LdG}(\boldsymbol{Q}) + \mathcal{F}_s(\boldsymbol{Q}). \tag{2.43}$$

Following the same non-dimensionalization procedure leading to (2.21), using $a = l$, we have

$$\tilde{\mathcal{E}}(\tilde{\boldsymbol{Q}}) := \frac{\mathcal{E}(\boldsymbol{Q})}{Ll} = \int_{\mathbb{R}^3\setminus \boldsymbol{B}_1(0)} \frac{1}{2}\left|\tilde{\nabla}\tilde{\boldsymbol{Q}}\right|^2 + \frac{1}{\varepsilon^2}\tilde{f}\left(\tilde{\boldsymbol{Q}}\right) \mathrm{d}\tilde{x} + \tilde{w}\int_{\partial \boldsymbol{B}_1(0)} \left|\tilde{\boldsymbol{Q}} - \boldsymbol{Q}_b\right|^2 \mathrm{d}\tilde{\sigma} \tag{2.44}$$

where $\tilde{w} = wl/2L$. Typically w ranges from 10^{-7} to 10^{-3} J m^{-2} (Ravnik & Žumer 2009; Blinov, Kabayenkov & Sonin 1989). Using $L \sim 10^{-11}$ N and l ranging from 10^{-9} m to 10^{-6} m, we have $\tilde{w}$ ranging from 10^{-5} to 10^{2}. From now on, we will omit the tilde and refer to w as the non-dimensional anchoring strength.

The first condition in (2.41) is called a weak anchoring condition for $\boldsymbol{Q}$. Naturally, in the case of infinite anchoring strength, $w = \infty$ the boundary conditions reduces to the Dirichlet problem $\boldsymbol{Q} = \boldsymbol{Q}_b$ on $\partial\Omega$. In this case $\boldsymbol{Q}$ is said to satisfy a strong anchoring condition. In § 3.1, we will choose $\boldsymbol{Q}_b$ a 'hedgehog' type so as to have an explicit solution for $\boldsymbol{Q}$.

REMARK 2. *The problem* (2.36), (2.40), (2.41) *describes the flow of a nematic liquid crystal in the exterior of a colloidal particle under various scenarios. We emphasize that the quantity* $\boldsymbol{v}_b$ *is defined in the frame associated with the moving particle.*

(*a*) *For a passive particle, the condition* $\boldsymbol{v}_b = 0$ *describes no-slip boundary conditions on the surface of a particle that is stationary with respect to an inertial frame. The second condition in* (2.40) *imposes the constant velocity* $\boldsymbol{v}_*$ *of the flow at infinity.*

(*b*) *Now suppose the passive particle moves in the nematic fluid with an externally imposed velocity* $\boldsymbol{v}_c$ *subject to the no-slip boundary condition, while the nematic is stationary at infinity, then the velocity on the boundary of the particle and at infinity equals* $\boldsymbol{v}_b = \boldsymbol{v}_c$ *and* $\boldsymbol{v}_* = 0$*, respectively. In this case, if we go to a frame moving*

https://doi.org/10.1017/jfm.2025.10821 Published online by Cambridge University Press

with the particle, then the velocity of the nematic liquid crystal at infinity will equal $\boldsymbol{v}_* = -\boldsymbol{v}_c$ *and the velocity on the surface of the particle will vanish, that is,* $\boldsymbol{v}_b = 0$*. However, this change of frame will induce an additional forcing term in* (2.32) *due to the presence of the convective derivative* $\boldsymbol{v}\cdot\nabla\boldsymbol{Q}$ *of* $\boldsymbol{Q}$*. This term will be described more explicitly in* § 4*, in particular,* (4.28) *and the discussion afterward.*

(*c*) *For a general active particle,* $\boldsymbol{v}_b$ *is typically prescribed and non-constant on the surface of the particle. Similar to the previous paragraph, if the particle moves with constant velocity* $\boldsymbol{v}_c$*, then changing to a frame moving with the particle, we can replace* $\boldsymbol{v}_b$ *and* $\boldsymbol{v}_*$ *by* $\boldsymbol{v}_b - \boldsymbol{v}_c$ *and* $\boldsymbol{v}_* = -\boldsymbol{v}_c$*. The value of* $\boldsymbol{v}_c$ *can be determined by solving the problem* (2.36), (2.40)–(2.41) *and choosing* $\boldsymbol{v}_c$ *so that the total stress on the surface of the particle vanishes.*

As a final remark, we point out that it is certainly advantageous to consider our problem in the frame of the (moving) particle so that the domain does not change in time. Thus, in the case of passive particle which is the emphasis of the current paper, we set $\boldsymbol{v}_b = 0$ and $\boldsymbol{v}_*$ to be some prescribed value. (As mentioned above, the extension to active particle in the current framework is achieved by setting $\boldsymbol{v}_b$ to be some general non-constant function. See Lighthill (1952) for examples of such a function.) Our goal is then to compute and analyse the flow pattern of the nematic fluid.

3. Preliminary information

Here we describe known explicit solutions for $\boldsymbol{Q}$ and $\boldsymbol{v}$, which will be used in determining the flow pattern in our anisotropic Stokes system. At this point, we have non-dimensionalized the system so that the domain Ω is now taken to be $\mathbb{R}^3\backslash\boldsymbol{B}_1(0)$.

3.1. *Stationary state for* $\boldsymbol{Q}$

Under the physical regime and boundary conditions considered in the § § 2.3 and 2.4, we are looking for a $\boldsymbol{Q}$-tensor function satisfying

$$\triangle\boldsymbol{Q} = 0, \quad \text{in } \Omega, \tag{3.1}$$

$$\frac{1}{w}\frac{\partial\boldsymbol{Q}}{\partial\nu} = \boldsymbol{Q}_b - \boldsymbol{Q} \quad \text{on } \partial\Omega, \tag{3.2}$$

$$\boldsymbol{Q} = \boldsymbol{Q}_* \quad \text{at } |x| = \infty \tag{3.3}$$

where $w = O(1)$ is the non-dimensional anchoring strength. The work Alama–Bronsard–Lamy (Alama *et al.* 2016) gives the following explicit solution:

$$\boldsymbol{Q} = \left(1 - \frac{w}{1+w}\frac{1}{r}\right)\boldsymbol{Q}_* + \frac{w}{3+w}\frac{1}{r^3}\boldsymbol{Q}_b, \quad r > 1, \tag{3.4}$$

$$\text{where} \quad \boldsymbol{Q}_* = s_*\left(n_*\otimes n_* - \frac{\boldsymbol{I}}{3}\right), \quad \text{with a given unit vector } n_*, \tag{3.5}$$

$$\text{and} \quad \boldsymbol{Q}_b = s_*\left(\widehat{x}\otimes\widehat{x} - \frac{\boldsymbol{I}}{3}\right), \quad \widehat{x} = \frac{x}{|x|}, \tag{3.6}$$

with parameters $s_* > 0$. Note that the boundary function $\boldsymbol{Q}_b$ is of 'hedgehog' type. This boundary behaviour corresponds to $\boldsymbol{Q}$ satisfying the so-called weak homeotropic anchoring condition. Note that the above $\boldsymbol{Q}$ is harmonic and has the following far-field asymptotics:

https://doi.org/10.1017/jfm.2025.10821 Published online by Cambridge University Press

$$\boldsymbol{Q} \sim \boldsymbol{Q}_* + O\left(\frac{1}{r}\right) \quad \text{and} \quad \nabla \boldsymbol{Q} \sim O\left(\frac{1}{r^2}\right), \quad \text{for } r \gg 1. \tag{3.7}$$

REMARK 3. *We remark that Alama et al. (2016) derives the above equation in the small particle regime $a^2 \ll L$, corresponding to $\varepsilon \gg 1$. For large particle, $a^2 \gg L$, corresponding to $\varepsilon \ll 1$, the solution $\boldsymbol{Q}$ tends to a map taking the form, $\boldsymbol{Q}(x) = s_*(n(x) \otimes n(x) - (\boldsymbol{I}/3))$ for some unit vector field $n(\cdot)$. We point out here the work (Alama et al. 2023) in which it is shown that in the director model, $n(x)$ decays as $(1/r)$ in the region away of a particle. This result is fairly robust with respect to the boundary condition – it relies mostly on the energy minimizing property of the director field. The explicit formula (3.4) for $\boldsymbol{Q}(x)$ is consistent with this behaviour. We expect that similar asymptotics will also hold in the intermediate particle size regime as $\boldsymbol{Q}$ satisfies (2.35). Due to the stabilizing term $\partial \mathcal{E}_{LdG}(\boldsymbol{Q})/\partial \boldsymbol{Q}$, Green's function for the linearized system has better decay properties. It is certainly of interest to make this statement more precise and also investigate the asymptotics and expansions of the solution as a function of Er and ε.*

On the other hand, the decay property of the velocity field $\boldsymbol{v}$ is much more involved and requires a different consideration. It depends on the interaction between Green's function for Stokes system and the inhomogeneous terms which are directly linked to the explicit expression for $\boldsymbol{Q}$ in (3.4). The main technical component of the rest of this paper is to understand this interaction.

3.2. *Green's function for classical isotropic Stokes system*

We introduce here the fundamental solution $(\boldsymbol{E}, \boldsymbol{q})$ of the Stokes system which solves the following system of equations:

$$\begin{cases} -\Delta \boldsymbol{E}_{ij}(x) - \dfrac{\partial}{\partial x_i} \boldsymbol{q}_j(x) = \delta_{ij}\delta_0(x), \\ \dfrac{\partial}{\partial x_i} \boldsymbol{E}_{ij}(x) = 0. \end{cases} \tag{3.8}$$

Following Galdi (2011, Chapter 4.2, p. 238), $(\boldsymbol{E}, \boldsymbol{q})$ is given as

$$\boldsymbol{E}(x) = \frac{1}{8\pi}\left[\frac{\boldsymbol{I}}{r} + \frac{x \otimes x}{r^3}\right], \quad \text{i.e.} \quad \boldsymbol{E}_{ij}(x) = \frac{1}{8\pi}\left[\frac{\delta_{ij}}{r} + \frac{x_i x_j}{r^3}\right], \quad i, j = 1, 2, 3, \tag{3.9}$$

$$\boldsymbol{q}(x) = -\frac{1}{4\pi}\frac{x}{r^3}, \quad \text{i.e.} \quad \boldsymbol{q}_i(x) = -\frac{x_i}{r^3}, \quad i = 1, 2, 3. \tag{3.10}$$

Note that

$$\boldsymbol{E}(x) \sim \frac{1}{r}, \quad \text{and} \quad \boldsymbol{q}(x) \sim \frac{1}{r^2} \quad \text{for} \quad r \gg 1. \tag{3.11}$$

The above fundamental solution can be used to produce solutions of Stokes system on the entire space. More precisely, if $(\boldsymbol{u}, p)$ solves

$$\begin{aligned} -\Delta \boldsymbol{u} + \nabla p &= \boldsymbol{f}, \quad \text{on } \mathbb{R}^3, \\ \operatorname{div} \boldsymbol{u} &= 0, \quad \text{on } \mathbb{R}^3, \\ \boldsymbol{u} &= 0, \quad \text{at } |x| = \infty, \end{aligned} \tag{3.12}$$

then it is given by

$$\boldsymbol{u}(x) = \int_{\mathbb{R}^3} \boldsymbol{E}(x - y)\boldsymbol{f}(y)\,\mathrm{d}y \quad \text{and} \quad p(x) = \int_{\mathbb{R}^3} -\boldsymbol{q}(x - y) \cdot \boldsymbol{f}(y)\,\mathrm{d}y. \tag{3.13}$$

https://doi.org/10.1017/jfm.2025.10821 Published online by Cambridge University Press

The above integrals are well-defined for $\boldsymbol{f}$ with sufficient spatial decay (Galdi 1999, 2011).

Similarly, in the case of a Stokes system in an exterior domain, for example,

$$\begin{aligned} -\Delta \boldsymbol{u} + \nabla p &= \boldsymbol{f}, \quad \text{on } \Omega, \\ \operatorname{div} \boldsymbol{u} &= 0, \quad \text{on } \Omega, \\ \boldsymbol{u} &= 0, \quad \text{at } |x| = \infty, \end{aligned} \tag{3.14}$$

then $\boldsymbol{u}$ and p can be represented by

$$\begin{aligned} \boldsymbol{u}(x) = &\int_\Omega \boldsymbol{E}(x-y)\boldsymbol{f}(y)\,\mathrm{d}y \\ &+ \int_{\partial\Omega} \big\langle \boldsymbol{E}(x-y),\, \boldsymbol{T}(\boldsymbol{u},\, p)(y)\nu_y \big\rangle \,\mathrm{d}\sigma_y - \int_{\partial\Omega} \big\langle \boldsymbol{T}(\boldsymbol{E},\, \boldsymbol{q})(x-y)\nu_y,\, \boldsymbol{u}(y) \big\rangle \,\mathrm{d}\sigma_y, \end{aligned} \tag{3.15}$$

$$\begin{aligned} p(x) = &\int_\Omega -\boldsymbol{q}(x-y)\cdot \boldsymbol{f}(y)\,\mathrm{d}y \\ &- \int_{\partial\Omega} \big\langle \boldsymbol{T}(\boldsymbol{u},\, p)(y)\nu_y,\, \boldsymbol{q}(x-y) \big\rangle \,\mathrm{d}\sigma_y + 2\int_{\partial\Omega} \big\langle \nabla_x \boldsymbol{q}(x-y)\nu_y,\, \boldsymbol{u}(y) \big\rangle \,\mathrm{d}\sigma_y, \end{aligned} \tag{3.16}$$

where $\boldsymbol{T}$ is the stress tensor defined for any given vector and scalar fields $\boldsymbol{w}$ and π as

$$\boldsymbol{T}(\boldsymbol{w}, \pi) = \nabla \boldsymbol{w} + (\nabla \boldsymbol{w})^T - \pi \boldsymbol{I}, \tag{3.17}$$

and for any matrix and vector fields $\boldsymbol{M}$ and $\boldsymbol{g}$ and vector v, $\boldsymbol{T}(\boldsymbol{M}, \boldsymbol{g})v$ is a matrix with its ith row given by

$$\big(\boldsymbol{T}(\boldsymbol{M}, \boldsymbol{g})v\big)_i = \boldsymbol{T}(\boldsymbol{M}_i, \boldsymbol{g}_i)v. \tag{3.18}$$

We also recall the convention as stated in item (g) at the end of the Introduction.

In the above and the bulk of this paper, we will be dealing with solutions $\boldsymbol{u}$ that converge to their far-field limits with rate $(1/r)$. With this in mind, we expect the following estimates for the boundary integrals:

$$\left| \int_{\partial\Omega} \big\langle \boldsymbol{E}(x,-y),\, \boldsymbol{T}(\boldsymbol{u},\, p)(y)\nu_y \big\rangle \,\mathrm{d}\sigma_y \right| \lesssim \frac{1}{r}, \tag{3.19}$$

$$\left| \int_{\partial\Omega} \big\langle \boldsymbol{T}(\boldsymbol{E},\, \boldsymbol{q}_j)(x-y)\nu_y,\, \boldsymbol{u}(y) \big\rangle \,\mathrm{d}\sigma_y \right| \lesssim \frac{1}{r^2}, \tag{3.20}$$

$$\left| \int_{\partial\Omega} \big\langle \boldsymbol{T}(\boldsymbol{u},\, p)(y)\nu_y,\, \boldsymbol{q}(x-y) \big\rangle \,\mathrm{d}\sigma_y \right| \lesssim \frac{1}{r^2}, \tag{3.21}$$

$$\left| \int_{\partial\Omega} \big\langle \nabla_x \boldsymbol{q}(x-y)\nu_y,\, \boldsymbol{u}(y) \big\rangle \,\mathrm{d}\sigma_y \right| \lesssim \frac{1}{r^3}. \tag{3.22}$$

Clearly (3.19) gives the dominating far-field behaviour. It can be decomposed as

$$\begin{aligned} &\int_{\partial\Omega} \big\langle \boldsymbol{E}(x-y),\, \boldsymbol{T}(\boldsymbol{u},\, p)(y)\nu_y \big\rangle \,\mathrm{d}\sigma_y \\ &= \left\langle \boldsymbol{E}(x),\, \int_{\partial\Omega} \boldsymbol{T}(\boldsymbol{u},\, p)(y)\nu_y \mathrm{d}\sigma_y \right\rangle + \int_{\partial\Omega} \big\langle \boldsymbol{E}(x-y) - \boldsymbol{E}(x),\, \boldsymbol{T}(\boldsymbol{u},\, p)(y)\nu_y \big\rangle \mathrm{d}\sigma_y \\ &= \langle \boldsymbol{E}(x),\, \mathcal{F} \rangle + O\left(\frac{1}{r^2}\right) \end{aligned} \tag{3.23}$$

https://doi.org/10.1017/jfm.2025.10821 Published online by Cambridge University Press

where

$$\mathcal{F} := \int_{\partial\Omega} \boldsymbol{T}(\boldsymbol{u}, p)(y)\nu_y \mathrm{d}\sigma_y \tag{3.24}$$

denotes the boundary stress or drag force on the particle. The decomposition (3.23) is the same as Chang & Finn (1961, Theorem 1, (4.2a)).

A word of caution is in order. The anticipated $(1/r)$ rate of decay for $\boldsymbol{u}$ relies crucially on the mean-zero condition on the inhomogeneous function $\boldsymbol{f}$ which appears in the bulk integral $\int_\Omega \boldsymbol{E}(x-y)\boldsymbol{f}(y)\,\mathrm{d}y$ in (3.15). This and other related far-field asymptotics of the bulk integrals and the method of solution for the Stokes system (2.32) will be given in the Appendices and Supplementary materials. In particular, see Appendix A.3 and A.4.

3.3. *Uniform Stokes flow*

Here we provide the solution of a uniform Stokes flow $\boldsymbol{U}$ with far-field velocity $\boldsymbol{U}_*$, passing a sphere of radius a. It solves the following system of equations:

$$-\Delta \boldsymbol{U} + \nabla p = 0, \quad \text{for } |x| > a; \tag{3.25}$$

$$\operatorname{div} \boldsymbol{U} = 0, \quad \text{for } |x| > a; \tag{3.26}$$

$$\boldsymbol{U} = 0, \quad \text{at } |x| = a; \tag{3.27}$$

$$\boldsymbol{U} = \boldsymbol{U}_*, \quad \text{at } |x| = \infty. \tag{3.28}$$

Using the spherical coordinates (following the physicists' convention) with θ being the polar angle (measured from the polar axis) and ϕ being the azimuthal angle (measured from the meridian plane), we can write the velocity flowing along the polar axis as $\boldsymbol{U} = (u_r, u_\theta, u_\phi = 0)$. Following Acheson (1990, § 7.2), we have

$$u_r = \frac{1}{r^2 \sin\theta}\frac{\partial \Psi}{\partial \theta}, \quad \text{and} \quad u_\theta = -\frac{1}{r\sin\theta}\frac{\partial \Psi}{\partial r}, \tag{3.29}$$

where

$$\Psi(r,\theta) = f(r)\sin^2\theta, \quad f(r) = \frac{V}{4}\left(2r^2 - 3ar + \frac{a^3}{r}\right), \quad V = |\boldsymbol{U}_*|, \tag{3.30}$$

$$u_r = \frac{V}{4}\left(2 - \frac{3a}{r} + \frac{a^3}{r^3}\right)2\cos\theta, \tag{3.31}$$

$$u_\theta = -\frac{V}{4}\left(4 - \frac{3a}{r} - \frac{a^3}{r^3}\right)\sin\theta. \tag{3.32}$$

We note that the form of f is found by solving $((\partial^2/\partial r^2) - (2/r^2))^2 f(r) = 0$. The method of finding f in a bounded (annular) domain will be presented in Appendix C.

If the flow is in the direction of the x_1-axis, i.e. $\boldsymbol{U}_* = Ve_1$, then we have in Cartesian coordinates that

https://doi.org/10.1017/jfm.2025.10821 Published online by Cambridge University Press

$$\begin{aligned}\boldsymbol{U} &= V\left(e_1 - \frac{3a}{4}\left(\frac{x_1 x + r^2 e_1}{r^3}\right) - \frac{a^3}{4}\left(\frac{r^2 e_1 - 3x_1 x}{r^5}\right)\right)\\ &= V\left(e_1 - \frac{3a}{4}\left(\frac{2x_1^2 + x_2^2 + x_3^2,\, x_1x_2,\, x_1x_3}{r^3}\right)\right.\\ &\quad\left. - \frac{a^3}{4}\left(\frac{-2x_1^2 + x_2^2 + x_3^2,\, -3x_1x_2,\, -3x_1x_3}{r^5}\right)\right),\end{aligned} \tag{3.33}$$

$$p = p_\infty - \frac{3}{2}\frac{Va}{r^2}\cos\theta = p_\infty - \frac{3}{2}\frac{Va}{r^2}\frac{x_1}{\sqrt{x_1^2 + x_2^2}}. \tag{3.34}$$

More generally, in vector form, we have

$$\begin{aligned}\boldsymbol{U} &= \boldsymbol{U}_* - \frac{3a}{4}\left(\frac{x \otimes x\boldsymbol{U}_* + r^2\boldsymbol{U}_*}{r^3}\right) - \frac{a^3}{4}\left(\frac{r^2\boldsymbol{U}_* - 3x \otimes x\boldsymbol{U}_*}{r^5}\right)\\ &= \left[\boldsymbol{I} - \frac{3a}{4}\left(\frac{x \otimes x + r^2\boldsymbol{I}}{r^3}\right) + \frac{a^3}{4}\left(\frac{3x \otimes x - r^2\boldsymbol{I}}{r^5}\right)\right]\boldsymbol{U}_*.\end{aligned} \tag{3.35}$$

Making use of Green's function $\boldsymbol{E}$ (3.9) and upon introducing

$$\boldsymbol{F}(x) = \frac{3x \otimes x - r^2\boldsymbol{I}}{r^5}, \tag{3.36}$$

we have

$$\boldsymbol{U} = \boldsymbol{U}_* - 6\pi a\boldsymbol{E}(x)\boldsymbol{U}_* + \frac{a^3}{4}\boldsymbol{F}(x)\boldsymbol{U}_*, \tag{3.37}$$

or more compactly,

$$\boldsymbol{U} = \boldsymbol{E}_S\boldsymbol{U}_*, \quad \text{where} \quad \boldsymbol{E}_S = \boldsymbol{I} - 6\pi a\boldsymbol{E}(x) + \frac{a^3}{4}\boldsymbol{F}(x). \tag{3.38}$$

We note the following asymptotics:

$$\boldsymbol{E}(x) \sim O\left(\frac{1}{r}\right), \quad \boldsymbol{F}(x) \sim O\left(\frac{1}{r^3}\right), \tag{3.39}$$

so that

$$\boldsymbol{U} \sim \boldsymbol{U}_* + O\left(\frac{1}{r}\right), \quad \text{and} \quad \nabla\boldsymbol{U},\ \boldsymbol{A},\ \boldsymbol{W} \sim O\left(\frac{1}{r^2}\right), \quad \text{for } r \gg 1. \tag{3.40}$$

Next, we compute the drag force $\mathcal{F}$ (3.24) on the moving particle. For this purpose, the components of $\boldsymbol{T}(\boldsymbol{u}, p)$ on $\partial\boldsymbol{B}_a$, expressed in spherical coordinates are

$$\begin{aligned}\boldsymbol{T}_{rr} &= -p + 2\frac{\partial u_r}{\partial r} = -p_\infty + \frac{3}{2}\frac{V}{a}\cos\theta,\\ \boldsymbol{T}_{r\theta} &= r\frac{\partial}{\partial r}\left(\frac{u_\theta}{r}\right) + \frac{1}{r}\frac{\partial u_r}{\partial\theta} = -\frac{3}{2}\frac{U}{a}\sin\theta,\\ \boldsymbol{T}_{r\phi} &= 0.\end{aligned} \tag{3.41}$$

With the above, $\mathcal{F}$, in the direction of $\boldsymbol{U}_*$, is given by

$$\mathcal{F} = \int_0^{2\pi}\int_0^{\pi}\left(T_{rr}\cos\theta - \boldsymbol{T}_{r\theta}\sin\theta\right)a^2\sin\theta\,\mathrm{d}\theta\mathrm{d}\phi = 6\pi aV \tag{3.42}$$

https://doi.org/10.1017/jfm.2025.10821 Published online by Cambridge University Press

or in vector form, written as

$$\mathcal{F} = 6\pi a \boldsymbol{U}_*, \tag{3.43}$$

which is the celebrated Stokes Law.

REMARK 4. *The classical isotropic Stokeslet fundamental solution given by*

$$\boldsymbol{v}_s = \boldsymbol{E}\boldsymbol{\alpha}, \quad p_s = \boldsymbol{q}\cdot\boldsymbol{\alpha}, \tag{3.44}$$

for any $\boldsymbol{\alpha}\in\mathbb{R}^3$ corresponds to Stokes flow driven by a point source of strength $\boldsymbol{\alpha}$ located at the origin. Note that the far-field behaviour of the Stokeslet is the same as the leading-order asymptotics of classical Stokes flow in the exterior of a spherical domain. See Chwang & Wu (1975) for an explanation and application of such a notion.

4. Structure of the anisotropic Stokes (2.37)

Here we start our analysis for the stationary system (2.37) with boundary conditions (2.40)–(2.41). The main conclusion of this section is that we can write the (2.37) in the form (4.18) which is that of a second-order, linear system of equations with constant coefficients. All the inhomogeneous terms can be explicitly expressed in terms of the tensor field $\boldsymbol{Q}$ which is given by (3.4)–(3.6). Equation (4.18) is then used to understand the far-field behaviour ($r\gg 1$) of $\boldsymbol{v}$.

To proceed, we first substitute form (3.4) for $\boldsymbol{Q}$ into (2.37) for $\boldsymbol{v}$ and estimate various quantities for $r\gg 1$.

(a) Recall the decay property (3.7) of $\boldsymbol{Q}$: $\boldsymbol{Q}=\boldsymbol{Q}_*+O(1/r)$ and $\nabla\boldsymbol{Q}=O(1/r^2)$. We look for a solution $\boldsymbol{v}$ satisfying $\boldsymbol{v}=\boldsymbol{v}_*+O(1/r)$ and $\nabla\boldsymbol{v}=O(1/r^2)$. Hence, we expect

$$\begin{aligned}
&\boldsymbol{A},\quad \boldsymbol{W}\sim O\left(\frac{1}{r^2}\right),\\
&\boldsymbol{Q}=\boldsymbol{v}\cdot\nabla\boldsymbol{Q}+\boldsymbol{Q}\boldsymbol{W}-\boldsymbol{W}\boldsymbol{Q}\\
&\quad=\underbrace{\boldsymbol{v}_*\cdot\nabla\boldsymbol{Q}+\boldsymbol{Q}_*\boldsymbol{W}-\boldsymbol{W}\boldsymbol{Q}_*}_{O\left(\frac{1}{r^2}\right)}+\underbrace{(\boldsymbol{v}-\boldsymbol{v}_*)\cdot\nabla\boldsymbol{Q}+(\boldsymbol{Q}-\boldsymbol{Q}_*)\boldsymbol{W}-\boldsymbol{W}(\boldsymbol{Q}-\boldsymbol{Q}_*)}_{O\left(\frac{1}{r^3}\right)}\\
&\quad\sim O\left(\frac{1}{r^2}\right).
\end{aligned}\tag{4.1}$$

(b) With the above, the right-hand side of (2.37) becomes

$$\mathcal{D}_\gamma := -\left(\gamma_1\boldsymbol{Q}+\gamma_2\boldsymbol{A}+\frac{\gamma_3}{2}(\boldsymbol{A}\boldsymbol{Q}+\boldsymbol{Q}\boldsymbol{A})+\gamma_9(\boldsymbol{A}\cdot\boldsymbol{Q})\boldsymbol{Q}\right)\cdot\partial_i\boldsymbol{Q}\mathbf{e}_i\sim O\left(\frac{1}{r^4}\right). \tag{4.2}$$

(c) Next, we analyse the terms constituting the viscous stress $\boldsymbol{T}^v_{SV}$ given by (2.38).

(i) The γ_1-term:

$$\begin{aligned}
\left[\boldsymbol{Q}\boldsymbol{Q}-\boldsymbol{Q}\boldsymbol{Q}\right]&=\left[\boldsymbol{Q}\left(\boldsymbol{v}\cdot\nabla\boldsymbol{Q}+\boldsymbol{Q}\boldsymbol{W}-\boldsymbol{W}\boldsymbol{Q}\right)-\left(\boldsymbol{v}\cdot\nabla\boldsymbol{Q}+\boldsymbol{Q}\boldsymbol{W}-\boldsymbol{W}\boldsymbol{Q}\right)\boldsymbol{Q}\right]\\
&=\left[\boldsymbol{Q}\left(\boldsymbol{v}\cdot\nabla\boldsymbol{Q}\right)-\left(\boldsymbol{v}\cdot\nabla\boldsymbol{Q}\right)\boldsymbol{Q}\right]+\left[\boldsymbol{Q}^2\boldsymbol{W}-2\boldsymbol{Q}\boldsymbol{W}\boldsymbol{Q}+\boldsymbol{W}\boldsymbol{Q}^2\right].
\end{aligned}\tag{4.3}$$

https://doi.org/10.1017/jfm.2025.10821 Published online by Cambridge University Press

For the first bracketed term in (4.3), we have the following decomposition:

$$\begin{aligned}\left[\boldsymbol{Q}\left(\boldsymbol{v}\cdot\nabla\boldsymbol{Q}\right)-\left(\boldsymbol{v}\cdot\nabla\boldsymbol{Q}\right)\boldsymbol{Q}\right] &= \left[\boldsymbol{Q}_*(\boldsymbol{v}_*\cdot\nabla\boldsymbol{Q})-(\boldsymbol{v}_*\cdot\nabla\boldsymbol{Q})\boldsymbol{Q}_*\right]\\ &\quad+\left[\boldsymbol{Q}_*(\boldsymbol{v}-\boldsymbol{v}_*)\cdot\nabla\boldsymbol{Q}-(\boldsymbol{v}-\boldsymbol{v}_*)\cdot(\nabla\boldsymbol{Q})\boldsymbol{Q}_*\right]\\ &\quad+\left[(\boldsymbol{Q}-\boldsymbol{Q}_*)\boldsymbol{v}\cdot\nabla\boldsymbol{Q}-(\boldsymbol{v}\cdot\nabla\boldsymbol{Q})(\boldsymbol{Q}-\boldsymbol{Q}_*)\right]\\ &= \left[\boldsymbol{Q}_*(\boldsymbol{v}_*\cdot\nabla\boldsymbol{Q})-(\boldsymbol{v}_*\cdot\nabla\boldsymbol{Q})\boldsymbol{Q}_*\right]+O\left(\frac{1}{r^3}\right)\\ &=: \mathcal{A}_1(x)+O\left(\frac{1}{r^3}\right).\end{aligned} \tag{4.4}$$

For the second bracketed term in (4.3), we have

$$\begin{aligned}\left[\boldsymbol{Q}^2\boldsymbol{W}-2\boldsymbol{Q}\boldsymbol{W}\boldsymbol{Q}+\boldsymbol{W}\boldsymbol{Q}^2\right] &= \left[\boldsymbol{Q}_*^2\boldsymbol{W}-2\boldsymbol{Q}_*\boldsymbol{W}\boldsymbol{Q}_*+\boldsymbol{W}\boldsymbol{Q}_*^2\right]+O\left(\frac{1}{r^3}\right)\\ &=: \mathcal{B}_1[\nabla\boldsymbol{v}]+O\left(\frac{1}{r^3}\right).\end{aligned} \tag{4.5}$$

In the above, $\mathcal{A}_1$ and $\mathcal{B}_1$ are linear in $\boldsymbol{v}_*\cdot\nabla\boldsymbol{Q}$ and $\nabla\boldsymbol{v}$, respectively, both having coefficients depending only on $\boldsymbol{Q}_*$. Furthermore, both $\mathcal{A}_1$ and $\mathcal{B}_1$ decay as r^{-2}. A similar structure exists for all the remaining terms in the stress tensor as it will become clear while we proceed through the rest of this computation.

(ii) The γ_2-term:

$$\begin{aligned}&\left[\boldsymbol{Q}+\boldsymbol{Q}\boldsymbol{A}-\boldsymbol{A}\boldsymbol{Q}\right]\\ &=\left[\boldsymbol{v}\cdot\nabla\boldsymbol{Q}+\boldsymbol{Q}\nabla\boldsymbol{v}-(\nabla\boldsymbol{v})\boldsymbol{Q}\right]\\ &=\left[\boldsymbol{v}_*\cdot\nabla\boldsymbol{Q}+\boldsymbol{Q}_*\nabla\boldsymbol{v}-(\nabla\boldsymbol{v})\boldsymbol{Q}_*\right]+\left[(\boldsymbol{v}-\boldsymbol{v}_*)\cdot\nabla\boldsymbol{Q}+(\boldsymbol{Q}-\boldsymbol{Q}_*)\nabla\boldsymbol{v}-\nabla\boldsymbol{v}(\boldsymbol{Q}-\boldsymbol{Q}_*)\right]\\ &=\mathcal{A}_2(x)+\mathcal{B}_2[\nabla\boldsymbol{v}]+O\left(\frac{1}{r^3}\right),\end{aligned} \tag{4.6}$$

where

$$\mathcal{A}_2(x):=\boldsymbol{v}_*\cdot\nabla\boldsymbol{Q}\quad\text{and}\quad\mathcal{B}_2[\nabla\boldsymbol{v}]:=\boldsymbol{Q}_*\nabla\boldsymbol{v}-(\nabla\boldsymbol{v})\boldsymbol{Q}_*. \tag{4.7}$$

(iii) The γ_3-term:

$$\begin{aligned}&\frac{1}{2}\left(\boldsymbol{Q}\boldsymbol{Q}+\boldsymbol{Q}\boldsymbol{Q}+\boldsymbol{Q}^2\boldsymbol{A}-\boldsymbol{A}\boldsymbol{Q}^2\right)\\ &=\frac{1}{2}\left(\boldsymbol{Q}_*\left(\boldsymbol{v}_*\cdot\nabla\boldsymbol{Q}+\boldsymbol{Q}_*\boldsymbol{W}-\boldsymbol{W}\boldsymbol{Q}_*\right)+\left(\boldsymbol{v}_*\cdot\nabla\boldsymbol{Q}+\boldsymbol{Q}_*\boldsymbol{W}-\boldsymbol{W}\boldsymbol{Q}_*\right)\boldsymbol{Q}_*\right.\\ &\quad\left.+\boldsymbol{Q}_*^2\boldsymbol{A}-\boldsymbol{A}\boldsymbol{Q}_*^2\right)+O\left(\frac{1}{r^3}\right)\\ &=\frac{1}{2}\left(\boldsymbol{Q}_*(\boldsymbol{v}_*\cdot\nabla\boldsymbol{Q})+(\boldsymbol{v}_*\cdot\nabla\boldsymbol{Q})\boldsymbol{Q}_*+\boldsymbol{Q}_*^2(\nabla\boldsymbol{v})-(\nabla\boldsymbol{v})\boldsymbol{Q}_*^2\right)+O\left(\frac{1}{r^3}\right)\\ &=\mathcal{A}_3(x)+\mathcal{B}_3[\nabla\boldsymbol{v}]+O\left(\frac{1}{r^3}\right),\end{aligned} \tag{4.8}$$

https://doi.org/10.1017/jfm.2025.10821 Published online by Cambridge University Press

where

$$\begin{aligned}\mathcal{A}_3(x) &:= \frac{1}{2}\left(\boldsymbol{Q}_*(\boldsymbol{v}_*\cdot\nabla\boldsymbol{Q}) + (\boldsymbol{v}_*\cdot\nabla\boldsymbol{Q})\boldsymbol{Q}_*\right),\\ \mathcal{B}_3[\nabla\boldsymbol{v}] &:= \frac{1}{2}\left(\boldsymbol{Q}_*^2(\nabla\boldsymbol{v}) - (\nabla\boldsymbol{v})\boldsymbol{Q}_*^2\right).\end{aligned} \tag{4.9}$$

(iv) The γ_4-term:

$$\boldsymbol{Q}\boldsymbol{A} + \boldsymbol{A}\boldsymbol{Q} = \boldsymbol{Q}_*\boldsymbol{A} + \boldsymbol{A}\boldsymbol{Q}_* + O\left(\frac{1}{r^3}\right) =: \mathcal{B}_4[\nabla\boldsymbol{v}] + O\left(\frac{1}{r^3}\right). \tag{4.10}$$

(v) The γ_5-term:

$$\boldsymbol{Q}^2\boldsymbol{A} + \boldsymbol{A}\boldsymbol{Q}^2 = \boldsymbol{Q}_*^2\boldsymbol{A} + \boldsymbol{A}\boldsymbol{Q}_*^2 + O\left(\frac{1}{r^3}\right) =: \mathcal{B}_5[\nabla\boldsymbol{v}] + O\left(\frac{1}{r^3}\right). \tag{4.11}$$

(vi) The γ_6-term:

$$(\boldsymbol{A}\cdot\boldsymbol{Q})\boldsymbol{Q} = (\boldsymbol{A}\cdot\boldsymbol{Q}_*)\boldsymbol{Q}_* + O\left(\frac{1}{r^3}\right) =: \mathcal{B}_6[\nabla\boldsymbol{v}] + O\left(\frac{1}{r^3}\right). \tag{4.12}$$

(vii) The γ_7-term:

$$|\boldsymbol{Q}^2|\boldsymbol{A} = |\boldsymbol{Q}_*^2|\boldsymbol{A} + O\left(\frac{1}{r^3}\right) =: \mathcal{B}_7[\nabla\boldsymbol{v}] + O\left(\frac{1}{r^3}\right). \tag{4.13}$$

(viii) The γ_9-term:

$$\begin{aligned}(\boldsymbol{Q}\cdot\boldsymbol{Q})\boldsymbol{Q} &= \Big((\boldsymbol{v}\cdot\nabla\boldsymbol{Q} + \boldsymbol{Q}\boldsymbol{W} - \boldsymbol{W}\boldsymbol{Q})\cdot\boldsymbol{Q}\Big)\boldsymbol{Q} = \Big((\boldsymbol{v}\cdot\nabla\boldsymbol{Q})\cdot\boldsymbol{Q}\Big)\boldsymbol{Q}\\ &= \Big((\boldsymbol{v}_*\cdot\nabla\boldsymbol{Q})\cdot\boldsymbol{Q}_*\Big)\boldsymbol{Q}_* + O\left(\frac{1}{r^3}\right)\\ &= \mathcal{A}_9(x) + O\left(\frac{1}{r^3}\right),\end{aligned} \tag{4.14}$$

where we have used the fact that $(\boldsymbol{Q}\boldsymbol{W} - \boldsymbol{W}\boldsymbol{Q})\cdot\boldsymbol{Q} = 0$ as $(\boldsymbol{C}\boldsymbol{D} - \boldsymbol{D}\boldsymbol{C})\cdot\boldsymbol{C} = 0$ for any $\boldsymbol{C}, \boldsymbol{D} \in M^{3\times 3}$ with $\boldsymbol{C}$ symmetric.

(ix) The γ_{10}-term:

$$\begin{aligned}\left(\boldsymbol{Q}^2\cdot\boldsymbol{A}\right)\boldsymbol{Q} + (\boldsymbol{Q}\cdot\boldsymbol{A})\boldsymbol{Q}^2 &= \left(\boldsymbol{Q}_*^2\cdot\boldsymbol{A}\right)\boldsymbol{Q}_* + (\boldsymbol{Q}_*\cdot\boldsymbol{A})\boldsymbol{Q}_*^2 + O\left(\frac{1}{r^3}\right)\\ &=: \mathcal{B}_{10}[\nabla\boldsymbol{v}] + O\left(\frac{1}{r^3}\right).\end{aligned} \tag{4.15}$$

(x) The γ_{11}-term:

$$|\boldsymbol{Q}|^2(\boldsymbol{A}\cdot\boldsymbol{Q})\boldsymbol{Q} = |\boldsymbol{Q}_*|^2(\boldsymbol{A}\cdot\boldsymbol{Q}_*)\boldsymbol{Q}_* + O\left(\frac{1}{r^3}\right) =: \mathcal{B}_{11}[\nabla\boldsymbol{v}] + O\left(\frac{1}{r^3}\right). \tag{4.16}$$

From the above, we note that

$$\mathcal{A}_4 = \mathcal{A}_5 = \mathcal{A}_6 = \mathcal{A}_7 = \mathcal{A}_{10} = \mathcal{A}_{11} = 0 \text{ and } \mathcal{B}_9 = 0. \tag{4.17}$$

Taking into account the items (a)–(c) above, we can now write (2.37) as

$$-\left(\Delta\boldsymbol{v} + \operatorname{div}\left[\mathcal{B}_\gamma[\nabla\boldsymbol{v}] + \mathcal{A}_\gamma(x) + \mathcal{C}_\gamma(x)\right]\right) + \nabla p = \mathcal{D}_\gamma(x) \tag{4.18}$$

https://doi.org/10.1017/jfm.2025.10821 Published online by Cambridge University Press

where

$$\mathcal{B}_\gamma[\nabla \boldsymbol{v}] = \mathcal{B}_{\gamma,\boldsymbol{Q}_*}[\nabla \boldsymbol{v}] := \sum_{i=1,\neq 8,9}^{11} \gamma_i \mathcal{B}_i[\nabla \boldsymbol{v}], \tag{4.19}$$

$$\mathcal{A}_\gamma(x) = \mathcal{A}_{\gamma,\boldsymbol{Q}_*}[\boldsymbol{v}_* \cdot \nabla \boldsymbol{Q}] := \sum_{i=1,2,3,9} \gamma_i \mathcal{A}_i(x) = O\left(\frac{1}{r^2}\right), \tag{4.20}$$

$$\mathcal{C}_\gamma(x) = \mathcal{C}_\gamma(\boldsymbol{v}, x) := \boldsymbol{T}^{\nu}_{SV} - \boldsymbol{A} - \mathcal{B}_\gamma[\nabla \boldsymbol{v}] - \mathcal{A}_\gamma(x) = O\left(\frac{1}{r^3}\right), \tag{4.21}$$

$$\begin{aligned}\mathcal{D}_\gamma(x) = \mathcal{D}_\gamma(\boldsymbol{v}, x) &:= -\left(\gamma_1 \boldsymbol{Q} + \gamma_2 \boldsymbol{A} + \frac{\gamma_3}{2}(\boldsymbol{A}\boldsymbol{Q} + \boldsymbol{Q}\boldsymbol{A}) + \gamma_9 (\boldsymbol{A} \cdot \boldsymbol{Q})\boldsymbol{Q}\right) \cdot \partial_i \boldsymbol{Q} \mathbf{e}_i \\ &= O\left(\frac{1}{r^4}\right).\end{aligned} \tag{4.22}$$

In the above and what follows, we will use the symbol γ to denote an expression or quantity that genuinely depends on $\gamma_1, \ldots, \gamma_{11}$. Furthermore, we set

$$|\gamma| := \max\{|\gamma_1|, \ldots, |\gamma_{11}|\}. \tag{4.23}$$

We might omit γ if the dependence is clear from the context.

The advantage of representation (4.18)–(4.22) is highlighted as follows.

(*a*) The linear operator $\mathcal{B}_\gamma[\cdot]$ in $\nabla \boldsymbol{v}$ corresponds to the leading-order far-field contribution to the diffusivity matrix originating from the stress tensor. In particular, $\operatorname{div}[\mathcal{B}_\gamma[\nabla v]]$ is linear in $D^2 \boldsymbol{v}$ with constant coefficients depending only on $\boldsymbol{Q}_*$. More explicitly, (4.19) can be written as

$$\operatorname{div}\left[\mathcal{B}_\gamma[\nabla \boldsymbol{v}]\right] = \mathcal{M}_\gamma : D^2 \boldsymbol{v} \tag{4.24}$$

for some constant fourth-order tensor $\mathcal{M}_\gamma$. Upon introducing the coordinates $\mathcal{M}_\gamma = (\mathcal{M}_{i,j;k,l})$, the right-hand side of the above is understood as

$$\left(\mathcal{M}_\gamma : D^2 \boldsymbol{v}\right)_i = \mathcal{M}_{i,j;k,l} \partial_{kl} \boldsymbol{v}_j, \quad \text{for } i = 1, 2, 3. \tag{4.25}$$

(*b*) The term $\operatorname{div}[\mathcal{A}_\gamma(x)]$ decays as r^{-3} for $r \gg 1$. It can be treated as a purely inhomogeneous forcing term involving $D^2 \boldsymbol{Q}$, $\boldsymbol{v}_*$ and $\boldsymbol{Q}_*$. Note that it is linear in the expression $\boldsymbol{v}_* \cdot \nabla \boldsymbol{Q}$ so it vanishes if $\boldsymbol{v}_* = 0$.

(*c*) The terms $\operatorname{div}[\mathcal{C}_\gamma(x)]$ and $\mathcal{D}_\gamma(x)$ decay as r^{-4} for $r \gg 1$ and hence they are integrable in the exterior domain Ω,

$$\int_\Omega \left|\operatorname{div}[\mathcal{C}_\gamma(x)]\right| \mathrm{d}x, \quad \int_\Omega \left|\mathcal{D}_\gamma(x)\right| \mathrm{d}x < \infty. \tag{4.26}$$

The explicit calculation of $\operatorname{div}[\mathcal{A}_\gamma(x)]$, $\operatorname{div}[\mathcal{B}_\gamma[\nabla \boldsymbol{v}]]$, $\operatorname{div}[\mathcal{C}_\gamma(x)]$ and $\mathcal{D}_\gamma(x)$ will be presented in Appendix B. We point out that the presence of $\mathcal{A}_\gamma$ and $\mathcal{D}_\gamma$ is due to the dependence of the interacting potential function R on $\boldsymbol{Q}$ so that only γ_1, γ_2, γ_3 and γ_9 appear in the expressions for $\mathcal{A}_\gamma$ and $\mathcal{D}_\gamma$. (See the form (2.12) of R.)

For the purpose of analysing (4.18), we will keep $\operatorname{div}[\mathcal{B}_\gamma[\nabla \boldsymbol{v}]]$ in the left-hand side but move $\mathcal{A}_\gamma, \mathcal{C}_\gamma, \mathcal{D}_\gamma$ to the right of that equation which now becomes

$$-\Delta \boldsymbol{v} - \operatorname{div}\left[\mathcal{B}_\gamma[\nabla \boldsymbol{v}]\right] + \nabla p = \operatorname{div}\left[\mathcal{A}_\gamma(x)\right] + \operatorname{div}\left[\mathcal{C}_\gamma(x)\right] + \mathcal{D}_\gamma(x). \tag{4.27}$$

https://doi.org/10.1017/jfm.2025.10821 Published online by Cambridge University Press

Note that $-\Delta \boldsymbol{v} - \operatorname{div}[\mathcal{B}_\gamma[\nabla \boldsymbol{v}]]$ is a second-order differential operator in $\boldsymbol{v}$ with constant coefficients. Its Green's function can be computed using Fourier transform and enjoys similar properties as the Newtonian potential. This is performed in the Supplementary materials § D.

Combining the above with the explicit expression (3.4) of $\boldsymbol{Q}$, the terms on the right-hand side of (4.27) take the following forms:

$$\operatorname{div} \mathcal{A}_\gamma(x) = \gamma \frac{\boldsymbol{F}(\hat{x})}{r^3} + O\left(\frac{1}{r^4}\right), \tag{4.28}$$

$$\operatorname{div} \mathcal{C}_\gamma(x) + \mathcal{D}_\gamma(x) = \gamma \left(\frac{\boldsymbol{G}(\hat{x})}{r^4} + \frac{\boldsymbol{H}(\hat{x}) : (\boldsymbol{v} - \boldsymbol{v}_*)}{r^3} + \frac{\boldsymbol{I}(\hat{x}) : D\boldsymbol{v}}{r^2} + \frac{\boldsymbol{J}(\hat{x}) : D^2\boldsymbol{v}}{r} \right) + O\left(\frac{1}{r^5}\right) \tag{4.29}$$

where $\boldsymbol{F}$, $\boldsymbol{G}$, $\boldsymbol{H}$, $\boldsymbol{I}$, $\boldsymbol{J}$ are some bounded vector or tensor fields defined on the unit sphere $\mathbb{S}^2$ depending only on $\boldsymbol{Q}$ and $\boldsymbol{Q}_*$ but not on $\boldsymbol{v}$ and $\boldsymbol{v}_*$. We again recall the convention about the symbol ':' stated in item (g) at the end of the Introduction. The precise forms of the contractions between tensors are not too important for our analysis. The key is the homogeneity in r leading to appropriate spatial decay. The presence of γ on the right-hand side refers to the fact that the terms are multiplied by γ_i. In particular, $\mathcal{A}_\gamma$, $\mathcal{B}_\gamma$, $\mathcal{C}_\gamma$, $\mathcal{D}_\gamma$ are all bounded in magnitude by $O(|\gamma|)$. Hence, if $|\gamma| = 0$, then (4.27) simply becomes the classical isotropic Stokes (3.25).

Relating back to § 2.4, Remark 2, note that the system (2.37) with boundary conditions (2.40)–(2.41) is solvable for any $\boldsymbol{v}_b$ and $\boldsymbol{v}_*$. From the form of $\mathcal{A}_\gamma$ written in (4.28), it seems the system becomes simpler by setting $\boldsymbol{v}_* = 0$. This can be achieved by a change of frame or simply consider the new vector field $\boldsymbol{v}' = \boldsymbol{v} - \boldsymbol{v}_*$. However, due to the presence of the convective derivative $\boldsymbol{v} \cdot \nabla \boldsymbol{Q}$ of $\boldsymbol{Q}$, either of these procedures will necessarily give rise to the term $\boldsymbol{v}_* \nabla \boldsymbol{Q}$ which at leading order is embedded in $\mathcal{A}_\gamma$.

5. Properties of the anisotropic Stokes flow (2.37)

Collecting the expressions from (4.28) and (4.29), we rewrite (4.27) as

$$\mathcal{L}_\gamma \boldsymbol{v} + \nabla p = \boldsymbol{f}_\gamma(\boldsymbol{v}), \quad \text{for } |x| > a, \tag{5.1}$$

$$\operatorname{div} \boldsymbol{v} = 0, \quad \text{for } |x| > a, \tag{5.2}$$

$$\boldsymbol{v} = \boldsymbol{v}_b \ (= 0), \quad \text{on } \partial \boldsymbol{B}_a, \tag{5.3}$$

$$\boldsymbol{v} = \boldsymbol{v}_*, \quad \text{at } |x| = \infty; \tag{5.4}$$

where

$$\mathcal{L}_\gamma \boldsymbol{v} := -\left(\Delta \boldsymbol{v} + \mathcal{M}_\gamma : D^2 \boldsymbol{v}\right), \tag{5.5}$$

$$\begin{aligned} \boldsymbol{f}_\gamma(\boldsymbol{v}) &:= \operatorname{div} \mathcal{A}_\gamma(x) + \operatorname{div} \mathcal{C}_\gamma(x) + \mathcal{D}_\gamma(x), \\ &= \gamma \left(\frac{\boldsymbol{F}(\hat{x})}{r^3} + \frac{\boldsymbol{G}(\hat{x})}{r^4} + \frac{\boldsymbol{H}(\hat{x}) : (\boldsymbol{v} - \boldsymbol{v}_*)}{r^3} + \frac{\boldsymbol{I}(\hat{x}) : D\boldsymbol{v}}{r^2} + \frac{\boldsymbol{J}(\hat{x}) : D^2\boldsymbol{v}}{r} \right) \\ &\quad + O\left(\frac{1}{r^5}\right). \end{aligned} \tag{5.6}$$

https://doi.org/10.1017/jfm.2025.10821 Published online by Cambridge University Press

Note that given $\boldsymbol{Q}$, the dependence of $\boldsymbol{f}_\gamma$ in its argument is in fact linear so that

$$\boldsymbol{f}_\gamma(\boldsymbol{u}_1) - \boldsymbol{f}_\gamma(\boldsymbol{u}_2) = \boldsymbol{f}_\gamma(\boldsymbol{u}_1 - \boldsymbol{u}_2) \tag{5.7}$$

making the above a linear system which we designate as our anisotropic Stokes system.

We remark again that the above system describes the flow in the moving frame attached to the particle. The far-field velocity $\boldsymbol{v}_*$ is prescribed. For passive particle which is the case in this paper, we take $\boldsymbol{v}_b = 0$ while for active particle, it is in general some prescribed, non-constant function. Note also that if $\boldsymbol{v}_b = 0$ and $\boldsymbol{v}_* = 0$, then we have only the trivial solution $\boldsymbol{v} = 0$.

Upon introducing

$$\boldsymbol{T}_\gamma(\boldsymbol{w}, \pi) = \nabla \boldsymbol{w} + (\nabla \boldsymbol{w})^T + \mathcal{B}_\gamma(\nabla \boldsymbol{v}) - \pi \boldsymbol{I}, \tag{5.8}$$

we can also write (5.1) as

$$-\operatorname{div} \boldsymbol{T}_\gamma(\boldsymbol{v}, p) = \boldsymbol{f}_\gamma(\boldsymbol{v}). \tag{5.9}$$

Similar to classical Stokes solution (3.40), we look for a solution $\boldsymbol{v}$ for (5.1) with spatial decay $\boldsymbol{v} - \boldsymbol{v}_* \approx (1/r)$. The existence of such a $\boldsymbol{v}$ will be provided in the Supplementary materials. Here we will concentrate on its representation formula and its usage in analysing properties of the solution.

As $\mathcal{L}_\gamma$ is a second-order differential operator, we infer that there are functions $\boldsymbol{G}_\gamma$ and $\boldsymbol{h}_\gamma$ with homogeneous degrees -1 and -2,

$$\boldsymbol{G}_\gamma(x) = \frac{\boldsymbol{G}_\gamma(\hat{x})}{|x|} \quad \text{and} \quad \boldsymbol{h}_\gamma(x) = \frac{\boldsymbol{h}_\gamma(\hat{x})}{|x|^2} \tag{5.10}$$

such that $\boldsymbol{v}$ can be represented as

$$\begin{aligned}\boldsymbol{v}(x) = &\int_\Omega \boldsymbol{G}_\gamma(x-y)\boldsymbol{f}_\gamma(\boldsymbol{v}(y))\,\mathrm{d}y + \int_{\partial\Omega} \left\langle \boldsymbol{G}_\gamma(x-y), \boldsymbol{T}_\gamma(\boldsymbol{v}, p)(y)\nu_y \right\rangle \mathrm{d}\sigma_y \\ &- \int_{\partial\Omega} \left\langle \boldsymbol{T}_\gamma(\boldsymbol{G}_\gamma, \boldsymbol{h}_\gamma)(x-y)\nu_y, \boldsymbol{v}(y) \right\rangle \mathrm{d}\sigma_y + \boldsymbol{v}_*. \end{aligned} \tag{5.11}$$

The functions $\boldsymbol{G}_\gamma$ and $\boldsymbol{h}_\gamma$ will be constructed using Fourier transform in the Supplementary materials. The above integral representation of $\boldsymbol{v}$ will be used to analyse its far-field decay property and deviation from the classical Stokes flow.

First, similar to (3.19)–(3.22), for the boundary integrals in (5.11), we have

$$\begin{aligned}&\left| \int_{\partial\Omega} \left\langle \boldsymbol{G}_\gamma(x-y), \boldsymbol{T}_\gamma(\boldsymbol{v}, p)(y)\nu_y \right\rangle \mathrm{d}\sigma_y \right| \lesssim \frac{1}{r}, \quad \text{and} \\ &\left| \int_{\partial\Omega} \left\langle \boldsymbol{T}_\gamma(\boldsymbol{G}_\gamma, \boldsymbol{h}_\gamma)(x-y)\nu_y, \boldsymbol{v}(y) \right\rangle \mathrm{d}\sigma_y \right| \lesssim \frac{1}{r^2}. \end{aligned} \tag{5.12}$$

In order to have $\boldsymbol{v} - \boldsymbol{v}_* \approx r^{-1}$, we need that the bulk term satisfies the following estimate:

$$\int_\Omega \boldsymbol{G}_\gamma(x-y)\boldsymbol{f}_\gamma(\boldsymbol{v}(y))\,\mathrm{d}y \lesssim \frac{1}{r}. \tag{5.13}$$

This crucially depends on the decay property of $\boldsymbol{f}_\gamma(\boldsymbol{v})$. Note that by (5.6), the dominant term of $\boldsymbol{f}_\gamma$ is given by

$$\operatorname{div} \mathcal{A}_\gamma(x) = \gamma \left(\frac{\boldsymbol{F}(\hat{x})}{r^3} \right) \approx \frac{1}{r^3}. \tag{5.14}$$

https://doi.org/10.1017/jfm.2025.10821 Published online by Cambridge University Press

According to (A21), the validity of (5.13) requires $\boldsymbol{F}$ to satisfy the mean zero condition:

$$\int_{\mathbb{S}^2} \boldsymbol{F}(\hat{x})\,\mathrm{d}\sigma = 0. \tag{5.15}$$

That it is true will be shown in Appendix A.4.

Second, we investigate the precisely far-field behaviour of $\boldsymbol{v}$, in particular, its deviation from the classical Stokes solution. For this purpose, we rearrange (5.11) in the following form:

$$\boldsymbol{v} - \boldsymbol{v}_* = \left\langle \boldsymbol{G}_\gamma(x), \int_{\partial\Omega} \boldsymbol{T}_\gamma(\boldsymbol{v}, p)(y)\nu_y\,\mathrm{d}\sigma_y \right\rangle \tag{5.16}$$

$$+ \int_\Omega \boldsymbol{G}_\gamma(x-y)\mathrm{div}\,\mathcal{A}_\gamma(y)\,\mathrm{d}y + \boldsymbol{G}_\gamma(x)\left(\int_\Omega \big(\mathrm{div}\,\mathcal{C}_\gamma(\boldsymbol{v}) + \mathcal{D}_\gamma(\boldsymbol{v})\big)(y)\,\mathrm{d}y\right) \tag{5.17}$$

$$+ \int_{\partial\Omega} \big\langle \boldsymbol{G}_\gamma(x-y) - \boldsymbol{G}_\gamma(x),\, \boldsymbol{T}_\gamma(\boldsymbol{v}, p)(y)\nu_y \big\rangle\,\mathrm{d}\sigma_y \tag{5.18}$$

$$- \int_{\partial\Omega} \big\langle \boldsymbol{T}_\gamma(\boldsymbol{G}_\gamma, \boldsymbol{h}_\gamma)(x-y)\nu_y,\, \boldsymbol{v}(y) \big\rangle\,\mathrm{d}\sigma_y \tag{5.19}$$

$$+ \int_\Omega (\boldsymbol{G}_\gamma(x-y) - \boldsymbol{G}_\gamma(x))\big(\mathrm{div}\,\mathcal{C}_\gamma(\boldsymbol{v}) + \mathcal{D}_\gamma(\boldsymbol{v})\big)(y)\,\mathrm{d}y. \tag{5.20}$$

Note that for $|x| \gg 1$, we have

$$\begin{aligned}
(5.17) &= \frac{O(1)}{|x|},\\
(5.18) &= \frac{O(\gamma)}{|x|},\\
(5.1) \text{ and } (5.20) &= \frac{O(1)}{|x|^2},\\
(5.21) &= \frac{O(\gamma)\log|x|}{|x|^2} \quad \text{(by (A5))}.
\end{aligned} \tag{5.21}$$

Hence, up to $O(\gamma)$, (5.16) and (5.17) are the dominant terms in the expression for the anisotropic flow.

We next describe asymptotically (5.16) and (5.17) for $\gamma \ll 1$.

5.1. *Precise asymptotics: deviation from isotropic Stokes flow*

The purpose of this section is to reveal more clearly the difference between $\boldsymbol{v}$ and the classical Stokes flow $\boldsymbol{v}_0$ which is set to satisfy

$$\begin{aligned}
-\Delta\boldsymbol{v}_0 + \nabla p_0 &= 0, \quad \text{for } |x| > a,\\
\mathrm{div}\,(\boldsymbol{v}_0) &= 0, \quad \text{for } |x| > a,\\
\boldsymbol{v}_0 &= 0, \quad \text{on } |x| = a,\\
\boldsymbol{v}_0 &= \boldsymbol{v}_*, \quad \text{at } |x| = \infty.
\end{aligned} \tag{5.22}$$

https://doi.org/10.1017/jfm.2025.10821 Published online by Cambridge University Press

Define $\varphi_\gamma := \boldsymbol{v} - \boldsymbol{v}_0$. Then we have

$$\begin{aligned}-\Delta\varphi_\gamma + \nabla(p - p_0) &= -\mathcal{M}_\gamma : D^2\boldsymbol{v} + \boldsymbol{f}_\gamma(\boldsymbol{v}) \\ &= -\mathcal{M}_\gamma : D^2\boldsymbol{v}_0 + \boldsymbol{f}_\gamma(\boldsymbol{v}_0) \\ &\quad + \Big(\boldsymbol{f}_\gamma(\boldsymbol{v}) - \boldsymbol{f}_\gamma(\boldsymbol{v}_0) - \mathcal{M}_\gamma : \big(D^2\boldsymbol{v} - D^2\boldsymbol{v}_0\big)\Big). \end{aligned} \tag{5.23}$$

Note that $|\mathcal{M}_\gamma|$, $|\boldsymbol{f}_\gamma(\boldsymbol{v}_0)| \lesssim |\gamma|$ and $|\boldsymbol{f}_\gamma(\boldsymbol{v}) - \boldsymbol{f}_\gamma(\boldsymbol{v}_0)| = |\boldsymbol{f}_\gamma(\boldsymbol{v} - \boldsymbol{v}_0)| \lesssim |\gamma|\|\boldsymbol{v} - \boldsymbol{v}_0\|_{\mathcal{S}}$. Now let $\overline{\varphi}_\gamma$ solve

$$-\Delta\overline{\varphi}_\gamma + \nabla(\overline{p}_\gamma) = -\mathcal{M}_\gamma : D^2\boldsymbol{v}_0 + \boldsymbol{f}_\gamma(\boldsymbol{v}_0), \tag{5.24}$$

$$\operatorname{div}(\overline{\varphi}_\gamma) = 0, \quad \text{for } |x| > a, \tag{5.25}$$

$$\overline{\varphi}_\gamma = 0, \quad \text{on } |x| = 0 \text{ and at } |x| = \infty. \tag{5.26}$$

Then the same approach in deriving estimates for $\boldsymbol{v}$ gives

$$\|\overline{\varphi}_\gamma\|_{\mathcal{S}} \lesssim O(\gamma), \quad \text{and} \quad \|\overline{\varphi}_\gamma - \varphi_\gamma\|_{\mathcal{S}} \lesssim O\big(\gamma^2\big). \tag{5.27}$$

Hence, we have

$$\boldsymbol{v} = \boldsymbol{v}_0 + \overline{\varphi}_\gamma + O\big(\gamma^2\big). \tag{5.28}$$

Finally, using Green's function $\boldsymbol{E}$ (3.9) for the classical Stokes flow, we have the following representation of $\overline{\varphi}_\gamma$:

$$\begin{aligned}\overline{\varphi}_\gamma(x) &= \int_\Omega \boldsymbol{E}(x - y)\big(-\mathcal{M}_\gamma : D^2\boldsymbol{v}_0 + \boldsymbol{f}_\gamma(\boldsymbol{v}_0(y))\big)\,\mathrm{d}y \\ &\quad + \int_{\partial\Omega} \big\langle \boldsymbol{E}(x - y),\, \boldsymbol{T}(\overline{\varphi}_\gamma, \overline{p}_\gamma)(y)\nu_y \big\rangle\,\mathrm{d}\sigma_y \\ &= \int_\Omega \boldsymbol{E}(x - y)\big(-\mathcal{M}_\gamma : D^2\boldsymbol{v}_0 + \boldsymbol{f}_\gamma(\boldsymbol{v}_0(y))\big)\,\mathrm{d}y + \boldsymbol{E}(x)\int_{\partial\Omega} \boldsymbol{T}(\overline{\varphi}_\gamma, \overline{p}_\gamma)(y)\nu_y\,\mathrm{d}\sigma_y \\ &\quad + \int_{\partial\Omega} \big\langle \boldsymbol{E}(x - y) - \boldsymbol{E}(x),\, \boldsymbol{T}(\overline{\varphi}_\gamma, \overline{p}_\gamma)(y)\nu_y \big\rangle\,\mathrm{d}\sigma_y, \end{aligned} \tag{5.29}$$

where $\boldsymbol{T}$ is the Stokes stress tensor (3.17). Note that the last term in the above decays as $\frac{1}{|x|^2}$. Hence, we have

$$\overline{\varphi}_\gamma(x) = \mathcal{I}_\gamma(x) + \boldsymbol{E}(x)\mathcal{J}_\gamma + O\left(\frac{1}{|x|^2}\right), \tag{5.30}$$

$$\text{where} \quad \mathcal{I}_\gamma(x) := \int_\Omega \boldsymbol{E}(x - y)\big(-\mathcal{M}_\gamma : D^2\boldsymbol{v}_0 + \boldsymbol{f}_\gamma(\boldsymbol{v}_0(y))\big)\,\mathrm{d}y, \tag{5.31}$$

$$\mathcal{J}_\gamma := \int_{\partial\Omega} \boldsymbol{T}(\overline{\varphi}_\gamma, \overline{p}_\gamma)(y)\nu_y \mathrm{d}\sigma_y. \tag{5.32}$$

The rest of this section will describe more explicitly the bulk and boundary integrals $\mathcal{I}_\gamma$ and $\mathcal{J}_\gamma$.

https://doi.org/10.1017/jfm.2025.10821 Published online by Cambridge University Press

5.1.1. *Estimating* $\mathcal{I}_\gamma$

Recalling from (3.38) that $\boldsymbol{v}_0 = \boldsymbol{E}_S \boldsymbol{v}_*$, we have

$$\begin{aligned}
\mathcal{I}_\gamma(x) &= \int_\Omega \boldsymbol{E}(x-y)\big[-\mathcal{M}_\gamma : D^2\boldsymbol{v}_0 + \boldsymbol{f}_\gamma(\boldsymbol{v}_0(y))\big]\,\mathrm{d}y \\
&= \int_\Omega \boldsymbol{E}(x-y)\Big[6\pi a\mathcal{M}_\gamma : D^2\boldsymbol{E}(y)\boldsymbol{v}_* - \frac{a^3}{4}\mathcal{M}_\gamma : D^2\boldsymbol{F}(y)\boldsymbol{v}_* \\
&\qquad + \operatorname{div}\mathcal{A}_\gamma(y) + \operatorname{div}\mathcal{C}_\gamma(y) + \mathcal{D}_\gamma(y)\Big]\,\mathrm{d}y \\
&= \int_\Omega \boldsymbol{E}(x-y)\big[6\pi a\mathcal{M}_\gamma : D^2\boldsymbol{E}(y)\boldsymbol{v}_* + \operatorname{div}\mathcal{A}_\gamma(y)\big]\,\mathrm{d}y \qquad (5.33) \\
&\quad + \boldsymbol{E}(x)\int_\Omega \left[-\frac{a^3}{4}\mathcal{M}_\gamma : D^2\boldsymbol{F}(y)\boldsymbol{v}_* + \operatorname{div}\mathcal{C}_\gamma(y) + \mathcal{D}_\gamma(y)\right]\,\mathrm{d}y \\
&\quad + \int_\Omega (\boldsymbol{E}(x-y) - \boldsymbol{E}(x))\left[-\frac{a^3}{4}\mathcal{M}_\gamma : D^2\boldsymbol{F}(y)\boldsymbol{v}_* + \operatorname{div}\mathcal{C}_\gamma(y) + \mathcal{D}_\gamma(y)\right]\,\mathrm{d}y \\
&=: I_1 + I_2 + I_3. \qquad (5.34)
\end{aligned}$$

Note that I_2 decays as $\boldsymbol{E}(x) \sim (1/|x|)$ because the integrand $\sim (1/|x|^4)$ is integrable. By (A5), the integral I_3 decays as $(\log|x|/|x|^2)$.

For I_1, we show in Appendix A.4 that $D^2\boldsymbol{E}(x) \approx (1/r^3)$ satisfies the mean zero condition,

$$\int_{\mathbb{S}^2} D^2\boldsymbol{E}(\hat{x})\,\mathrm{d}\sigma = 0. \qquad (5.35)$$

By (A21), we can then infer that $I_1(x)$ decays as $\frac{1}{|x|}$. (Recall that such a condition is also verified for $\operatorname{div}\mathcal{A}_\gamma$ in Appendix A.4.)

With the above, we can conclude that

$$\begin{aligned}
\mathcal{I}_\gamma(x) &= \frac{1}{|x|}\int_{\mathbb{S}^2} \boldsymbol{H}(\hat{x},\omega)\big[6\pi a\mathcal{M}_\gamma : D^2\boldsymbol{E}(\omega)\boldsymbol{v}_* + \operatorname{div}\mathcal{A}_\gamma(\omega)\big]\,\mathrm{d}\sigma_\omega \qquad (5.36) \\
&\quad + \boldsymbol{E}(x)\int_\Omega \left[-\frac{a^3}{4}\mathcal{M}_\gamma : D^2\boldsymbol{F}(y)\boldsymbol{v}_* + \operatorname{div}\mathcal{C}_\gamma(y) + \mathcal{D}_\gamma(y)\right]\,\mathrm{d}y \\
&\quad + O\left(\frac{\log|x|}{|x|^2}\right). \qquad (5.37)
\end{aligned}$$

In § 5.2, we will demonstrate that all the terms in the above expression either have symbolic representations or are amenable to numerical computation.

5.1.2. *Estimating* $\mathcal{J}_\gamma$

To obtain an explicit formula for the boundary integral $\mathcal{J}_\gamma$ associated with $\overline{\varphi}_\gamma$, we multiply (5.24) by a test function given by $\tilde{\boldsymbol{v}}_0 - \tilde{\boldsymbol{v}}_*$ where $\tilde{\boldsymbol{v}}_0$ solves the following equation:

$$\begin{aligned}
-\Delta\tilde{\boldsymbol{v}}_0 + \nabla\tilde{p}_0 &= 0, \quad \text{for } |x| > a, \\
\operatorname{div}(\tilde{\boldsymbol{v}}_0) &= 0, \quad \text{for } |x| > a, \\
\tilde{\boldsymbol{v}}_0 &= 0, \quad \text{on } |x| = a, \\
\tilde{\boldsymbol{v}}_0 &= \tilde{\boldsymbol{v}}_*, \quad \text{at } |x| = \infty, \qquad (5.38)
\end{aligned}$$

https://doi.org/10.1017/jfm.2025.10821 Published online by Cambridge University Press

with an arbitrary $\tilde{\boldsymbol{v}}_*$. Using integration by parts (see Ladyzhenskaya (1969, p.53 (10), (11)), we obtain

$$-\int_{\partial\Omega}\left\langle \boldsymbol{T}(\overline{\varphi}_\gamma,\overline{p}_\gamma)\nu_y,\left(\tilde{\boldsymbol{v}}_0-\tilde{\boldsymbol{v}}_*\right)\right\rangle \mathrm{d}\sigma_y+\int_{\partial\Omega}\left\langle \boldsymbol{T}(\tilde{\boldsymbol{v}}_0,\tilde{p}_0)\nu_y,\overline{\varphi}_\gamma\right\rangle \mathrm{d}\sigma_y$$
$$=\int_\Omega\left\langle -\mathcal{M}_\gamma:D^2\boldsymbol{v}_0+\boldsymbol{f}_\gamma(\boldsymbol{v}_0(y)),\tilde{\boldsymbol{v}}_0-\tilde{\boldsymbol{v}}_*\right\rangle \mathrm{d}y. \tag{5.39}$$

The above is justified by the decay estimates for $\overline{\varphi}_\gamma$ and $\tilde{\boldsymbol{v}}_0-\tilde{\boldsymbol{v}}_*$,

$$\left|\int_{\{|x|=R\}}\left\langle \boldsymbol{T}(\overline{\varphi}_\gamma,\overline{p}_\gamma)\nu_y,\left(\tilde{\boldsymbol{v}}_0-\tilde{\boldsymbol{v}}_*\right)\right\rangle \mathrm{d}\sigma_y\right|\lesssim\frac{1}{R^2}\frac{1}{R}R^2=\frac{1}{R}$$
$$\left|\int_{\{|x|=R\}}\left\langle \boldsymbol{T}(\tilde{\boldsymbol{v}}_0,\tilde{p}_0)\nu_y,\overline{\varphi}_\gamma\right\rangle \mathrm{d}\sigma_y\right|\lesssim\frac{1}{R^2}\frac{1}{R}R^2=\frac{1}{R}$$
$$\int_{\{|x|>R\}}\left|-\mathcal{M}_\gamma:D^2\boldsymbol{v}_0+\boldsymbol{f}(\boldsymbol{v}_0(y))\right|\left|\tilde{\boldsymbol{v}}_0-\boldsymbol{v}_*\right|\mathrm{d}y\lesssim\int_R^\infty\frac{1}{r^3}\frac{1}{r}r^2\,\mathrm{d}r\lesssim\frac{1}{R} \tag{5.40}$$

which all vanish as $R\longrightarrow 0$. Hence, we have

$$\int_{\partial\Omega}\left\langle \boldsymbol{T}(\overline{\varphi}_\gamma,\overline{p}_\gamma)\nu_y,\left(\tilde{\boldsymbol{v}}_0-\tilde{\boldsymbol{v}}_*\right)\right\rangle \mathrm{d}\sigma_y$$
$$=\int_{\partial\Omega}\left\langle \boldsymbol{T}(\tilde{\boldsymbol{v}}_0,\tilde{p}_0)\nu_y,\overline{\varphi}_\gamma\right\rangle \mathrm{d}\sigma_y-\int_\Omega\left\langle -\mathcal{M}_\gamma:D^2\boldsymbol{v}_0+\boldsymbol{f}(\boldsymbol{v}_0(y)),\tilde{\boldsymbol{v}}_0-\tilde{\boldsymbol{v}}_*\right\rangle \mathrm{d}y. \tag{5.41}$$

As $\tilde{\boldsymbol{v}}_0=\overline{\varphi}_\gamma=0$ on $\partial\Omega$, the following holds for any $\tilde{\boldsymbol{v}}_*$:

$$\int_{\partial\Omega}\left\langle \boldsymbol{T}(\overline{\varphi}_\gamma,\overline{p}_\gamma)\nu_y,\tilde{\boldsymbol{v}}_*\right\rangle \mathrm{d}\sigma_y=\int_\Omega\left\langle -\mathcal{M}_\gamma:D^2\boldsymbol{v}_0+\boldsymbol{f}_\gamma(\boldsymbol{v}_0(y)),\tilde{\boldsymbol{v}}_0-\tilde{\boldsymbol{v}}_*\right\rangle \mathrm{d}y$$
$$=\int_\Omega\left\langle -\mathcal{M}_\gamma:D^2\boldsymbol{E}_S(y)\boldsymbol{v}_*+\boldsymbol{f}_\gamma(\boldsymbol{E}_S(y)\boldsymbol{v}_*),(\boldsymbol{E}_S-\boldsymbol{I})\tilde{\boldsymbol{v}}_*\right\rangle \mathrm{d}y. \tag{5.42}$$

To conclude, we have

$$\begin{aligned}\mathcal{J}_\gamma&=\int_{\partial\Omega}\boldsymbol{T}(\overline{\varphi}_\gamma,\overline{p}_\gamma)\nu_y\,\mathrm{d}\sigma_y\\&=\int_\Omega(\boldsymbol{E}_S-\boldsymbol{I})\left[-\mathcal{M}_\gamma:D^2\boldsymbol{E}_S(y)\boldsymbol{v}_*+\boldsymbol{f}_\gamma\left(\boldsymbol{E}_S(y)\boldsymbol{v}_*\right)\right]\mathrm{d}y\\&=\int_\Omega(\boldsymbol{E}_S-\boldsymbol{I})\left[-\mathcal{M}_\gamma:D^2\boldsymbol{E}_S(y)\boldsymbol{v}_*\right.\\&\quad\left.+\operatorname{div}\mathcal{A}_\gamma(y)+\operatorname{div}\mathcal{C}_\gamma\left(\boldsymbol{E}_S(y)\boldsymbol{v}_*,y\right)+\mathcal{D}_\gamma\left(\boldsymbol{E}_S(y)\boldsymbol{v}_*,y\right)\right]\mathrm{d}y.\end{aligned} \tag{5.43}$$

Again, similar to $\mathcal{I}_\gamma$, as demonstrated in the next section, all the terms in the above either have symbolic representations or are amenable to numerical computation.

5.2. *Analytical expressions*

In this section, we calculate explicitly (5.36), (5.37) and (5.43). In principle, we can handle all the terms as they only involve homogeneous functions of negative integral degrees.

https://doi.org/10.1017/jfm.2025.10821 Published online by Cambridge University Press

More precisely, we have

$$\begin{aligned}
\boldsymbol{E}(x)\ (3.9): &\quad \frac{\delta_{ij}}{r},\ \frac{x_i x_j}{r^3},\\
\boldsymbol{F}(x)\ (3.36): &\quad \frac{\delta_{ij}}{r^3},\ \frac{x_i x_j}{r^5}\\
\boldsymbol{Q}\ (3.4): &\quad \frac{\delta_{ij}}{r},\ \frac{\delta_{ij}}{r^3},\ \frac{x_i x_j}{r^5}
\end{aligned} \tag{5.44}$$

and $\boldsymbol{v} = \boldsymbol{E}_S \boldsymbol{v}_*$ with $\boldsymbol{E}_S = \boldsymbol{I} - 6\pi a \boldsymbol{E}(x) + (a^3/4)\boldsymbol{F}(x)$ (3.38). Furthermore, the terms $\mathcal{C}_\gamma$ and $\mathcal{D}_\gamma$ involve multiplications between the following matrices:

$$\boldsymbol{A},\ \boldsymbol{W},\ \boldsymbol{Q}_*,\ \boldsymbol{Q},\ \ \boldsymbol{v}_* \cdot \nabla \boldsymbol{Q},\ \ \boldsymbol{v} \cdot \nabla \boldsymbol{Q}. \tag{5.45}$$

For convenience, we introduce the following conventions:

$$[A, B, C, \ldots] = \text{arbitrary linear combinations and products between } A, B, C, \text{ and their powers;} \tag{5.46}$$

$$\{A, B, C, \ldots\} = \text{linear combinations between } A, B, C. \tag{5.47}$$

From Appendix B.3, we have ,

$$\mathcal{M}_\gamma : D^2\boldsymbol{E}(x) \in \frac{1}{r^3}\big[1, \langle n_*, \hat{x}\rangle\big]\big\{\boldsymbol{I},\ \ n_* \otimes n_*,\ \ n_* \otimes \hat{x},\ \ \hat{x} \otimes n_*,\ \ \hat{x} \otimes \hat{x}\big\}, \tag{5.48}$$

$$\mathcal{M}_\gamma : D^2\boldsymbol{F}(x) \in \frac{1}{r^5}\big[1, \langle n_*, \hat{x}\rangle\big]\big\{\boldsymbol{I},\ \ n_* \otimes n_*,\ \ n_* \otimes \hat{x},\ \ \hat{x} \otimes n_*,\ \ \hat{x} \otimes \hat{x}\big\} \tag{5.49}$$

so that ,

$$\mathcal{M}_\gamma : D^2\boldsymbol{E}(x)\boldsymbol{v}_* \in \frac{1}{r^3}\big[1,\ \ \langle n_*, \hat{x}\rangle,\ \ \langle n_*, \boldsymbol{v}_*\rangle,\ \ \langle \hat{x}, \boldsymbol{v}_*\rangle\big]\big\{\boldsymbol{v}_*,\ \ n_*,\ \ \hat{x}\big\} \tag{5.50}$$

$$\mathcal{M}_\gamma : D^2\boldsymbol{F}(x)\boldsymbol{v}_* \in \frac{1}{r^5}\big[1,\ \ \langle n_*, \hat{x}\rangle,\ \ \langle n_*, \boldsymbol{v}_*\rangle,\ \ \langle \hat{x}, \boldsymbol{v}_*\rangle\big]\big\{\boldsymbol{v}_*,\ \ n_*,\ \ \hat{x}\big\}. \tag{5.51}$$

From Appendix B.1 and B.4, we have

$$\operatorname{div} \mathcal{A}_\gamma \in \left\{\frac{1}{r^3}, \frac{1}{r^4}\right\}\big[1,\ \ \langle \hat{x}, n_*\rangle,\ \ \langle \hat{x}, \boldsymbol{v}_*\rangle,\ \ \langle n_*, \boldsymbol{v}_*\rangle\big]\big\{\hat{x},\ \ n_*,\ \ \boldsymbol{v}_*\big\}, \tag{5.52}$$

$$\begin{aligned}
\mathcal{C}_\gamma \in \left[\frac{1}{r^3}, \ldots, \frac{1}{r^6}\right]&\big[1,\ \ \langle \hat{x}, n_*\rangle,\ \ \langle \hat{x}, \boldsymbol{v}_*\rangle,\ \ \langle n_*, \boldsymbol{v}_*\rangle\big]\times \\
&\big\{\boldsymbol{I},\ \ n_* \otimes n_*,\ \ n_* \otimes \boldsymbol{v}_*,\ \ \boldsymbol{v}_* \otimes n_*,\ \ n_* \otimes \hat{x},\ \ \hat{x} \otimes n_*,\ \ \boldsymbol{v}_* \otimes \hat{x},\ \ \hat{x} \otimes \boldsymbol{v}_*,\ \ \hat{x} \otimes \hat{x}\big\},
\end{aligned} \tag{5.53}$$

$$\mathcal{D}_\gamma \in \left[\frac{1}{r^4}, \ldots, \frac{1}{r^9}\right]\big[1,\ \ \langle \hat{x}, n_*\rangle,\ \ \langle \hat{x}, \boldsymbol{v}_*\rangle,\ \ \langle n_*, \boldsymbol{v}_*\rangle\big]\big\{\hat{x},\ \ n_*,\ \ \boldsymbol{v}_*\big\}. \tag{5.54}$$

All the terms above either have explicit analytical expressions or are amenable to symbolic or numerical calculations.

Now we proceed to obtain symbolic representations of the bulk and boundary terms appearing in (5.36), (5.37) and (5.43). For convenience, in what follows, we will introduce quantities $A_i(\hat{y})$ for $i \geq 1$ which are appropriate polynomial functions of $\langle \hat{y}, n_*\rangle$, $\langle \hat{y}, \boldsymbol{v}_*\rangle$, $\langle n_*, \boldsymbol{v}_*\rangle$.

https://doi.org/10.1017/jfm.2025.10821 Published online by Cambridge University Press

(i) Here $\int_\Omega \boldsymbol{E}(x-y)[6\pi a\mathcal{M}_\gamma : D^2\boldsymbol{E}(y)\boldsymbol{v}_* + \operatorname{div}\mathcal{A}_\gamma(y)]\,\mathrm{d}y$. By (A21), we have

$$\begin{aligned}
&\int_\Omega \boldsymbol{E}(x-y)\big[6\pi a\mathcal{M}_\gamma : D^2\boldsymbol{E}(y)\boldsymbol{v}_* + \operatorname{div}\mathcal{A}_\gamma(y)\big]\,\mathrm{d}y\\
&= \frac{1}{|x|}\int_{\mathbb{S}^2} \boldsymbol{H}(\hat{x},\hat{y})\big[6\pi a\mathcal{M}_\gamma : D^2\boldsymbol{E}(\hat{y})\boldsymbol{v}_* + \operatorname{div}\mathcal{A}_\gamma(\hat{y})\big]\,\mathrm{d}\sigma(\hat{y}) + O\left(\frac{1}{|x|^2}\right)\\
&= \frac{1}{|x|}\int_{\mathbb{S}^2} \boldsymbol{H}(\hat{x},\hat{y})\big[A_1(\hat{y})\hat{y} + A_2(\hat{y})n_* + A_3(\hat{y})\boldsymbol{v}_*\big]\,\mathrm{d}\sigma(\hat{y}) + O\left(\frac{1}{|x|^2}\right), \qquad (5.55)
\end{aligned}$$

where $\boldsymbol{H}$ given by (A19), is recorded here,

$$\boldsymbol{H}(\hat{x},\hat{y}) = \lim_{\epsilon\to 0}\left[\int_\epsilon^\infty \frac{\boldsymbol{E}(\hat{x}-r\hat{y})}{r}\,\mathrm{d}r + \boldsymbol{E}(\hat{x})\ln(\epsilon)\right]. \qquad (5.56)$$

(ii) Here $\int_\Omega [-(a^3/4)\mathcal{M}_\gamma : D^2\boldsymbol{F}(y)\boldsymbol{v}_* + \operatorname{div}\mathcal{C}_\gamma(y) + \mathcal{D}_\gamma(y)]\,\mathrm{d}y$. The terms $D^2\boldsymbol{F}$ and $\mathcal{D}_\gamma$ decay at least r^{-4} and hence are integrable. Using their forms, we have

$$\int_\Omega \left[-\frac{a^3}{4}\mathcal{M}_\gamma : D^2\boldsymbol{F}(y)\boldsymbol{v}_* + \mathcal{D}_\gamma(y)\right]\mathrm{d}y = \int_{\mathbb{S}^2}\big[A_4(\hat{y})\hat{y} + A_5(\hat{y})n_* + A_6(\hat{y})\boldsymbol{v}_*\big]\,\mathrm{d}\sigma(\hat{y}). \qquad (5.57)$$

For $\operatorname{div}\mathcal{C}_\gamma = O(1/r^3)$, it can be conveniently represented using divergence theorem,

$$\int_\Omega \operatorname{div}\mathcal{C}_\gamma(y)\,\mathrm{d}y = \int_{\mathbb{S}^2}\langle\mathcal{C}_\gamma(\hat{y}),\hat{y}\rangle\,\mathrm{d}\sigma(\hat{y}) = \int_{\mathbb{S}^2}\big[A_7(\hat{y})\hat{y} + A_8(\hat{y})n_* + A_9(\hat{y})\boldsymbol{v}_*\big]\,\mathrm{d}\sigma(\hat{y}). \qquad (5.58)$$

(iii) Here $\int_\Omega (\boldsymbol{E}_S - \boldsymbol{I})[-\mathcal{M}_\gamma : D^2\boldsymbol{E}_S(y)\boldsymbol{v}_* + \operatorname{div}\mathcal{A}_\gamma(y) + \operatorname{div}\mathcal{C}_\gamma(\boldsymbol{E}_S(y)\boldsymbol{v}_*, y) + \mathcal{D}_\gamma(\boldsymbol{E}_S(y)\boldsymbol{v}_*, y)]\,\mathrm{d}y$. As $\boldsymbol{E}_S - \boldsymbol{I}$ decays at least as r^{-1}, the following integral is integrable:

$$\begin{aligned}
&\int_\Omega (\boldsymbol{E}_S - \boldsymbol{I})\big[-\mathcal{M}_\gamma : D^2\boldsymbol{E}_S(y)\boldsymbol{v}_* + \operatorname{div}\mathcal{A}_\gamma(\boldsymbol{v}_*, y) + \mathcal{D}_\gamma\big(\boldsymbol{E}_S(y)\boldsymbol{v}_*, y\big)\big]\,\mathrm{d}y\\
&= \int_{\mathbb{S}^2}\big[A_{10}(\hat{y})\hat{y} + A_{11}(\hat{y})n_* + A_{12}(\hat{y})\boldsymbol{v}_*\big]\,\mathrm{d}\sigma(\hat{y}), \qquad (5.59)
\end{aligned}$$

where we recall the form of $\boldsymbol{E}_S$ from (3.38). The remaining term with $\operatorname{div}\mathcal{C}_\gamma$ can also be dealt with using the divergence theorem,

$$\begin{aligned}
&\int_\Omega (\boldsymbol{E}_S - \boldsymbol{I})\operatorname{div}\mathcal{C}_\gamma\big(\boldsymbol{E}_S(y)\boldsymbol{v}_*, y\big)\,\mathrm{d}y\\
&= \int_{\mathbb{S}^2}\big\langle(\boldsymbol{E}_S(\hat{y}) - \boldsymbol{I}), \mathcal{C}_\gamma(\hat{y})\hat{y}\big\rangle\,\mathrm{d}\sigma(\hat{y}) - \int_\Omega \big\langle\nabla\boldsymbol{E}_S(y), \mathcal{C}_\gamma(y)\big\rangle\,\mathrm{d}y\\
&= \int_{\mathbb{S}^2}\big[A_{13}(\hat{y})\hat{y} + A_{14}(\hat{y})n_* + A_{15}(\hat{y})\boldsymbol{v}_*\big]\,\mathrm{d}\sigma(\hat{y}). \qquad (5.60)
\end{aligned}$$

Before moving onto the next section, we consider one 'simplistic model' in which $\boldsymbol{Q}$ is taken to be uniform in space, i.e. it equals its end state $\boldsymbol{Q}_*$. Such an approximation was in fact used in some works (see e.g. Kneppe *et al.* 1991; Heuer *et al.* 1992; Gómez-González

https://doi.org/10.1017/jfm.2025.10821 Published online by Cambridge University Press

& del Álamo 2013; Kos & Ravnik 2018). In this case, all the terms $\mathcal{A}_\gamma$, $\mathcal{C}_\gamma$ and $\mathcal{D}_\gamma$ vanish as they involve either $\nabla \boldsymbol{Q}$ or $\boldsymbol{Q} - \boldsymbol{Q}_*$. Then we have

$$\mathcal{I}_\gamma(x) = \frac{1}{|x|}\int_{\mathbb{S}^2} \boldsymbol{H}(\hat{x},\omega)\big[6\pi a \mathcal{M}_\gamma : D^2\boldsymbol{E}(\omega)\boldsymbol{v}_*\big]\,\mathrm{d}\sigma_\omega + \boldsymbol{E}(x)\int_\Omega \left[-\frac{a^3}{4}\mathcal{M}_\gamma : D^2\boldsymbol{F}(y)\boldsymbol{v}_*\right]\mathrm{d}y, \tag{5.61}$$

$$\mathcal{J}_\gamma = \int_\Omega (\boldsymbol{E}_S - \boldsymbol{I})\big[-\mathcal{M}_\gamma : D^2\boldsymbol{E}_S(y)\boldsymbol{v}_*\big]\,\mathrm{d}y. \tag{5.62}$$

As demonstrated numerically in § 6.1, we see that the actual velocity flow $\boldsymbol{v}$ does depend on the overall structure of $\boldsymbol{Q}$, not just its end state $\boldsymbol{Q}_*$.

6. Numerical simulations

Here we provide numerical simulations to illustrate our analysis. The simulations are performed using a commercial finite elements software package, COMSOL. For validation, we used this package to compute the classical Stokes flow. The results are benchmarked against analytical solutions in a finite domain, more precisely in the annulus $a \le r \le R$. For details, we refer to Appendix C.

Next, we record our numerical results for the anisotropic Stokes system (2.37). We first make the following remarks which apply to all of our simulations.

(*a*) For simplicity, we assume that only γ_1 and γ_2 are non-zero. For § § 6.1 and 6.2, they are fixed to be $\gamma_1 = 1$ and $\gamma_2 = 0.9$. In § 6.3, they vary, in fact decrease to zero.

(*b*) Our analytical results (5.16)–(5.20) show that $\boldsymbol{v} = \boldsymbol{v}_* + O(\frac{1}{r})$. To better illustrate this, we will plot rescaled versions of components of $\boldsymbol{v}$. More precisely, if $\boldsymbol{v}_*$ is along e_i, then we plot the following quantity for $a < r < R$:

$$r\left(\frac{\boldsymbol{v}_i}{|\boldsymbol{v}_*|} - 1\right) \quad \text{and} \quad r\left(\frac{\boldsymbol{v}_j}{|\boldsymbol{v}_*|}\right) \quad \text{for } j \neq i \tag{6.1}$$

along various 2-D cross-sections.

(*c*) All of our plots indicate that the quantities in (6.1) are of $O(1)$ in the whole domain numerically demonstrating the validity of our prediction $\boldsymbol{v} = \boldsymbol{v}_* + O(\frac{1}{r})$. However, due to boundary effect, the numerical solution is only consistent with the true solution for the range $a < r \ll R$. Such a phenomenon is made more precise in Appendix C. For all of the following simulations, we set $a = 1$ and $R = 10^5$. For the zoomed-in version of the figures, the results are plotted in the range: $1 < r < 20$.

6.1. *Far field condition:* $\boldsymbol{v}_* = e_1$, $n_* = e_3$

In this section, we choose $\boldsymbol{v}_*$ and n_* to be non-parallel to each other. Besides plotting various (rescaled) components of $\boldsymbol{v}_i$, we aim to illustrate the clear differences between the solution $\boldsymbol{v}$ of our anisotropic Stokes system when $\boldsymbol{Q}$ is set to be $\boldsymbol{Q}_*$ and given by (3.4). The choice of setting the order parameter to be spatially uniform is also used in the works Kneppe *et al.* (1991), Heuer *et al.* (1992), Gómez-González & del Álamo (2013) and Kos & Ravnik (2018). The rescaled version of $\boldsymbol{v}_1$ in yz-plane are shown in figures 1 and 2. Note that the difference between the velocity fields for these two choices are at the order of $O(|\gamma|)$ and are clearly revealed by the distinction between the formulae (5.36), (5.37), (5.43) and (5.61), (5.62).

The following figures 3–5 are 2-D zoomed-in plots ($1 < r < 20$) for different choices of $\boldsymbol{v}_i$ so as to remove the influence of the artificial boundary of the computational domain.

https://doi.org/10.1017/jfm.2025.10821 Published online by Cambridge University Press

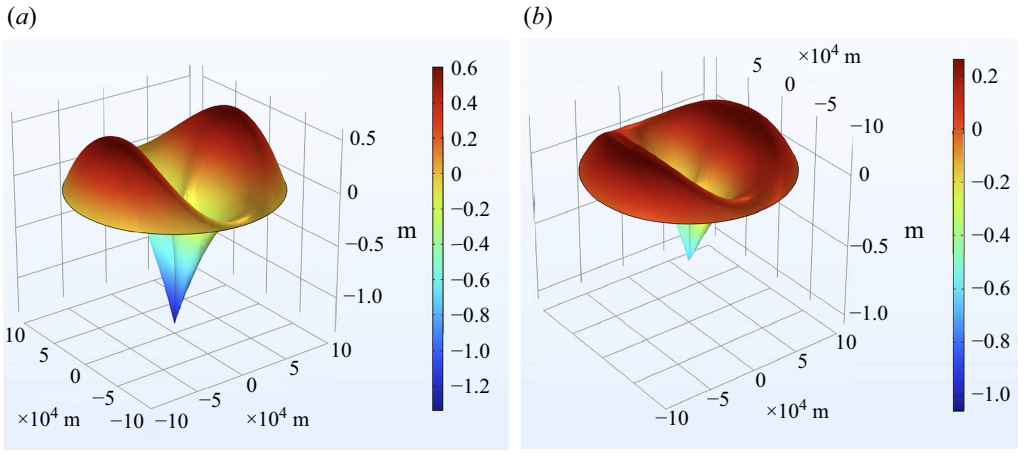

Figure 1. A 3-D plot of the rescaled $\boldsymbol{v}_1$ in the yz-plane on the whole computational domain $1 < r < 10^5$. Note that the behaviour of interest is near the tip of the conical section of the surface plot. The remaining part of the surface is determined by the finite size of the domain. Here (*a*) $\boldsymbol{Q}$ is set to be $\boldsymbol{Q}_*$; (*b*) $\boldsymbol{Q}$ is given by (3.4).

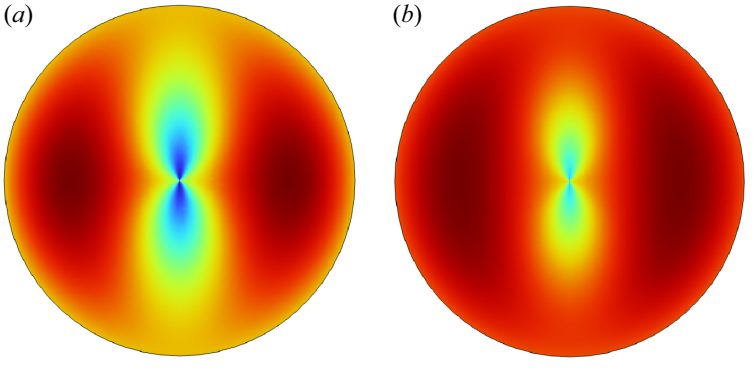

Figure 2. A 2-D plot of rescaled $\boldsymbol{v}_1$ in the yz-plane on the whole computational domain $1 < r < 10^5$ (cf. figure 1). Here (*a*) $\boldsymbol{Q}$ is set to be $\boldsymbol{Q}_*$; (*b*) $\boldsymbol{Q}$ is given by (3.4). Note again the distinction between the two plots.

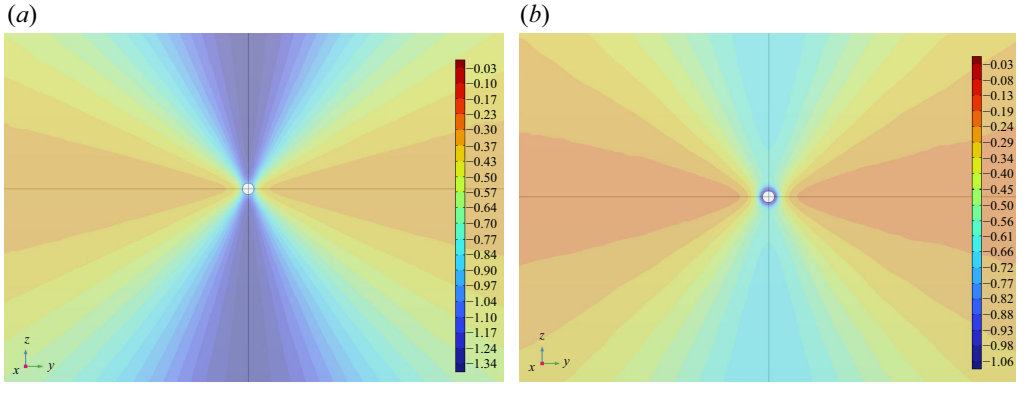

Figure 3. Zoomed-in 2-D plot ($1 < r < 20$) of the rescaled $\boldsymbol{v}_1$ in the yz-plane (cf. figure 2). Here (*a*) $\boldsymbol{Q}$ is set to be $\boldsymbol{Q}_*$; (*b*) $\boldsymbol{Q}$ is given by (3.4).

https://doi.org/10.1017/jfm.2025.10821 Published online by Cambridge University Press

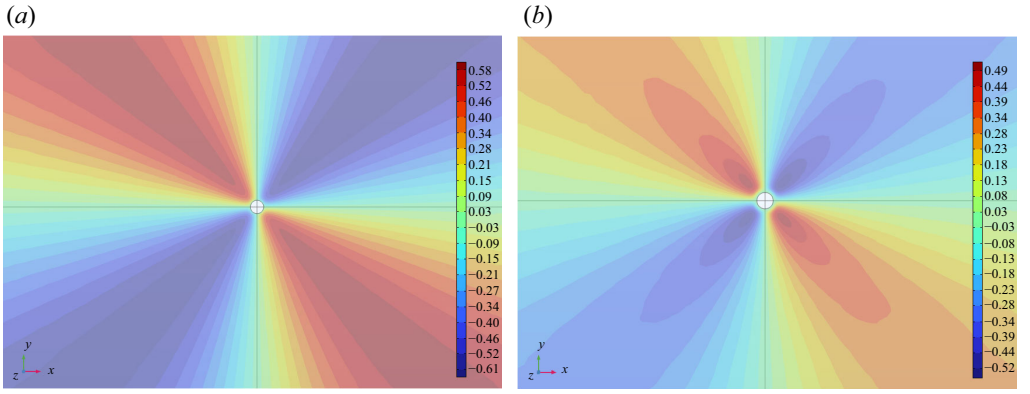

Figure 4. Zoomed-in 2-D, rescaled plot ($1 < r < 20$) of $\boldsymbol{v}_2$ in the xy-plane. Here (a) $\boldsymbol{Q}$ is set to be $\boldsymbol{Q}_*$; (b) $\boldsymbol{Q}$ is given by (3.4).

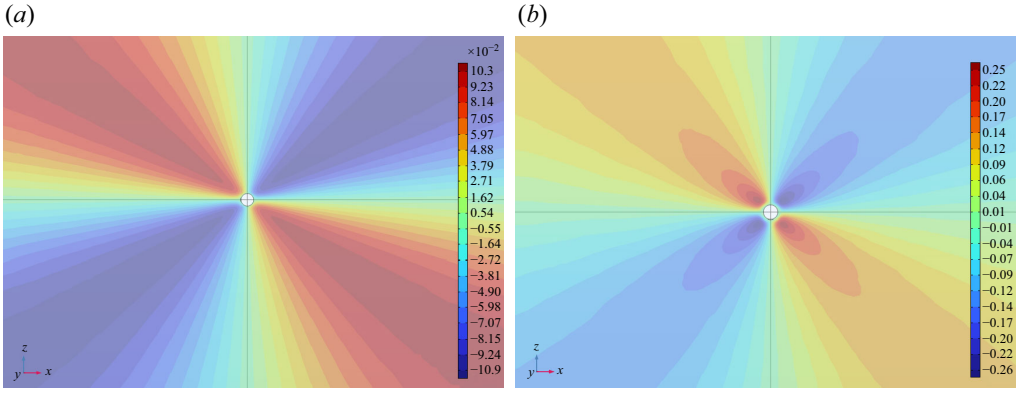

Figure 5. Zoomed-in, 2-D, rescaled plot ($1 < r < 20$) of $\boldsymbol{v}_3$ in the xz-plane. Here (a) $\boldsymbol{Q}$ is set to be $\boldsymbol{Q}_*$; (b) $\boldsymbol{Q}$ is given by (3.4).

Note that the distinction between the two plots in each respective figure is evident. Furthermore, in figures 1–3, there is reflection symmetry for $\boldsymbol{v}_1$ in the yz-plane with respect to both the y- and z-axes. This is due to the fact that the yz-plane is perpendicular to the xz-plane, the plane spanned by $\boldsymbol{v}_*$ and n_*.

6.2. *Far field condition:* $\boldsymbol{v}_* = e_3$, $n_* = e_3$

In this section, the $\boldsymbol{v}_*$ and n_* are parallel to each other, both pointing in the direction of z-axis. In this case, $\boldsymbol{v}_3$ should be rotational symmetric with respect to the z-axis. This is clearly demonstrated in figure 6, the plots for $\boldsymbol{v}_3$ in the xy-plane. See also figure 7 for $\boldsymbol{v}_3$ in the xz-plane.

Next, we plot several other velocity profiles to further illustrate the underlying symmetry. Note that the behaviour of $\boldsymbol{v}_1$ in the xz-plane and $\boldsymbol{v}_2$ in the yz-plane should be 'identical', as illustrated by figures 8 and 9.

https://doi.org/10.1017/jfm.2025.10821 Published online by Cambridge University Press

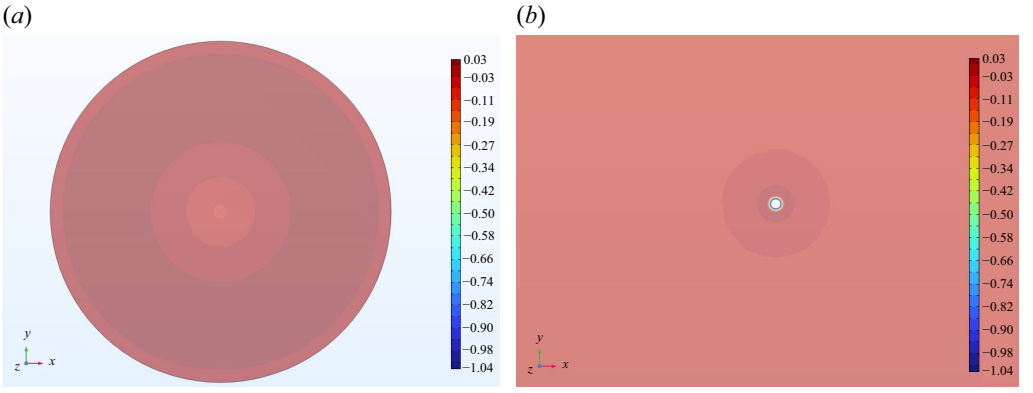

Figure 6. A 2-D, rescaled plot of $\boldsymbol{v}_3$ in the xy-plane: (a) whole computational domain, $1 < r < 10^5$; (b) zoomed-in version, $1 < r < 20$.

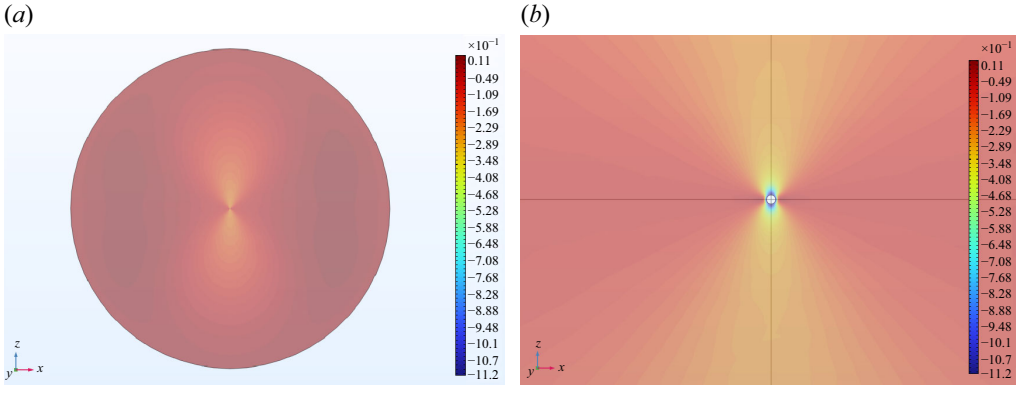

Figure 7. A 2-D, rescaled plot of $\boldsymbol{v}_3$ in the xz-plane: (a) whole computational domain, $1 < r < 10^5$; (b) zoomed-in version, $1 < r < 20$.

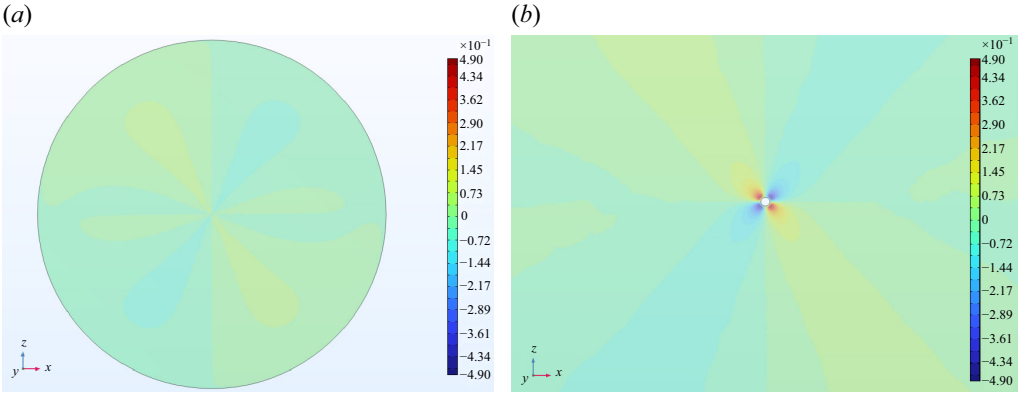

Figure 8. A 2-D, rescaled plot of $\boldsymbol{v}_1$ in the xz-plane: (a) whole computational domain, $1 < r < 10^5$; (b) zoomed-in version, $1 < r < 20$.

https://doi.org/10.1017/jfm.2025.10821 Published online by Cambridge University Press

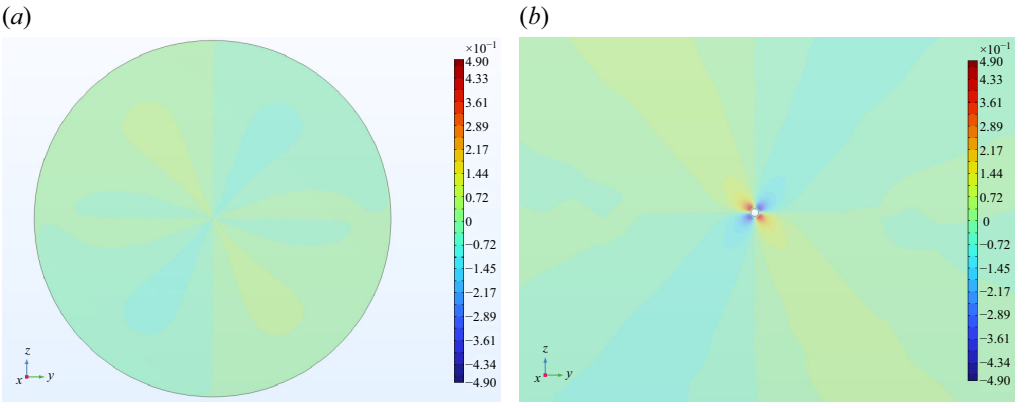

Figure 9. A 2-D, rescaled plot of $\boldsymbol{v}_2$ in the yz-plane: (a) whole computational domain, $1 < r < 10^5$; (b) zoomed-in version, $1 < r < 20$.

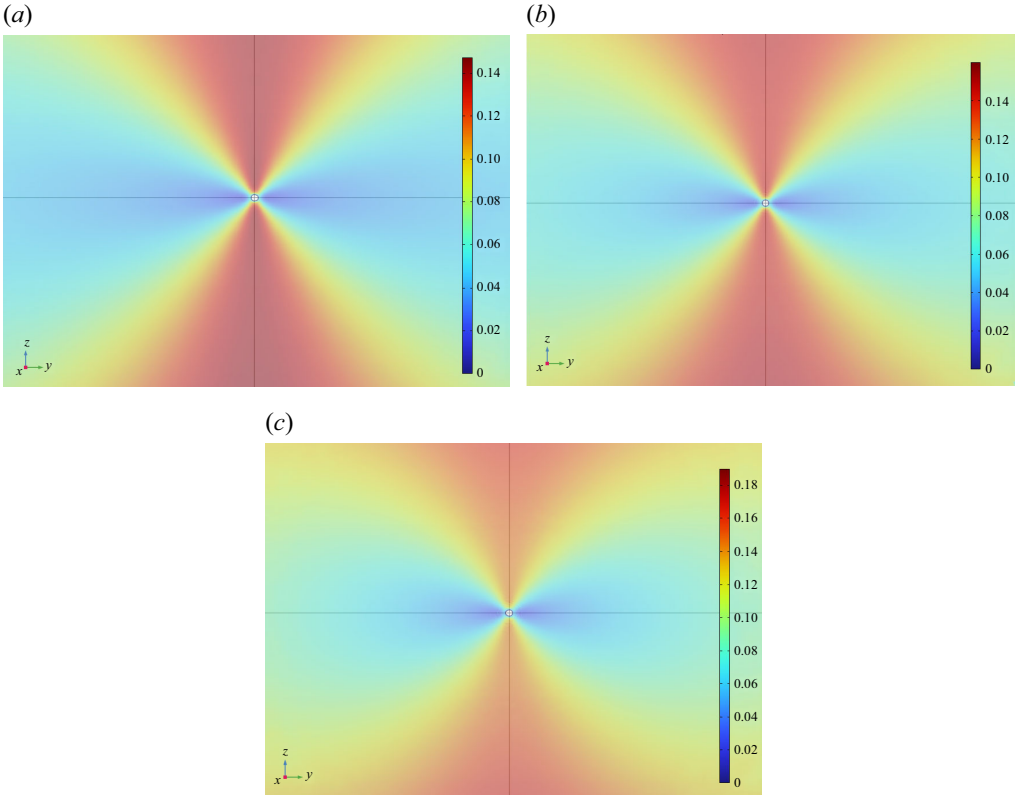

Figure 10. A 2-D, rescaled plot ($1 < r < 20$) of $\boldsymbol{v}_1 - \boldsymbol{v}_{01}$ in the yz-plane: (a) $\gamma_1 = 0.2$, $\gamma_2 = 0.18$; (b) $\gamma_1 = 0.1$, $\gamma_2 = 0.09$; (c) $\gamma_1 = 0.05$, $\gamma_2 = 0.045$.

6.3. *Far field condition:* $\boldsymbol{v}_* = e_3$, $n_* = e_3$

In this section, we demonstrate the decomposition (5.28). This is validated by plotting

$$r\left(\frac{\boldsymbol{v}_i - \boldsymbol{v}_{0i}}{|\boldsymbol{v}_*|\gamma_1}\right) = r\left(\frac{\overline{\varphi}_{\gamma i}}{|\boldsymbol{v}_*|\gamma_1}\right) = r\,O\left(\frac{\overline{\varphi}_\gamma}{|\gamma|}\right), \quad \text{for } i = 1, 2, 3, \tag{6.2}$$

https://doi.org/10.1017/jfm.2025.10821 Published online by Cambridge University Press

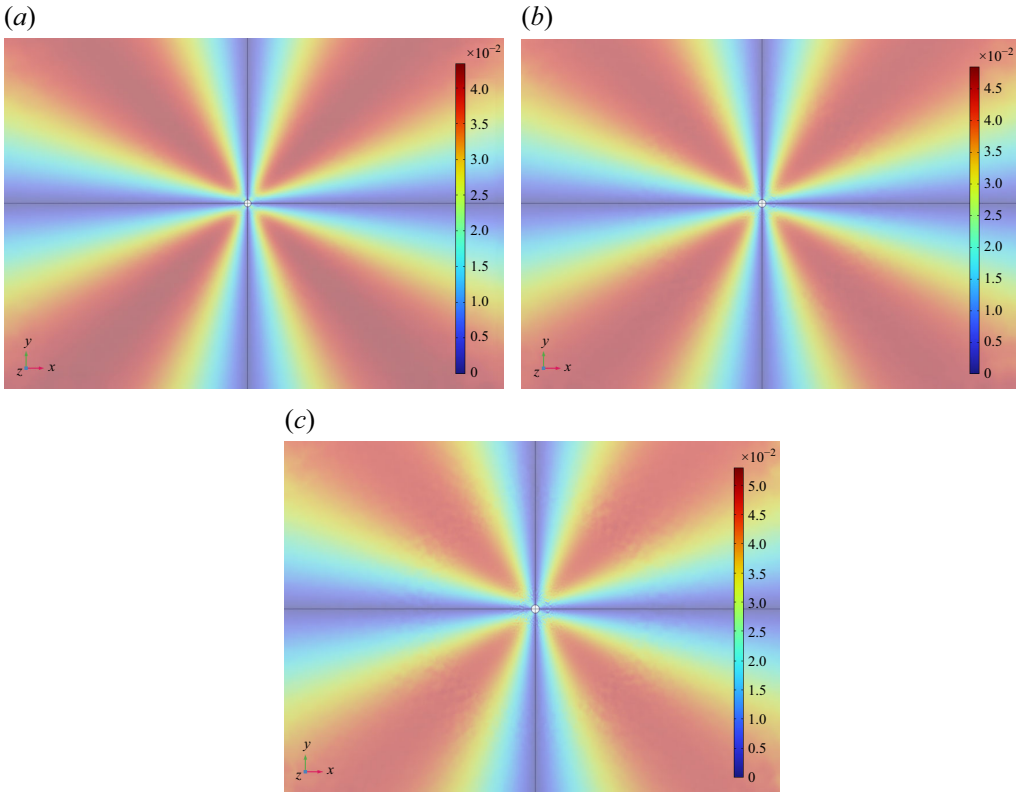

Figure 11. A 2-D, rescaled plot ($1 < r < 20$) of $\boldsymbol{v}_2 - \boldsymbol{v}_{02}$ in the xy-plane: (a) $\gamma_1 = 0.2$, $\gamma_2 = 0.18$; (b) $\gamma_1 = 0.1$, $\gamma_2 = 0.09$; (c) $\gamma_1 = 0.05$, $\gamma_2 = 0.045$.

with three samples of γ_1 and γ_2,

$$(a)\gamma_1 = 0.2,\ \gamma_2 = 0.18;\ (b)\gamma_1 = 0.1,\ \gamma_2 = 0.09;\ (c)\gamma_1 = 0.05,\ \gamma_2 = 0.045. \tag{6.3}$$

As $|\gamma| \longrightarrow 0$, we expect that the expression $r(\overline{\varphi}_\gamma/|\gamma|)$ converges to some fixed function, asymptotically determined by the property of (5.24). This is clearly demonstrated in figures 10–12, in terms of both the pattern and order of magnitude.

7. Conclusion

In this work, we analyse the velocity flow $\boldsymbol{v}$ of a nematic liquid crystal medium in the exterior of a small spherical particle in an anisotropic Stokes regime. The elastic energy of the nematic is described by the Landau–de Gennes energy functional defined over the exterior of a fixed spherical particle. Compared with previous results, in the limit of small Ericksen and Reynolds Numbers, we make use of an exact expression for the energy-minimizing $\boldsymbol{Q}$-tensor field. This expression then enters into an inhomogeneous Stokes system for $\boldsymbol{v}$. We are able to obtain analytical expression for the far-field asymptotics of $\boldsymbol{v}$, in particular, revealing its deviation from the classical isotropic Stokes flow.

The results obtained here for a single particle can provide useful information to model multiparticle systems in a complex fluid. Further investigations include characterization of the drag force on the particle, understanding the effect of defect patterns on or near the particle surface and the interaction between particles. From an analytical perspective, it will also be useful to consider the asymptotics of the solution as a function or an expansion

https://doi.org/10.1017/jfm.2025.10821 Published online by Cambridge University Press

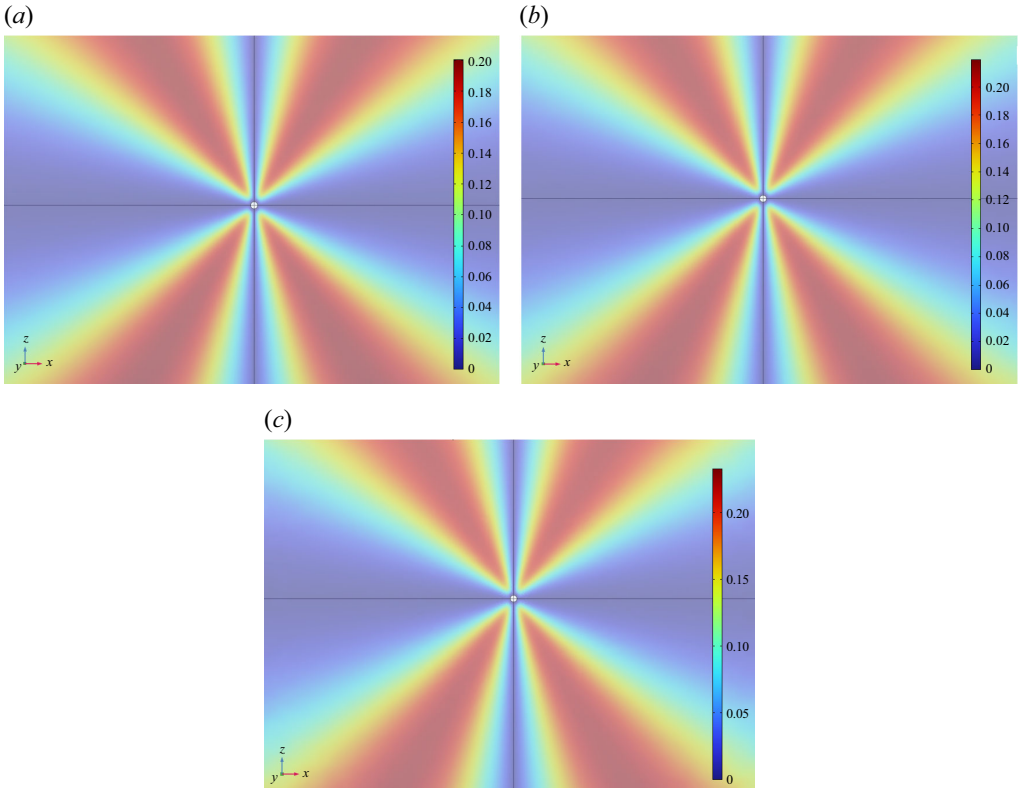

Figure 12. A 2-D, rescaled plot ($1 < r < 20$) of $\boldsymbol{v}_3 - \boldsymbol{v}_{03}$ in the xz-plane: (a) $\gamma_1 = 0.2$, $\gamma_2 = 0.18$; (b) $\gamma_1 = 0.1$, $\gamma_2 = 0.09$; (c) $\gamma_1 = 0.05$, $\gamma_2 = 0.045$.

in terms of the Ericksen Number and/or particle size which might take on intermediate values.

Supplementary material. Supplementary material is available at https://doi.org/10.1017/jfm.2025.10821.

Acknowledgements. The authors would like to acknowledge useful discussions with L. Berlyand and M. Potomkin.

Funding. The work of D.G. was partially supported by the NSF grant DMS-2106551.

Declaration of interests. The authors report no conflict of interest.

Appendix A. Far-field behaviour of bulk integrals

Here we analyse the asymptotics of the bulk integral

$$I(x) = \int_{\mathbb{R}^3 \setminus \mathcal{B}_1(0)} \boldsymbol{G}_\gamma(x - y)\, \boldsymbol{f}(y)\, \mathrm{d}y \tag{A1}$$

where $\boldsymbol{G}_\gamma = \boldsymbol{G}_{\gamma\,\gamma}$. Such an integral appears in the representation (5.11) of the solution $\boldsymbol{v}$ of (5.1). (The asymptotics of the boundary integrals is much simpler and will be given and used in Supplementary materials § E, step (II) of the proof of the existence of solution $\boldsymbol{v}$.) The property of being homogeneous of degree -1 (5.10) for $\boldsymbol{G}_\gamma$ plays an important role in our analysis. The precise asymptotics naturally also depends on the far-field behaviour of $\boldsymbol{f}$. We present these results in the following cases.

https://doi.org/10.1017/jfm.2025.10821 Published online by Cambridge University Press

A.1 *Case I*

We assume that $\|\boldsymbol{f}\|_{L^\infty(\mathbb{R}^3\setminus\boldsymbol{\mathcal{B}}_1(0))} < \infty$ and

$$\int_{\mathbb{R}^3\setminus\boldsymbol{B}_1(0)} |\boldsymbol{f}(y)|\,\mathrm{d}y < \infty. \tag{A2}$$

We compute

$$\begin{aligned}
&\int_{\mathbb{R}^3\setminus\boldsymbol{B}_1(0)} \boldsymbol{G}_\gamma(x-y)\boldsymbol{f}(y)\,\mathrm{d}y \\
&= \boldsymbol{G}_\gamma(x)\left(\int_{\mathbb{R}^3\setminus\boldsymbol{B}_1(0)} \boldsymbol{f}(y)\,\mathrm{d}y\right) + \int_{\mathbb{R}^3\setminus\boldsymbol{B}_1(0)} (\boldsymbol{G}_\gamma(x-y)-\boldsymbol{G}_\gamma(x))\boldsymbol{f}(y)\,\mathrm{d}y \\
&= \boldsymbol{G}_\gamma(x)\left(\int_{\mathbb{R}^3\setminus\boldsymbol{B}_1(0)} \boldsymbol{f}(y)\,\mathrm{d}y\right) + \frac{1}{|x|}\int_{\mathbb{R}^3\setminus\boldsymbol{B}_1(0)} \left(\boldsymbol{G}_\gamma(\hat{x}-\frac{y}{|x|})-\boldsymbol{G}_\gamma(\hat{x})\right)\boldsymbol{f}(y)\,\mathrm{d}y \\
&= \boldsymbol{G}_\gamma(x)\left(\int_{\mathbb{R}^3\setminus\boldsymbol{B}_1(0)} \boldsymbol{f}(y)\,\mathrm{d}y\right) + o\left(\frac{1}{|x|}\right).
\end{aligned} \tag{A3}$$

In order to characterize the $o(1/|x|)$ term, we assume that

$$\boldsymbol{f}(y) \lesssim \frac{1}{|y|^4}. \tag{A4}$$

Let $L \gg 1$. Then we have

$$\begin{aligned}
&\left|\frac{1}{|x|}\int_{\mathbb{R}^3\setminus\boldsymbol{B}_1(0)} \left(\boldsymbol{G}_\gamma(\hat{x}-\frac{y}{|x|})-\boldsymbol{G}_\gamma(\hat{x})\right)\boldsymbol{f}(y)\,\mathrm{d}y\right| \\
&= \left|\frac{1}{|x|}\int_{1\le|y|<\frac{|x|}{L}} + \int_{\frac{|x|}{L}\le|y|<L|x|} + \int_{L|x|\le|y|} \left(\frac{\boldsymbol{G}_\gamma(\widehat{\hat{x}-\frac{y}{|x|}})}{\left|\hat{x}-\frac{y}{|x|}\right|}-\boldsymbol{G}_\gamma(\hat{x})\right)\boldsymbol{f}(y)\,\mathrm{d}y\right| \\
&\lesssim \frac{1}{|x|}\int_{1\le|y|<\frac{|x|}{L}} \frac{|y|}{|x|}\frac{1}{|y|^4}\,\mathrm{d}y + \frac{1}{|x|}\int_{\frac{|x|}{L}\le|y|<L|x|} \frac{1}{|y|^4}\,\mathrm{d}y + \frac{1}{|x|}\int_{L|x|\le|y|} \frac{|x|}{|y|}\frac{1}{|y|^4}\,\mathrm{d}y \\
&\lesssim \frac{1}{|x|^2}\int_1^{\frac{|x|}{L}} \frac{r^2}{r^3}\,\mathrm{d}r + \frac{1}{|x|}\int_{\frac{|x|}{L}}^{L|x|} \frac{r^2}{r^4}\,\mathrm{d}r + \int_{L|x|}^{\infty} \frac{r^2}{r^5}\,\mathrm{d}r \\
&\lesssim \frac{\log|x|}{|x|^2} + \frac{1}{|x|^2} \\
&\lesssim \frac{\log|x|}{|x|^2}.
\end{aligned} \tag{A5}$$

Note that in the above, we have used the fact that $(1/|\hat{x}-(y/|x|)|)$ is an integrable singularity at $y\sim x$ in $\mathbb{R}^3$.

A.2 *Case II*

Next, we assume that f has the following large spatial asymptotic behaviour:

$$|\boldsymbol{f}| \le O\left(\frac{A+B\ln r}{r^k}\right) \quad \text{for some } k\ge 3 \text{ and all } r\gg 1. \tag{A6}$$

https://doi.org/10.1017/jfm.2025.10821 Published online by Cambridge University Press

Then we compute

$$\begin{aligned}
&\left|\int_{\mathbb{R}^3\setminus \boldsymbol{B}_1(0)} \boldsymbol{G}_\gamma(x-y)\boldsymbol{f}(y)\,\mathrm{d}y\right| \\
&\lesssim \int_{\mathbb{R}^3\setminus \boldsymbol{B}_1(0)} \frac{A+B\ln|y|}{|y|^k}\frac{1}{|x-y|}\,\mathrm{d}y \\
&\lesssim \frac{1}{|x|}\int_{\mathbb{R}^3\setminus \mathcal{B}_{\frac{1}{|x|}}(0)} \frac{A+B\ln|z|+B\ln|x|}{|x|^k|z|^k}\frac{1}{|\widehat{x}-z|}\,|x|^3 dz \quad (\text{where } \widehat{x}=\tfrac{x}{|x|} \text{ and } z=\tfrac{y}{|x|}) \\
&\lesssim \frac{1}{|x|^{k-2}}\left[\int_1^\infty \frac{A+B\ln|r|+B\ln|x|}{r^{k+1}}\,r^2\mathrm{d}r + \int_{\frac{1}{|x|}}^1 \frac{A+B\ln|r|+B\ln|x|}{r^k}\,r^2\mathrm{d}r\right] \\
&\quad \text{(note that the singularity at } \widehat{x} \text{ is integrable)} \\
&\lesssim \begin{cases} \dfrac{A\ln|x|+B\ln|x|+B(\ln|x|)^2}{|x|}, & \text{if } k=3, \\ \dfrac{A+B\ln|x|}{|x|}, & \text{if } k>3. \end{cases}
\end{aligned} \tag{A7}$$

Similarly,

$$\left|\int_{\mathbb{R}^3\setminus \boldsymbol{B}_1(0)} -\boldsymbol{q}(x-y)\cdot\boldsymbol{f}(y)\,\mathrm{d}y\right| \lesssim \int_{\mathbb{R}^3\setminus \boldsymbol{B}_1(0)} \frac{A+B\ln|y|}{|y|^k}\frac{1}{|x-y|^2}\,\mathrm{d}y \tag{A8}$$

$$\lesssim \begin{cases} \dfrac{A\ln|x|+B\ln|x|+B(\ln|x|)^2}{|x|^2}, & \text{if } k=3, \\ \dfrac{A+B\ln|x|}{|x|^2}, & \text{if } k>3. \end{cases} \tag{A9}$$

Note that for $k=3$, even if $B=0$, a $\ln|x|$ term can appear in the bulk integrals.

A.3 *Case III*

In order to do a more careful analysis of the case $k=3$ of which we are concerned most, we further assume that $\boldsymbol{f}$ is homogeneous of degree -3, i.e.

$$\boldsymbol{f}(\lambda x)=\lambda^{-3}\boldsymbol{f}(x) \quad \text{so that} \quad \boldsymbol{f}(x)=\frac{\boldsymbol{f}(\hat{x})}{|x|^3}. \tag{A10}$$

Note that the integrand $\boldsymbol{G}_\gamma(x-\cdot)\boldsymbol{f}(\cdot)\sim(1/|y|^4)$ is integrable in $\mathbb{R}^3\setminus\boldsymbol{B}_1(0)$. Hence, we can use Fubini's Theorem to compute $\mathrm{d}y$ iteratively as $r^2\,\mathrm{d}\omega\,\mathrm{d}r$, where $r=|y|$ and $\omega=\hat{y}$. To this end, we have

$$\begin{aligned}
\int_{\mathbb{R}^3\setminus \boldsymbol{B}_1(0)} \boldsymbol{G}_\gamma(x-y)\boldsymbol{f}(y)\,\mathrm{d}y &= \int_{\mathbb{S}^2}\left[\int_1^\infty \boldsymbol{G}_\gamma(x-r\omega)\frac{\boldsymbol{f}(\omega)}{r^3}r^2\,\mathrm{d}r\right]\mathrm{d}\omega \\
&= \frac{1}{|x|}\int_{\mathbb{S}^2}\left[\int_1^\infty \boldsymbol{G}_\gamma(\hat{x}-\frac{r}{|x|}\omega)\frac{1}{r}\,\mathrm{d}r\right]\boldsymbol{f}(\omega)\,\mathrm{d}\omega \\
&= \frac{1}{|x|}\int_{\mathbb{S}^2}\left[\int_{\frac{1}{|x|}}^\infty \boldsymbol{G}_\gamma(\hat{x}-r\omega)\frac{1}{r}\,\mathrm{d}r\right]\boldsymbol{f}(\omega)\,\mathrm{d}\omega.
\end{aligned} \tag{A11}$$

https://doi.org/10.1017/jfm.2025.10821 Published online by Cambridge University Press

For $|x| > 2$, we write

$$\int_{\frac{1}{|x|}}^{\infty} \boldsymbol{G}_\gamma(\hat{x} - r\omega)\frac{1}{r}\,\mathrm{d}r = \int_{\frac{1}{2}}^{\infty} \boldsymbol{G}_\gamma(\hat{x} - r\omega)\frac{1}{r}\,\mathrm{d}r + \int_{\frac{1}{|x|}}^{\frac{1}{2}} \boldsymbol{G}_\gamma(\hat{x} - r\omega)\frac{1}{r}\,\mathrm{d}r. \quad \text{(A12)}$$

Now for $\omega \neq \hat{x}$, define

$$\boldsymbol{H}_1(\hat{x}, \omega) := \int_{\frac{1}{2}}^{\infty} \boldsymbol{G}_\gamma(\hat{x} - r\omega)\frac{1}{r}\,\mathrm{d}r = O(1). \quad \text{(A13)}$$

Then we have

$$\int_{\mathbb{S}^2}\left[\int_{\frac{1}{2}}^{\infty} \boldsymbol{G}_\gamma(\hat{x} - r\omega)\frac{1}{r}\,\mathrm{d}r\right]\boldsymbol{f}(\omega)\,\mathrm{d}\omega = \int_{\mathbb{S}^2} \boldsymbol{H}_1(\hat{x}, \omega)\boldsymbol{f}(\omega)\,\mathrm{d}\omega. \quad \text{(A14)}$$

On the other hand, we have $\displaystyle\int_{(1/|x|)}^{(1/2)} \boldsymbol{G}_\gamma(\hat{x} - r\omega)(1/r)\,\mathrm{d}r = O(\ln|x|)$. To analyse this term, we compute

$$\begin{aligned}
&\int_{\mathbb{S}^2}\left[\int_{\frac{1}{|x|}}^{\frac{1}{2}} \boldsymbol{G}_\gamma(\hat{x} - r\omega)\frac{1}{r}\,\mathrm{d}r\right]\boldsymbol{f}(\omega)\,\mathrm{d}\omega \\
&= \int_{\mathbb{S}^2}\left[\int_{\frac{1}{|x|}}^{\frac{1}{2}} \frac{\boldsymbol{G}_\gamma(\hat{x})}{r}\,\mathrm{d}r\right]\boldsymbol{f}(\omega)\,\mathrm{d}\omega + \int_{\mathbb{S}^2}\left[\int_{\frac{1}{|x|}}^{\frac{1}{2}} \frac{\boldsymbol{G}_\gamma(\hat{x} - r\omega) - \boldsymbol{G}_\gamma(\hat{x})}{r}\,\mathrm{d}r\right]\boldsymbol{f}(\omega)\,\mathrm{d}\omega \\
&= \boldsymbol{G}_\gamma(\hat{x})\ln\left(\frac{|x|}{2}\right)\int_{\mathbb{S}^2}\boldsymbol{f}(\omega)\,\mathrm{d}\omega + \int_{\mathbb{S}^2}\boldsymbol{H}_2(\hat{x}, \omega)\boldsymbol{f}(\omega)\,\mathrm{d}\omega \\
&\quad - \int_{\mathbb{S}^2}\left[\int_{0}^{\frac{1}{|x|}} \frac{\boldsymbol{G}_\gamma(\hat{x} - r\omega) - \boldsymbol{G}_\gamma(\hat{x})}{r}\,\mathrm{d}r\right]\boldsymbol{f}(\omega)\,\mathrm{d}\omega \qquad \text{(A15)}
\end{aligned}$$

where

$$\boldsymbol{H}_2(\hat{x}, \omega) := \int_{0}^{\frac{1}{2}} \frac{\boldsymbol{G}_\gamma(\hat{x} - r\omega) - \boldsymbol{G}_\gamma(\hat{x})}{r}\,\mathrm{d}r = O(1) \quad \text{(A16)}$$

because $(\boldsymbol{G}_\gamma(\hat{x} - r\omega) - \boldsymbol{G}_\gamma(\hat{x})/r) = O(1)$ as $r \to 0^+$. Lastly, we have

$$\int_{\mathbb{S}^2}\left[\int_{0}^{\frac{1}{|x|}} \frac{\boldsymbol{G}_\gamma(\hat{x} - r\omega) - \boldsymbol{G}_\gamma(\hat{x})}{r}\,\mathrm{d}r\right]\boldsymbol{f}(\omega)\,\mathrm{d}\omega = O\left(\frac{1}{|x|}\right). \quad \text{(A17)}$$

Combining (A13), (A15), (A16), we define

$$\begin{aligned}
\boldsymbol{H}(\hat{x}, \omega) &:= \boldsymbol{H}_1(\hat{x}, \omega) + \boldsymbol{H}_2(\hat{x}, \omega) - \boldsymbol{G}_\gamma(\hat{x})\ln(2) \\
&= \int_{0}^{\frac{1}{2}} \frac{\boldsymbol{G}_\gamma(\hat{x} - r\omega) - \boldsymbol{G}_\gamma(\hat{x})}{r}\,\mathrm{d}r + \int_{\frac{1}{2}}^{\infty} \frac{\boldsymbol{G}_\gamma(\hat{x} - r\omega)}{r}\,\mathrm{d}r - \boldsymbol{G}_\gamma(\hat{x})\ln(2). \quad \text{(A18)}
\end{aligned}$$

Note that the above does not depend on the choice of $(1/2)$. Hence, it can also be equivalently written as

$$\boldsymbol{H}(\hat{x}, \omega) = \lim_{\epsilon \to 0}\left[\int_{\epsilon}^{\infty} \frac{\boldsymbol{G}_\gamma(\hat{x} - r\omega)}{r}\,\mathrm{d}r + \boldsymbol{G}_\gamma(\hat{x})\ln(\epsilon)\right]. \quad \text{(A19)}$$

https://doi.org/10.1017/jfm.2025.10821 Published online by Cambridge University Press

Then we have for $|x| \gg 1$ that

$$\int_\Omega \boldsymbol{G}_\gamma(x-y)\boldsymbol{f}(y)\,\mathrm{d}y = \boldsymbol{G}_\gamma(x)\ln|x|\int_{\mathbb{S}^2}\boldsymbol{f}(\omega)\,\mathrm{d}\omega + \frac{1}{|x|}\int_{\mathbb{S}^2}\boldsymbol{H}(\hat{x},\omega)\boldsymbol{f}(\omega)\,\mathrm{d}\omega + O\left(\frac{1}{|x|^2}\right). \tag{A20}$$

Hence, if $\int_{\mathbb{S}^2}\boldsymbol{f}(\omega)\,\mathrm{d}\omega = 0$, then

$$\int_\Omega \boldsymbol{G}_\gamma(x-y)\boldsymbol{f}(y)\,\mathrm{d}y = \frac{1}{|x|}\int_{\mathbb{S}^2}\boldsymbol{H}(\hat{x},\omega)\boldsymbol{f}(\omega)\,\mathrm{d}\omega + O\left(\frac{1}{|x|^2}\right). \tag{A21}$$

A.4 *Mean zero condition of the inhomogeneous term*

The conclusion of the previous section, in particular (A21), will be used to handle two terms. One is the dominant term $\operatorname{div}\mathcal{A}_\gamma(x)$ in $f_\gamma(\boldsymbol{v})$ (see (5.11)). Another is $D^2\boldsymbol{E}$ in the analysis of I_1 in (5.34).

For $\operatorname{div}\mathcal{A}_\gamma(x)$, recall its form (4.28), $\operatorname{div}\mathcal{A}_\gamma(x) = \gamma(\boldsymbol{F}(\hat{x})/r^3) + O(1/r^4)$. We will show that

$$\int_{\mathbb{S}^2}\boldsymbol{F}(\hat{x})\,\mathrm{d}\sigma = 0. \tag{A22}$$

To this end, we write $\mathcal{A}_\gamma$ explicitly as

$$\begin{aligned}\mathcal{A}_\gamma &= \gamma_1\mathcal{A}_1 + \gamma_2\mathcal{A}_2 + \gamma_3\mathcal{A}_3 + \gamma_9\mathcal{A}_9\\ &= \gamma_1\big(\boldsymbol{Q}_*(\boldsymbol{v}_*\cdot\nabla\boldsymbol{Q}) - (\boldsymbol{v}_*\cdot\nabla\boldsymbol{Q})\boldsymbol{Q}_*\big) + \gamma_2\big(\boldsymbol{v}_*\cdot\nabla\boldsymbol{Q}\big)\\ &\quad + \frac{\gamma_3}{2}\big(\boldsymbol{Q}_*(\boldsymbol{v}_*\cdot\nabla\boldsymbol{Q}) + (\boldsymbol{v}_*\cdot\nabla\boldsymbol{Q})\boldsymbol{Q}_*\big) + \gamma_9\big((\boldsymbol{v}_*\cdot\nabla\boldsymbol{Q})\cdot\boldsymbol{Q}_*\big)\boldsymbol{Q}_*.\end{aligned} \tag{A23}$$

By considering only the dominating term $(1/r)$ in the expression (3.4) of $\boldsymbol{Q}$, we have

$$\begin{aligned}\boldsymbol{Q}-\boldsymbol{Q}_* &= \left(-\frac{w\boldsymbol{Q}_*}{1+w}\right)\frac{1}{r} + O\left(\frac{1}{r^2}\right),\\ \boldsymbol{v}_*\cdot\nabla\boldsymbol{Q} &= \left(-\frac{w\boldsymbol{Q}_*}{1+w}\right)\left\langle\boldsymbol{v}_*, \nabla\frac{1}{r}\right\rangle + O\left(\frac{1}{r^3}\right),\\ \boldsymbol{Q}_*(\boldsymbol{v}_*\cdot\nabla\boldsymbol{Q}),\quad (\boldsymbol{v}_*\cdot\nabla\boldsymbol{Q})\boldsymbol{Q}_* &= \left(-\frac{w\boldsymbol{Q}_*^2}{1+w}\right)\left\langle\boldsymbol{v}_*, \nabla\frac{1}{r}\right\rangle + O\left(\frac{1}{r^3}\right),\\ \big((\boldsymbol{v}_*\cdot\nabla\boldsymbol{Q})\cdot\boldsymbol{Q}_*\big)\boldsymbol{Q}_* &= \left(-\frac{w|\boldsymbol{Q}_*|^2\boldsymbol{Q}_*}{1+w}\right)\left\langle\boldsymbol{v}_*, \nabla\frac{1}{r}\right\rangle + O\left(\frac{1}{r^3}\right).\end{aligned} \tag{A24}$$

Hence, we can write for some constant 3×3 matrix $\boldsymbol{M}_* = (m_{ij})$ that

$$\operatorname{div}\mathcal{A}_\gamma = \operatorname{div}\left(\left\langle\boldsymbol{v}_*, \nabla\frac{1}{r}\right\rangle\boldsymbol{M}_*\right) + O\left(\frac{1}{r^4}\right). \tag{A25}$$

Note that the term in $\mathcal{A}_\gamma$ multiplied by γ_1 completely vanishes.

We next claim that

$$\int_{\mathbb{S}^2}\operatorname{div}\left(\left\langle\boldsymbol{v}_*, \nabla\frac{1}{r}\right\rangle\boldsymbol{M}_*\right)\Big|_{r=1}\,\mathrm{d}\sigma = 0. \tag{A26}$$

https://doi.org/10.1017/jfm.2025.10821 Published online by Cambridge University Press

To see this, let $g(r) = (1/r)$, and we compute for $i = 1, 2, 3$,

$$\operatorname{div}\left(\left\langle \boldsymbol{v}_*, \nabla\frac{1}{r}\right\rangle \boldsymbol{M}_*\right)_i = \partial_j\left(\boldsymbol{v}_{*k}\partial_k g(r) m_{ij}\right) = \boldsymbol{v}_{*k} m_{ij}\partial^2_{kj} g(r), \tag{A27}$$

and

$$\begin{aligned}\partial^2_{kj} g(r) &= g''(r)\partial_k r\partial_j r + g'(r)\partial^2_{kj} r\\ &= g''(r)\frac{x_k x_j}{r^2} + \frac{g'(r)}{r}\left(\delta_{kj} - \frac{x_k x_j}{r^2}\right)\\ &= \frac{g'(r)}{r}\delta_{kj} + \left(g''(r) - \frac{g'(r)}{r}\right)\frac{x_k x_j}{r^2}\\ &= -\frac{1}{r^3}\left(\delta_{kj} - 3\frac{x_k x_j}{r^2}\right)\end{aligned} \tag{A28}$$

where we have used the facts that $g'(r) = -(1/r^2)$ and $g''(r) = (2/r^3)$. As

$$\int_{\mathbb{S}^2} 3\hat{x}\otimes\hat{x}\,\mathrm{d}\sigma = 4\pi\boldsymbol{I}, \tag{A29}$$

we have for all k, j that

$$\int_{\mathbb{S}^2} \partial^2_{kj} g(r)\,\mathrm{d}\sigma = 0. \tag{A30}$$

Thus, (A26) holds and so does (A22).

For $D^2\boldsymbol{E}$, to show $\displaystyle\int_{\mathbb{S}^2} D^2\boldsymbol{E}(\hat{x})\,\mathrm{d}\sigma = 0$, by (B39), we have

$$\begin{aligned}\int_{\mathbb{S}^2} \partial_{kl}\boldsymbol{E}_{ij}(x)\,\mathrm{d}\sigma &= 4\pi\left(-\delta_{ij}\delta_{kl} + \delta_{ik}\delta_{jl} + \delta_{jk}\delta_{il}\right) - 4\pi\left(-\delta_{ij}\delta_{kl} + \delta_{ik}\delta_{jl} + \delta_{jk}\delta_{il}\right)\\ &\quad -4\pi\left(\delta_{il}\delta_{jk} + \delta_{jl}\delta_{ik} + \delta_{kl}\delta_{ij}\right) + 15\int_{\mathbb{S}^2}\hat{x}_i\hat{x}_j\hat{x}_k\hat{x}_l\,\mathrm{d}\sigma\\ &= -4\pi\left(\delta_{il}\delta_{jk} + \delta_{jl}\delta_{ik} + \delta_{kl}\delta_{ij}\right) + 15\int_{\mathbb{S}^2}\hat{x}_i\hat{x}_j\hat{x}_k\hat{x}_l\,\mathrm{d}\sigma.\end{aligned} \tag{A31}$$

Using spherical coordinates and considering symmetry, it suffices to check the following cases:

(*a*) $i \neq j, k \neq l, (k, l) = (i, j)$ or (j, i)

$$\begin{aligned}\int_{\mathbb{S}^2} \partial_{kl}\boldsymbol{E}_{ij}(x)\,\mathrm{d}\sigma &= -4\pi + 15\int_{\mathbb{S}^2}\hat{x}_1^2\hat{x}_2^2\,\mathrm{d}\sigma\\ &= -4\pi + 15\int_0^{\pi}\int_0^{2\pi}(\sin\phi\cos\theta)^2(\sin\phi\sin\theta)^2\sin\phi\,\mathrm{d}\phi\,\mathrm{d}\theta\\ &= -4\pi + 15\int_0^{\pi}\sin^5\phi\,\mathrm{d}\phi\int_0^{2\pi}\cos^2\theta\sin^2\theta\,\mathrm{d}\theta = 0;\end{aligned} \tag{A32}$$

(*b*) $i \neq j, k \neq l, (k, l) \neq (i, j), (j, i)$

$$\int_{\mathbb{S}^2} \partial_{kl}\boldsymbol{E}_{ij}(x)\,\mathrm{d}\sigma = 0; \tag{A33}$$

https://doi.org/10.1017/jfm.2025.10821 Published online by Cambridge University Press

(*c*) $i \neq j, k = l = i$ or $k = l = j$

$$\int_{\mathbb{S}^2} \partial_{kl} \boldsymbol{E}_{ij}(x)\, \mathrm{d}\sigma = +15 \int_{\mathbb{S}^2} \hat{x}_1^3 \hat{x}_2\, \mathrm{d}\sigma = 0; \tag{A34}$$

(*d*) $i \neq j, k = l, \neq i, j$

$$\int_{\mathbb{S}^2} \partial_{kl} \boldsymbol{E}_{ij}(x)\, \mathrm{d}\sigma = 0; \tag{A35}$$

(*e*) $i = j, k \neq l$

$$\int_{\mathbb{S}^2} \partial_{kl} \boldsymbol{E}_{ij}(x)\, \mathrm{d}\sigma = 0; \tag{A36}$$

(*f*) $i = j, k = l, \neq i, j$

$$\int_{\mathbb{S}^2} \partial_{kl} \boldsymbol{E}_{ij}(x)\, \mathrm{d}\sigma = -4\pi + 15 \int_{\mathbb{S}^2} \hat{x}_1^2 \hat{x}_2^2\, \mathrm{d}\sigma = 0, \quad \text{as in } (a); \tag{A37}$$

(*g*) $i = j = k = l$

$$\int_{\mathbb{S}^2} \partial_{kl} \boldsymbol{E}_{ij}(x)\, \mathrm{d}\sigma = -12\pi + 15 \int_{\mathbb{S}^2} \hat{x}_3^4\, \mathrm{d}\sigma = -12\pi + 15 \int_0^{\pi} \int_0^{2\pi} \cos^4\phi \sin\phi\, \mathrm{d}\theta\, \mathrm{d}\phi = 0. \tag{A38}$$

Thus, $D^2 \boldsymbol{E}$ does also satisfy the mean zero condition.

Appendix B. Calculation of div $\mathcal{A}_\gamma$, div $[\mathcal{B}_\gamma[\nabla \mathrm{v}]]$, $\mathcal{M}_\gamma$:$\mathrm{D}^2\boldsymbol{E}$, $\mathcal{M}_\gamma$:$\mathrm{D}^2\boldsymbol{F}$, $\mathcal{C}_\gamma$ and $\mathcal{D}_\gamma$

These quantities appear in the final expressions (5.36), (5.37) and (5.43) for $\mathcal{I}_\gamma$ and $\mathcal{J}_\gamma$. Before proceeding, we recall the conventions (5.46) and (5.47).

B.1 *Formula for div $\mathcal{A}_\gamma$*

By (A25), (A27) and (A28), we have for some matrix $\boldsymbol{M}_* = (m_{ij})$ that

$$\big(\mathrm{div}\,(\mathcal{A}_\gamma)\big)_i = \mathrm{div}\left(\left\langle \boldsymbol{v}_*, \nabla \frac{1}{r} \right\rangle \boldsymbol{M}_*\right)_i = -m_{ij}\big(\delta_{kj} - 3\hat{x}_k \hat{x}_j\big)\boldsymbol{v}_{*k} = -m_{ij}\boldsymbol{v}_{*j} + 3m_{ij}\hat{x}_j \langle \boldsymbol{v}_*, \hat{x}\rangle \tag{B1}$$

so that

$$\mathrm{div}\,(\mathcal{A}_\gamma) = -\boldsymbol{M}_*(\boldsymbol{I} - 3\hat{x} \otimes \hat{x})\boldsymbol{v}_*. \tag{B2}$$

Hence

$$\mathrm{div}\left(\left\langle \boldsymbol{v}_*, \nabla \frac{1}{r} \right\rangle \boldsymbol{M}_*\right) = \begin{cases} \big(-\langle \boldsymbol{v}_*, n_*\rangle + 3\langle n_*, \hat{x}\rangle\langle \boldsymbol{v}_*, \hat{x}\rangle\big)n_*, & \text{if } \boldsymbol{M}_* = n_* \otimes n_*, \\ -\boldsymbol{v}_* + 3\langle \boldsymbol{v}_*, \hat{x}\rangle \hat{x}, & \text{if } \boldsymbol{M}_* = \boldsymbol{I}. \end{cases} \tag{B3}$$

Using the form of $\boldsymbol{Q}_*$ from (3.5), we have

$$\boldsymbol{M}_* = -\frac{w}{1+w}\left[\left(\gamma_2 s_* + \frac{\gamma_3}{3}s_*^2 + \frac{2\gamma_9}{3}s_*^3\right) n_* \otimes n_* - \frac{1}{3}\left(\gamma_2 s_* - \frac{\gamma_3 s_*^2}{3} + \frac{2\gamma_9 s_*^3}{3}\right)\boldsymbol{I}\right]. \tag{B4}$$

https://doi.org/10.1017/jfm.2025.10821 Published online by Cambridge University Press

Hence

$$\begin{aligned}\operatorname{div}(\mathcal{A}_\gamma) &= -\frac{w}{1+w}\left[\left(\gamma_2 s_* + \frac{\gamma_3}{3}s_*^2 + \frac{2\gamma_9}{3}s_*^3\right)\left(-\langle \boldsymbol{v}_*, n_*\rangle + 3\langle n_*, \hat{x}\rangle\langle \boldsymbol{v}_*, \hat{x}\rangle\right)n_*\right.\\ &\qquad \left. -\frac{1}{3}\left(\gamma_2 s_* - \frac{\gamma_3 s_*^2}{3} + \frac{2\gamma_9 s_*^3}{3}\right)\left(-\boldsymbol{v}_* + 3\langle \boldsymbol{v}_*, \hat{x}\rangle\hat{x}\right)\right]\\ &= -\frac{w}{1+w}\left[\left(\gamma_2 s_* + \frac{\gamma_3}{3}s_*^2 + \frac{2\gamma_9}{3}s_*^3\right)\left(-n_*\otimes n_* + 3\langle n_*, \hat{x}\rangle n_*\otimes\hat{x}\right)\right.\\ &\qquad \left. -\left(\gamma_2 s_* - \frac{\gamma_3 s_*^2}{3} + \frac{2\gamma_9 s_*^3}{3}\right)\left(\hat{x}\otimes\hat{x} - \frac{1}{3}\boldsymbol{I}\right)\right]\boldsymbol{v}_*. \end{aligned} \tag{B5}$$

B.2 *Formula for div* $[\mathcal{B}_\gamma[\nabla \boldsymbol{v}]]$

In this section, we will identify $\mathcal{M}_{i,j;k,l}$ which appear in (4.24) and (4.25). We note the following symmetry of $\mathcal{M}_{i,j;k,l}$ with respect to k and l,

$$\mathcal{M}_{i,j;k,l}\partial_{kl}\boldsymbol{v}_j = \mathcal{M}_{i,j;l,k}\partial_{kl}\boldsymbol{v}_j. \tag{B6}$$

Furthermore, we emphasize that $\mathcal{M}_\gamma$ will only act on incompressible vector fields $\boldsymbol{v}$: $\partial_j \boldsymbol{v}_j = 0$.

Before proceeding, using (3.5), we record that

$$\boldsymbol{Q}_{*ij} = s_*\left(n_{*i}n_{*j} - \frac{1}{3}\delta_{ij}\right), \quad \boldsymbol{Q}^2_{*ij} = \frac{s_*^2}{3}\left(n_{*i}n_{*j} + \frac{1}{3}\delta_{ij}\right), \quad |\boldsymbol{Q}_*|^2 = \frac{2s_*^2}{3}. \tag{B7}$$

With that, we compute

(*a*) $\operatorname{div}(\mathcal{B}_1[\nabla \boldsymbol{v}])$:

$$\begin{aligned}&\operatorname{div}\left(\left[\boldsymbol{Q}_*^2\boldsymbol{W} + \boldsymbol{W}\boldsymbol{Q}_*^2 - 2\boldsymbol{Q}_*\boldsymbol{W}\boldsymbol{Q}_*\right]_i\right) = \partial_j\left[\boldsymbol{Q}_*^2\boldsymbol{W} + \boldsymbol{W}\boldsymbol{Q}_*^2 - 2\boldsymbol{Q}_*\boldsymbol{W}\boldsymbol{Q}_*\right]_{ij}\\ &= \partial_j\left[\frac{1}{2}(\boldsymbol{Q}_*^2)_{ik}(\partial_j\boldsymbol{v}_k - \partial_k\boldsymbol{v}_j) + \frac{1}{2}(\boldsymbol{Q}_*^2)_{kj}(\partial_k\boldsymbol{v}_i - \partial_i\boldsymbol{v}_k) - (\boldsymbol{Q}_*)_{ik}(\partial_l\boldsymbol{v}_k - \partial_k\boldsymbol{v}_l)(\boldsymbol{Q}_*)_{lj}\right]\\ &= \frac{1}{2}(\boldsymbol{Q}_*^2)_{ik}\partial_{jj}\boldsymbol{v}_k + \frac{1}{2}(\boldsymbol{Q}_*^2)_{kj}(\partial_{kj}\boldsymbol{v}_i - \partial_{ij}\boldsymbol{v}_k) - (\boldsymbol{Q}_*)_{ik}(\boldsymbol{Q}_*)_{lj}(\partial_{jl}\boldsymbol{v}_k - \partial_{jk}\boldsymbol{v}_l)\\ &= \left(\frac{1}{2}\delta_{k,l}\left(\boldsymbol{Q}_*^2\right)_{ij} + \frac{1}{2}\delta_{i,j}(\boldsymbol{Q}_*^2)_{kl} - \frac{1}{2}\delta_{i,l}(\boldsymbol{Q}_*^2)_{jk} - (\boldsymbol{Q}_*)_{ij}(\boldsymbol{Q}_*)_{lk} + (\boldsymbol{Q}_*)_{ik}(\boldsymbol{Q}_*)_{lj}\right)\partial_{kl}\boldsymbol{v}_j\\ &=: \mathcal{M}^1_{i,j;k,l}\partial_{kl}\boldsymbol{v}_j, \end{aligned} \tag{B8}$$

where

$$\begin{aligned}\mathcal{M}^1_{i,j;k,l} &= s_*^2\left[\frac{1}{6}\delta_{k,l}\left(n_{*i}n_{*j} + \frac{1}{3}\delta_{i,j}\right) + \frac{1}{6}\delta_{i,j}\left(n_{*k}n_{*l} + \frac{1}{3}\delta_{k,l}\right)\right.\\ &\qquad -\frac{1}{6}\delta_{i,l}\left(n_{*k}n_{*j} + \frac{1}{3}\delta_{k,j}\right) - \left(n_{*i}n_{*j} - \frac{1}{3}\delta_{i,j}\right)\left(n_{*k}n_{*l} - \frac{1}{3}\delta_{k,l}\right)\\ &\qquad \left. +\left(n_{*k}n_{*i} - \frac{1}{3}\delta_{k,i}\right)\left(n_{*j}n_{*l} - \frac{1}{3}\delta_{j,l}\right)\right]\\ &= \frac{s_*^2}{2}\left(\delta_{kl}n_{*i}n_{*j} + \delta_{ij}n_{*k}n_{*l} - \delta_{ik}n_{*l}n_{*j}\right). \end{aligned} \tag{B9}$$

https://doi.org/10.1017/jfm.2025.10821 Published online by Cambridge University Press

In the above, we have used the symmetry property (B6) of $\mathcal{M}$ and the incompressibility of $\boldsymbol{v}$:

$$\delta_{il}n_{*k}n_{*j}\partial_{kl}\boldsymbol{v}_j = \delta_{ik}n_{*l}n_{*j}\partial_{kl}\boldsymbol{v}_j \quad \text{and} \quad \delta_{il}\delta_{kj}\partial_{kl}\boldsymbol{v}_j = \delta_{ik}\delta_{lj}\partial_{kl}\boldsymbol{v}_j = \partial_{ij}\boldsymbol{v}_j = 0. \tag{B10}$$

The above property will be used in several places in what follows.

(*b*) $\operatorname{div}(\mathcal{B}_2[\nabla\boldsymbol{v}])$:

$$\begin{aligned}\operatorname{div}\left[\boldsymbol{Q}_*\nabla\boldsymbol{v} - (\nabla\boldsymbol{v})\boldsymbol{Q}_*\right]_i &= \partial_j\left[\left(\boldsymbol{Q}_*\right)_{ik}\partial_j\boldsymbol{v}_k - \partial_k\boldsymbol{v}_i\left(\boldsymbol{Q}_*\right)_{kj}\right]\\ &= \left(\boldsymbol{Q}_*\right)_{ik}\partial_{jj}\boldsymbol{v}_k - \left(\boldsymbol{Q}_*\right)_{kj}\partial_{kj}\boldsymbol{v}_i\\ &= \left(\delta_{k,l}\left(\boldsymbol{Q}_*\right)_{ij} - \delta_{i,j}\left(\boldsymbol{Q}_*\right)_{kl}\right)\partial_{kl}\boldsymbol{v}_j\\ &=: \mathcal{M}^2_{i,j;k,l}\partial_{kl}\boldsymbol{v}_j.\end{aligned} \tag{B11}$$

Here

$$\mathcal{M}^2_{i,j;k,l} = s_*\left(\delta_{k,l}n_{*i}n_{*j} - \delta_{i,j}n_{*k}n_{*l}\right). \tag{B12}$$

(*c*) $\operatorname{div}(\mathcal{B}_3[\nabla\boldsymbol{v}])$:

$$\begin{aligned}\frac{1}{2}\operatorname{div}\left[\boldsymbol{Q}_*^2\nabla\boldsymbol{v} - (\nabla\boldsymbol{v})\boldsymbol{Q}_*^2\right]_i &= \frac{1}{2}\left(\left(\boldsymbol{Q}_*^2\right)_{ik}\partial_{jj}\boldsymbol{v}_k - \left(\boldsymbol{Q}_*^2\right)_{kj}\partial_{kj}\boldsymbol{v}_i\right)\\ &= \frac{1}{2}\left(\delta_{k,l}\left(\boldsymbol{Q}_*^2\right)_{ij} - \delta_{i,j}\left(\boldsymbol{Q}_*^2\right)_{kl}\right)\partial_{kl}\boldsymbol{v}_j\\ &=: \mathcal{M}^3_{i,j;k,l}\partial_{kl}\boldsymbol{v}_j.\end{aligned} \tag{B13}$$

Here

$$\mathcal{M}^3_{i,j;k,l} = \frac{s_*^2}{6}\left(\delta_{k,l}n_{*i}n_{*j} - \delta_{i,j}n_{*k}n_{*l}\right). \tag{B14}$$

(*d*) $\operatorname{div}(\mathcal{B}_4[\nabla\boldsymbol{v}])$:

$$\begin{aligned}\operatorname{div}\left[\boldsymbol{Q}_*\boldsymbol{A} + \boldsymbol{A}\boldsymbol{Q}_*\right]_i &= \frac{1}{2}\left(\boldsymbol{Q}_*\right)_{ik}\partial_{jj}\boldsymbol{v}_k + \frac{1}{2}\left(\partial_{ij}\boldsymbol{v}_k + \partial_{kj}\boldsymbol{v}_i\right)\left(\boldsymbol{Q}_*\right)_{kj}\\ &= \frac{1}{2}\left(\delta_{k,l}\left(\boldsymbol{Q}_*\right)_{ij} + \delta_{i,l}\left(\boldsymbol{Q}_*\right)_{jk} + \delta_{i,j}\left(\boldsymbol{Q}_*\right)_{kl}\right)\partial_{kl}\boldsymbol{v}_j\\ &=: \mathcal{M}^4_{i,j;k,l}\partial_{kl}\boldsymbol{v}_j.\end{aligned} \tag{B15}$$

Here

$$\begin{aligned}\mathcal{M}^4_{i,j;k,l} &= \frac{s_*}{2}\left(\delta_{k,l}\left(n_{*i}n_{*j} - \frac{1}{3}\delta_{i,j}\right) + \delta_{i,l}\left(n_{*j}n_{*k} - \frac{1}{3}\delta_{j,k}\right)\right.\\ &\quad\left.+\delta_{i,j}\left(n_{*k}n_{*l} - \frac{1}{3}\delta_{k,l}\right)\right)\\ &= \frac{s_*}{2}\left(\delta_{kl}n_{*i}n_{*j} + \delta_{ij}n_{*k}n_{*l} + \delta_{ik}n_{*l}n_{*j} - \frac{2}{3}\delta_{kl}\delta_{ij}\right).\end{aligned} \tag{B16}$$

https://doi.org/10.1017/jfm.2025.10821 Published online by Cambridge University Press

(e) $\mathrm{div}(\mathcal{B}_5[\nabla \boldsymbol{v}])$:

$$\begin{aligned}\mathrm{div}\left[\boldsymbol{Q}_*^2\boldsymbol{A}+\boldsymbol{A}\boldsymbol{Q}_*^2\right]_i &= \frac{1}{2}\left(\boldsymbol{Q}_*^2\right)_{ik}\partial_{jj}\boldsymbol{v}_k+\frac{1}{2}\left(\partial_{ij}\boldsymbol{v}_k+\partial_{kj}\boldsymbol{v}_i\right)\left(\boldsymbol{Q}_*^2\right)_{kj}\\ &= \frac{1}{2}\left(\delta_{k,l}\left(\boldsymbol{Q}_*^2\right)_{ij}+\delta_{i,l}\left(\boldsymbol{Q}_*^2\right)_{jk}+\delta_{i,j}\left(\boldsymbol{Q}_*^2\right)_{kl}\right)\partial_{kl}\boldsymbol{v}_j\\ &=: \mathcal{M}^5_{i,j;k,l}\partial_{kl}\boldsymbol{v}_j. \end{aligned} \tag{B17}$$

Here

$$\begin{aligned}\mathcal{M}^5_{i,j;k,l} &= \frac{s_*^2}{6}\left(\delta_{k,l}\left(n_{*i}n_{*j}+\frac{1}{3}\delta_{i,j}\right)+\delta_{i,l}\left(n_{*j}n_{*k}+\frac{1}{3}\delta_{j,k}\right)\right.\\ &\quad\left.+\delta_{i,j}\left(n_{*k}n_{*l}+\frac{1}{3}\delta_{k,l}\right)\right)\\ &= \frac{s_*^2}{6}\left(\delta_{kl}n_{*i}n_{*j}+\delta_{ij}n_{*k}n_{*l}+\delta_{ik}n_{*l}n_{*j}+\frac{2}{3}\delta_{ij}\delta_{kl}\right). \end{aligned} \tag{B18}$$

(f) $\mathrm{div}(\mathcal{B}_6[\nabla \boldsymbol{v}])$:

$$\begin{aligned}\mathrm{div}\left[(\boldsymbol{A}\cdot\boldsymbol{Q}_*)\boldsymbol{Q}_*\right]_i &= \frac{1}{2}\left(\boldsymbol{Q}_*\right)_{ij}\left(\boldsymbol{Q}_*\right)_{kl}\left(\partial_{lj}\boldsymbol{v}_k+\partial_{kj}\boldsymbol{v}_l\right)\\ &= \frac{1}{2}\left(\left(\boldsymbol{Q}_*\right)_{ik}\left(\boldsymbol{Q}_*\right)_{jl}+\left(\boldsymbol{Q}_*\right)_{il}\left(\boldsymbol{Q}_*\right)_{kj}\right)\partial_{kl}\boldsymbol{v}_j\\ &=: \mathcal{M}^6_{i,j;k,l}\partial_{kl}\boldsymbol{v}_j. \end{aligned} \tag{B19}$$

Here

$$\begin{aligned}\mathcal{M}^6_{i,j;k,l} &= \frac{s_*^2}{2}\left(\left(n_{*i}n_{*k}-\frac{1}{3}\delta_{i,k}\right)\left(n_{*j}n_{*l}-\frac{1}{3}\delta_{j,l}\right)\right.\\ &\quad\left.+\left(n_{*i}n_{*l}-\frac{1}{3}\delta_{i,l}\right)\left(n_{*j}n_{*k}-\frac{1}{3}\delta_{j,k}\right)\right)\\ &= s_*^2\left(n_{*i}n_{*j}n_{*k}n_{*l}-\frac{1}{3}\delta_{ik}n_{*l}n_{*j}\right). \end{aligned} \tag{B20}$$

(g) $\mathrm{div}(\mathcal{B}_7[\nabla \boldsymbol{v}])$:

$$\mathrm{div}\left[|\boldsymbol{Q}_*|^2\boldsymbol{A}\right]_i = \mathrm{div}\left[\frac{2s_*^2}{3}\boldsymbol{A}\right]_i =: \mathcal{M}^7_{i,j;k,l}\partial_{kl}\boldsymbol{v}_j. \tag{B21}$$

Here

$$\mathcal{M}^7_{i,j;k,l} = \frac{s_*^2}{3}\delta_{k,l}\delta_{i,j}. \tag{B22}$$

(h) $\mathrm{div}(\mathcal{B}_{10}[\nabla \boldsymbol{v}])$:

$$\begin{aligned}\mathrm{div}\left[(\boldsymbol{Q}_*^2\cdot\boldsymbol{A})\boldsymbol{Q}_*+(\boldsymbol{Q}_*\cdot\boldsymbol{A})\boldsymbol{Q}_*^2\right]_i &= \frac{1}{2}\left(\left(\boldsymbol{Q}_*^2\right)_{kl}\left(\boldsymbol{Q}_*\right)_{ij}+\left(\boldsymbol{Q}_*\right)_{kl}\left(\boldsymbol{Q}_*^2\right)_{ij}\right)\left(\partial_{lj}\boldsymbol{v}_k+\partial_{kj}\boldsymbol{v}_l\right)\\ &= \left(\left(\boldsymbol{Q}_*^2\right)_{jk}\left(\boldsymbol{Q}_*\right)_{il}+\left(\boldsymbol{Q}_*\right)_{jk}\left(\boldsymbol{Q}_*^2\right)_{il}\right)\partial_{kl}\boldsymbol{v}_j\\ &=: \mathcal{M}^{10}_{i,j;k,l}\partial_{kl}\boldsymbol{v}_j. \end{aligned} \tag{B23}$$

https://doi.org/10.1017/jfm.2025.10821 Published online by Cambridge University Press

Here

$$\mathcal{M}^{10}_{i,j;k,l} = \frac{s_*^3}{3}\left(\left(n_{*j}n_{*k}+\frac{1}{3}\delta_{j,k}\right)\left(n_{*i}n_{*l}-\frac{1}{3}\delta_{i,l}\right) + \left(n_{*j}n_{*k}-\frac{1}{3}\delta_{j,k}\right)\left(n_{*i}n_{*l}+\frac{1}{3}\delta_{i,l}\right)\right) = \frac{2s_*^3}{3}n_{*i}n_{*j}n_{*k}n_{*l}. \tag{B24}$$

(i) $\operatorname{div}(\mathcal{B}_{11}[\nabla \boldsymbol{v}])$:

$$\operatorname{div}\left[|\boldsymbol{Q}_*|^2(\boldsymbol{A}\cdot\boldsymbol{Q}_*)\boldsymbol{Q}_*\right]_i = \frac{2s_*^2}{3}\left(\boldsymbol{Q}_*\right)_{il}\left(\boldsymbol{Q}_*\right)_{jk}\partial_{kl}\boldsymbol{v}_j =: \mathcal{M}^{11}_{i,j;k,l}\partial_{kl}\boldsymbol{v}_j. \tag{B25}$$

Here

$$\mathcal{M}^{11}_{i,j;k,l} = \frac{2s_*^4}{3}\left(n_{*i}n_{*l}-\frac{1}{3}\delta_{i,l}\right)\left(n_{*j}n_{*k}-\frac{1}{3}\delta_{j,k}\right) = \frac{2s_*^4}{3}\left(n_{*i}n_{*j}n_{*k}n_{*l}-\frac{1}{3}\delta_{ik}n_{*l}n_{*j}\right). \tag{B26}$$

Hence, the fourth-order tensor $\mathcal{M}_\gamma$ can be decomposed as

$$\mathcal{M}_{i,j;k,l} = \sum_{p=1,\dots,7,10,11}\gamma_p\mathcal{M}^p_{i,j;k,l}. \tag{B27}$$

From (B9) to (B26), the $\mathcal{M}^p_{i,j;k,l}$ are effectively given by a linear combination of the following tensors:

$$\delta_{kl}\delta_{ij},\quad \delta_{kl}n_{*i}n_{*j},\quad \delta_{ij}n_{*k}n_{*l},\quad \delta_{ik}n_{*l}n_{*j}\ \text{(or equivalently, } \delta_{il}n_{*k}n_{*j}),\quad n_{*i}n_{*j}n_{*k}n_{*l} \tag{B28}$$

where δ_{pq} is the delta-function $\delta_{pq}=1$ for $p=q$ and $\delta_{pq}=0$ for $p\neq q$.

B.3 *Formula for* $\mathcal{M}_\gamma : D^2\boldsymbol{F}$

Here we list the formulae for $\mathcal{M}_\gamma : D^2\boldsymbol{F}$ where $\boldsymbol{F}$ is some divergence free vector field with homogeneous degree $-k$, for $k=1,3,5$.

As a preparation, following (A28) for $g(r)=\frac{1}{r},\ \frac{1}{r^3},\ \frac{1}{r^5}$, we compute

$$\partial_k g(r) = g'(r)\frac{x_k}{r}, \tag{B29}$$

$$\partial_{kl}g(r) = \frac{g'(r)}{r}\delta_{kl}+\left(g''(r)-\frac{g'(r)}{r}\right)\frac{x_kx_l}{r^2}, \tag{B30}$$

$$\partial_{kl}\big(g(r)\delta_{ij}\big) = \left(\frac{g'(r)}{r}\delta_{kl}+\left(g''(r)-\frac{g'(r)}{r}\right)\frac{x_kx_l}{r^2}\right)\delta_{ij}, \tag{B31}$$

$$\partial_k\big(g(r)x_ix_j\big) = g(r)\big(\delta_{ik}x_j+\delta_{jk}x_i\big)+\frac{g'(r)}{r}x_ix_jx_k, \tag{B32}$$

$$\begin{aligned}\partial_{kl}\big(g(r)x_ix_j\big) &= g(r)\big(\delta_{ik}\delta_{jl}+\delta_{jk}\delta_{il}\big)\\ &\quad + rg'(r)\Big(\frac{\delta_{il}x_jx_k+\delta_{jl}x_ix_k+\delta_{kl}x_ix_j+\delta_{ik}x_jx_l+\delta_{jk}x_ix_l}{r^2}\Big)\\ &\quad + (r^2g''(r)-rg'(r))\frac{x_ix_jx_kx_l}{r^4}.\end{aligned} \tag{B33}$$

https://doi.org/10.1017/jfm.2025.10821 Published online by Cambridge University Press

Hence,

$$\partial_{kl}\left(\frac{\delta_{ij}}{r}\right)=\frac{1}{r^3}\left(-\delta_{kl}+3\hat{x}_k\hat{x}_l\right)\delta_{ij}, \tag{B34}$$

$$\partial_{kl}\left(\frac{\delta_{ij}}{r^3}\right)=\frac{1}{r^5}\left(-3\delta_{kl}+15\hat{x}_k\hat{x}_l\right)\delta_{ij}, \tag{B35}$$

$$\begin{aligned}\partial_{kl}\left(\frac{x_ix_j}{r^3}\right)=\frac{1}{r^3}\big[&\left(\delta_{ik}\delta_{jl}+\delta_{jk}\delta_{il}\right)\\&-3\left(\delta_{il}\hat{x}_j\hat{x}_k+\delta_{jl}\hat{x}_i\hat{x}_k+\delta_{kl}\hat{x}_i\hat{x}_j+\delta_{ik}\hat{x}_j\hat{x}_l+\delta_{jk}\hat{x}_i\hat{x}_l\right)\\&+15\hat{x}_i\hat{x}_j\hat{x}_k\hat{x}_l\big],\end{aligned} \tag{B36}$$

$$\begin{aligned}\partial_{kl}\left(\frac{x_ix_j}{r^5}\right)=\frac{1}{r^5}\big[&\left(\delta_{ik}\delta_{jl}+\delta_{jk}\delta_{il}\right)\\&-5\left(\delta_{il}\hat{x}_j\hat{x}_k+\delta_{jl}\hat{x}_i\hat{x}_k+\delta_{kl}\hat{x}_i\hat{x}_j+\delta_{ik}\hat{x}_j\hat{x}_l+\delta_{jk}\hat{x}_i\hat{x}_l\right)\\&+35\hat{x}_i\hat{x}_j\hat{x}_k\hat{x}_l\big].\end{aligned} \tag{B37}$$

The above are applied to $\boldsymbol{E}$, $\boldsymbol{F}$ and $\boldsymbol{Q}$:

(i) $\boldsymbol{E}(x)=\dfrac{1}{8\pi}\left[\dfrac{\boldsymbol{I}}{r}+\dfrac{x\otimes x}{r^3}\right]$,

$$\partial_k\boldsymbol{E}_{ij}(x)=\frac{1}{8\pi r^2}\left[-\delta_{ij}\hat{x}_k+\delta_{ik}\hat{x}_j+\delta_{jk}\hat{x}_i-3\hat{x}_i\hat{x}_j\hat{x}_k\right], \tag{B38}$$

$$\begin{aligned}\partial_{kl}\boldsymbol{E}_{ij}(x)=\frac{1}{8\pi r^3}\big[&\left(-\delta_{ij}\delta_{kl}+\delta_{ik}\delta_{jl}+\delta_{jk}\delta_{il}\right)\\&-3\left(-\delta_{ij}\hat{x}_k\hat{x}_l+\delta_{ik}\hat{x}_j\hat{x}_l+\delta_{jk}\hat{x}_i\hat{x}_l+\delta_{il}\hat{x}_j\hat{x}_k+\delta_{jl}\hat{x}_i\hat{x}_k+\delta_{kl}\hat{x}_i\hat{x}_j\right)\\&+15\hat{x}_i\hat{x}_j\hat{x}_k\hat{x}_l\big];\end{aligned} \tag{B39}$$

(ii) $\boldsymbol{F}(x)=\dfrac{3x\otimes x-r^2\boldsymbol{I}}{r^5}$,

$$\partial_k\boldsymbol{F}_{ij}(x)=\frac{1}{r^4}\left[3\left(\delta_{ij}\hat{x}_k+\delta_{ik}\hat{x}_j+\delta_{jk}\hat{x}_i\right)-15\hat{x}_i\hat{x}_j\hat{x}_k\right], \tag{B40}$$

$$\begin{aligned}\partial_{kl}\boldsymbol{F}_{ij}(x)=\frac{1}{r^5}\big[&3\left(\delta_{ik}\delta_{jl}+\delta_{jk}\delta_{il}+\delta_{kl}\delta_{ij}\right)\\&-15\left(\delta_{ij}\hat{x}_k\hat{x}_l+\delta_{il}\hat{x}_j\hat{x}_k+\delta_{jl}\hat{x}_i\hat{x}_k+\delta_{kl}\hat{x}_i\hat{x}_j+\delta_{ik}\hat{x}_j\hat{x}_l+\delta_{jk}\hat{x}_i\hat{x}_l\right)\\&+105\hat{x}_i\hat{x}_j\hat{x}_k\hat{x}_l\big]\end{aligned} \tag{B41}$$

(iii) $\boldsymbol{Q}(x)=\left(1-\dfrac{w}{1+w}\dfrac{1}{r}\right)\boldsymbol{Q}_*+\dfrac{w}{3+w}\dfrac{1}{r^3}\boldsymbol{Q}_b=\left(1-\dfrac{w}{1+w}\dfrac{1}{r}\right)\boldsymbol{Q}_*+\dfrac{ws_*}{3(3+w)}\boldsymbol{F}(x)$,

where $\boldsymbol{Q}_{*ij}=n_{*i}n_{*j}-\dfrac{1}{3}\delta_{ij}$,

$$\begin{aligned}\partial_k\boldsymbol{Q}_{ij}(x)=&\frac{w}{(1+w)r^2}\hat{x}_k\boldsymbol{Q}_{*ij}\\&+\frac{ws_*}{(3+w)r^4}\left[\delta_{ij}\hat{x}_k+\delta_{ik}\hat{x}_j+\delta_{jk}\hat{x}_i-5\hat{x}_i\hat{x}_j\hat{x}_k\right],\end{aligned} \tag{B42}$$

https://doi.org/10.1017/jfm.2025.10821 Published online by Cambridge University Press

$$\begin{aligned}\partial_{kl}\boldsymbol{Q}_{ij}(x) = &-\frac{w}{(1+w)r^3}\big[-\delta_{kl}+3\hat{x}_k\hat{x}_l\big]\boldsymbol{Q}_{*ij}\\ &+\frac{ws_*}{(3+w)r^5}\big[\big(\delta_{ik}\delta_{jl}+\delta_{jk}\delta_{il}+\delta_{kl}\delta_{ij}\big)\\ &-5\big(\delta_{ij}\hat{x}_k\hat{x}_l+\delta_{il}\hat{x}_j\hat{x}_k+\delta_{jl}\hat{x}_i\hat{x}_k+\delta_{kl}\hat{x}_i\hat{x}_j+\delta_{ik}\hat{x}_j\hat{x}_l+\delta_{jk}\hat{x}_i\hat{x}_l\big)\\ &+35\hat{x}_i\hat{x}_j\hat{x}_k\hat{x}_l\big].\end{aligned} \tag{B43}$$

We now recall the operation (4.24), (4.25) and (B27) for $\mathcal{B}_\gamma$:

$$\big(\operatorname{div}\big(\mathcal{B}_\gamma[\nabla \boldsymbol{v}]\big)\big)_i = \big(\mathcal{M}_\gamma : D^2\boldsymbol{v}\big)_i = \sum_{p=1,\dots 7,10,11}\gamma_p\mathcal{M}^p_{i,j;k,l}\partial_{kl}\boldsymbol{v}_j. \tag{B44}$$

Given any matrix valued function $\boldsymbol{F}(x)=\{\boldsymbol{F}_{ij}(x)\}_{1\le i,j\le 3}$, upon introducing the contraction

$$\big(\mathcal{M}^p : D^2\mathbf{F}big\big)_{ij} = \mathcal{M}^p_{i,m;,k,l}\partial_{kl}\mathbf{F}_{mj}, \tag{B45}$$

we have

$$\big(\mathcal{M}^p : D^2(\boldsymbol{F}\boldsymbol{v}_*)\big)_i = \big(\mathcal{M}^p_{i,m;k,l}\partial_{kl}\boldsymbol{F}_{mj}\big)\boldsymbol{v}_{*j}. \tag{B46}$$

Note that we will only consider those $\mathbf{F}$ such that $\mathbf{F}\boldsymbol{v}_*$ is divergence free for all $\boldsymbol{v}_*$, i.e.

$$\partial_i\mathbf{F}_{ik} = 0 \quad \text{for all } k. \tag{B47}$$

This condition is indeed satisfied by $\boldsymbol{F}=\boldsymbol{E}$ (3.9), $\boldsymbol{E}_S$ (3.38), and hence $\boldsymbol{F}$ (3.36).

With the above, we proceed to find the following expressions,

(i) Formula for $(\mathcal{M}^p : D^2\boldsymbol{E})_{ij}(x) = \mathcal{M}^p_{i,m;k,l}\partial_{kl}\boldsymbol{E}_{mj}(x)$. From (B28), we need to compute the following:

$$\begin{aligned}&\big\{\delta_{kl}\delta_{im},\quad \delta_{kl}n_{*i}n_{*m},\quad \delta_{im}n_{*k}n_{*l},\quad \delta_{ik}n_{*l}n_{*m},\quad n_{*i}n_{*m}n_{*k}n_{*l}\big\}\times\partial_{kl}\boldsymbol{E}_{mj}(x)\\ &=\big\{\delta_{kl}\delta_{im},\quad \delta_{kl}n_{*i}n_{*m},\quad \delta_{im}n_{*k}n_{*l},\quad \delta_{ik}n_{*l}n_{*m},\quad n_{*i}n_{*m}n_{*k}n_{*l}\big\}\times\\ &\quad\frac{1}{8\pi r^3}\big[\big(-\delta_{mj}\delta_{kl}+\delta_{mk}\delta_{jl}+\delta_{jk}\delta_{ml}\big)\\ &\qquad -3\big(-\delta_{mj}\hat{x}_k\hat{x}_l+\delta_{mk}\hat{x}_j\hat{x}_l+\delta_{jk}\hat{x}_m\hat{x}_l+\delta_{ml}\hat{x}_j\hat{x}_k+\delta_{jl}\hat{x}_m\hat{x}_k+\delta_{kl}\hat{x}_m\hat{x}_j\big)\\ &\qquad +15\hat{x}_m\hat{x}_j\hat{x}_k\hat{x}_l\big].\end{aligned} \tag{B48}$$

We tabulate the result in the following:

$$\begin{aligned}\delta_{kl}\delta_{im}\partial_{kl}\boldsymbol{E}_{mj}(x) &= \frac{1}{8\pi r^3}\big[2\delta_{ij}-6\hat{x}_i\hat{x}_j\big]\\ \delta_{kl}n_{*i}n_{*m}\partial_{kl}\boldsymbol{E}_{mj}(x) &= \frac{1}{8\pi r^3}\big[2n_{*i}n_{*j}-6n_{*i}\hat{x}_j\langle n,\hat{x}\rangle\big]\\ \delta_{im}n_{*k}n_{*l}\partial_{kl}\boldsymbol{E}_{mj}(x) &= \frac{1}{8\pi r^3}\big[-\delta_{ij}+2n_{*i}n_{*j}+3\delta_{ij}\langle n_*,\hat{x}\rangle^2\\ &\qquad -6(n_{*i}\hat{x}_j+n_{*j}\hat{x}_i)\langle n_*,\hat{x}\rangle-3\hat{x}_i\hat{x}_j+15\hat{x}_i\hat{x}_j\langle n_*,\hat{x}\rangle^2\big]\\ \delta_{ik}n_{*l}n_{*m}\partial_{kl}\boldsymbol{E}_{mj}(x) &= \frac{1}{8\pi r^3}\big[\delta_{ij}-3\delta_{ij}\langle n_*,\hat{x}\rangle^2-6n_{*i}x_j\langle n_*,\hat{x}\rangle-3\hat{x}_i\hat{x}_j\\ &\qquad +15\hat{x}_i\hat{x}_j\langle a,\hat{x}\rangle^2\big]\\ n_{*i}n_{*m}n_{*k}n_{*l}\partial_{kl}\boldsymbol{E}_{mj}(x) &= \frac{1}{8\pi r^3}\big[n_{*i}n_{*j}-3n_{*i}n_{*j}\langle n_*,\hat{x}\rangle^2-9n_{*i}\hat{x}_j\langle n_*,\hat{x}\rangle\\ &\qquad +15n_{*i}\hat{x}_j\langle n_*,\hat{x}\rangle^3\big].\end{aligned} \tag{B49}$$

https://doi.org/10.1017/jfm.2025.10821 Published online by Cambridge University Press

With the above, we have explicitly,

$$\begin{aligned}
\mathcal{M}^1 : D^2\boldsymbol{E}(x) &= \frac{s_*^2}{8\pi r^3}\big[-\big(1-3\langle n_*,\hat{x}\rangle^2\big)\boldsymbol{I}+2n_*\otimes n_*-3\langle n_*,\hat{x}\rangle\big(n_*\otimes\hat{x}+\hat{x}\otimes n_*\big)\big]\\
\mathcal{M}^2 : D^2\boldsymbol{E}(x) &= \frac{s_*}{8\pi r^3}\big[\big(1-3\langle n_*,\hat{x}\rangle^2\big)\boldsymbol{I}+3\big(1-5\langle n_*,\hat{x}\rangle^2\big)\hat{x}\otimes\hat{x}+6\langle n_*,\hat{x}\rangle\hat{x}\otimes n_*\big]\\
\mathcal{M}^3 : D^2\boldsymbol{E}(x) &= \frac{1}{8\pi r^3}\frac{s_*^2}{6}\big[\big(1-3\langle n_*,\hat{x}\rangle^2\big)\boldsymbol{I}+3\big(1-5\langle n_*,\hat{x}\rangle^2\big)\hat{x}\otimes\hat{x}+6\langle n_*,\hat{x}\rangle\hat{x}\otimes n_*\big]\\
\mathcal{M}^4 : D^2\boldsymbol{E}(x) &= \frac{s_*}{8\pi r^3}\big[-\frac{2}{3}\boldsymbol{I}+2n_*\otimes n_*-\big(1-15\langle n_*,\hat{x}\rangle^2\big)\hat{x}\otimes\hat{x}\\
&\qquad -9\langle n_*,\hat{x}\rangle n_*\otimes\hat{x}-3\langle n_*,\hat{x}\rangle\hat{x}\otimes n_*\big]\\
\mathcal{M}^5 : D^2\boldsymbol{E}(x) &= \frac{1}{8\pi r^3}\frac{s_*^2}{6}\Big[\frac{4}{3}\boldsymbol{I}+4n_*\otimes n_*-10\big(1-3\langle n_*,\hat{x}\rangle^2\big)\hat{x}\otimes\hat{x}\\
&\qquad -18\langle n_*,\hat{x}\rangle n_*\otimes\hat{x}-6\langle n_*,\hat{x}\rangle\hat{x}\otimes n_*\Big]\\
\mathcal{M}^6 : D^2\boldsymbol{E}(x) &= \frac{s_*^2}{8\pi r^3}\Big[-\Big(\frac{1}{3}-\langle n_*,\hat{x}\rangle^2\Big)\boldsymbol{I}+\big(1-3\langle n_*,\hat{x}\rangle^2\big)n_*\otimes n_*\\
&\qquad +\big(1-10\langle n_*,\hat{x}\rangle^2\big)\hat{x}\otimes\hat{x}-7\langle n_*,\hat{x}\rangle n_*\otimes\hat{x}+15\langle n_*,\hat{x}\rangle^3 n\otimes\hat{x}\Big]\\
\mathcal{M}^7 : D^2\boldsymbol{E}(x) &= \frac{s_*^2}{8\pi r^3}\Big[\frac{2}{3}\boldsymbol{I}-2\hat{x}\otimes\hat{x}\Big]\\
\mathcal{M}^{10} : D^2\boldsymbol{E}(x) &= \frac{1}{8\pi r^3}\frac{2s_*^3}{3}\big[\big(1-3\langle n_*,\hat{x}\rangle^2\big)n_*\otimes n_*-9\langle n_*,\hat{x}\rangle n_*\otimes\hat{x}\\
&\quad +15\langle n_*,\hat{x}\rangle^3 n_*\otimes\hat{x}\big]\\
\mathcal{M}^{11} : D^2\boldsymbol{E}(x) &= \frac{1}{8\pi r^3}\frac{2s_*^4}{3}\Big[-\Big(\frac{1}{3}-\langle n_*,\hat{x}\rangle^2\Big)\boldsymbol{I}+\big(1-3\langle n_*,\hat{x}\rangle^2\big)n_*\otimes n_*\\
&\quad +\big(1-10\langle n_*,\hat{x}\rangle^2\big)\hat{x}\otimes\hat{x}-7\langle n_*,\hat{x}\rangle n_*\otimes\hat{x}+15\langle n_*,\hat{x}\rangle^3 n_*\otimes\hat{x}\Big].
\end{aligned}\tag{B50}$$

We note that $\mathcal{M}^3=(s_*/6)\mathcal{M}^2$, $\mathcal{M}^{11}=(2s_*^2/3)\mathcal{M}^6$.

(ii) Formula for $\mathcal{M}_\gamma : D^2\boldsymbol{F}(x)$. Similarly, we need to compute the following:

$$\begin{aligned}
&\big\{\delta_{kl}\delta_{im},\quad \delta_{kl}n_{*i}n_{*m},\quad \delta_{im}n_{*k}n_{*l},\quad \delta_{ik}n_{*l}n_{*m},\quad n_{*i}n_{*m}n_{*k}n_{*l}\big\}\times\partial_{kl}\boldsymbol{F}_{mj}(x)\\
&=\big\{\delta_{kl}\delta_{im},\quad \delta_{kl}n_{*i}n_{*m},\quad \delta_{im}n_{*k}n_{*l},\quad \delta_{ik}n_{*l}n_{*m},\quad n_{*i}n_{*m}n_{*k}n_{*l}\big\}\times\\
&\quad\frac{1}{r^5}\big[3\big(\delta_{mk}\delta_{jl}+\delta_{jk}\delta_{ml}+\delta_{kl}\delta_{mj}\big)\\
&\qquad -15\big(\delta_{mj}\hat{x}_k\hat{x}_l+\delta_{ml}\hat{x}_j\hat{x}_k+\delta_{jl}\hat{x}_m\hat{x}_k+\delta_{kl}\hat{x}_m\hat{x}_j+\delta_{mk}\hat{x}_j\hat{x}_l+\delta_{jk}\hat{x}_m\hat{x}_l\big)\\
&\qquad +105\hat{x}_m\hat{x}_j\hat{x}_k\hat{x}_l\big].
\end{aligned}\tag{B51}$$

We again tabulate the result in the following:

$$\begin{aligned}
\delta_{kl}\delta_{im}\partial_{kl}\boldsymbol{F}_{mj}(x)&=0\\
\delta_{kl}n_{*i}n_{*m}\partial_{kl}\boldsymbol{F}_{mj}(x)&=0\\
\delta_{im}n_{*k}n_{*l}\partial_{kl}\boldsymbol{F}_{mj}(x)&=\frac{1}{r^5}\big[3\delta_{ij}-15\delta_{ij}\langle n_*,\hat{x}\rangle^2+6n_{*i}n_{*j}-15\hat{x}_i\hat{x}_j
\end{aligned}$$

https://doi.org/10.1017/jfm.2025.10821 Published online by Cambridge University Press

$$-30(n_{*i}\hat{x}_j + n_{*j}\hat{x}_i)\langle a,\hat{x}\rangle + 105\hat{x}_i\hat{x}_j\langle n_*,\hat{x}\rangle^2\big]$$

$$\delta_{ik}n_{*l}n_{*m}\partial_{kl}\boldsymbol{F}_{mj}(x) = \frac{1}{r^5}\big[3\delta_{ij} - 15\delta_{ij}\langle n_*,\hat{x}\rangle^2 + 6n_{*i}n_{*j} - 15\hat{x}_i\hat{x}_j$$
$$-30(n_{*i}x_j + n_{*j}\hat{x}_i)\langle a,\hat{x}\rangle + 105\hat{x}_i\hat{x}_j\langle n_*,\hat{x}\rangle^2\big]$$

$$n_{*i}n_{*m}n_{*k}n_{*l}\partial_{kl}\boldsymbol{F}_{mj}(x) = \frac{1}{r^5}\big[9n_{*i}n_{*j} - 45n_{*i}n_{*j}\langle a,\hat{x}\rangle^2 - 45n_{*i}\hat{x}_j\langle n_*,\hat{x}\rangle$$
$$+105n_{*i}\hat{x}_j\langle n_*,\hat{x}\rangle^3\big]. \tag{B52}$$

Similar to $\mathcal{M}_\gamma : D^2\boldsymbol{E}$, we have the following:

$$\mathcal{M}^1 : D^2\boldsymbol{F}(x) = 0$$

$$\mathcal{M}^2 : D^2\boldsymbol{F}(x) = -\frac{s_*}{r^5}\big[3\big(1-5\langle n_*,\hat{x}\rangle^2\big)\boldsymbol{I} + 6n_*\otimes n_* - 15(1-7\langle n_*,\hat{x}\rangle^2)\hat{x}\otimes\hat{x}$$
$$-30\langle n_*,\hat{x}\rangle\big(n_*\otimes\hat{x} + \hat{x}\otimes n_*\big)\big]$$

$$\mathcal{M}^3 : D^2\boldsymbol{F}(x) = -\frac{s_*^2}{6r^5}\big[3\big(1-5\langle n_*,\hat{x}\rangle^2\big)\boldsymbol{I} + 6n_*\otimes n_* - 15(1-7\langle n_*,\hat{x}\rangle^2)\hat{x}\otimes\hat{x}$$
$$-30\langle n_*,\hat{x}\rangle\big(n_*\otimes\hat{x} + \hat{x}\otimes n_*\big)\big]$$

$$\mathcal{M}^4 : D^2\boldsymbol{F}(x) = \frac{s_*}{r^5}\big[3\big(1-5\langle n_*,\hat{x}\rangle^2\big)\boldsymbol{I} + 6n_*\otimes n_* - 15(1-7\langle n,\hat{x}\rangle^2)\hat{x}\otimes\hat{x}$$
$$-30\langle n_*,\hat{x}\rangle\big(n_*\otimes\hat{x} + \hat{x}\otimes n_*\big)\big]$$

$$\mathcal{M}^5 : D^2\boldsymbol{F}(x) = \frac{s_*^2}{3r^5}\big[3\big(1-5\langle n_*,\hat{x}\rangle^2\big)\boldsymbol{I} + 6n_*\otimes n_* - 15(1-7\langle n_*,\hat{x}\rangle^2)\hat{x}\otimes\hat{x}$$
$$-30\langle n_*,\hat{x}\rangle\big(n_*\otimes\hat{x} + \hat{x}\otimes n_*\big)\big]$$

$$\mathcal{M}^6 : D^2\boldsymbol{F}(x) = \frac{s_*^2}{r^5}\big[-\big(1-5\langle n_*,\hat{x}\rangle^2\big)\boldsymbol{I} + \big(7-45\langle n_*,\hat{x}\rangle^2\big)n_*\otimes n_*$$
$$+5\big(1-7\langle n_*,\hat{x}\rangle^2\big)\hat{x}\otimes\hat{x} + 35\big(-\langle n_*,\hat{x}\rangle + 3\langle n_*,\hat{x}\rangle^3\big)n_*\otimes\hat{x}$$
$$+10\langle n_*,\hat{x}\rangle\hat{x}\otimes n_*\big]$$

$$\mathcal{M}^7 : D^2\boldsymbol{F}(x) = 0$$

$$\mathcal{M}^{10} : D^2\boldsymbol{F}(x) = \frac{2s_*^3}{3r^5}\big[9\big(1-5\langle n_*,\hat{x}\rangle^2\big)n_*\otimes n_* + \big(-45\langle n_*,\hat{x}\rangle + 105\langle n_*,\hat{x}\rangle^3\big)n_*\otimes\hat{x}\big]$$

$$\mathcal{M}^{11} : D^2\boldsymbol{F} = \frac{2s_*^4}{3r^5}\big[-\big(1-5\langle n_*,\hat{x}\rangle^2\big)\boldsymbol{I} + \big(7-45\langle n_*,\hat{x}\rangle^2\big)n_*\otimes n_*$$
$$+5\big(1-7\langle n_*,\hat{x}\rangle^2\big)\hat{x}\otimes\hat{x} + 35\big(-\langle n_*,\hat{x}\rangle + 3\langle n_*,\hat{x}\rangle^3\big)n_*\otimes\hat{x}$$
$$+10\langle n_*,\hat{x}\rangle\hat{x}\otimes n_*\big]. \tag{B53}$$

From the above, we can conclude that $\mathcal{M} : D^2\boldsymbol{E}$ and $\mathcal{M} : D^2\boldsymbol{F}$ are linear combinations of the following matrices:

$$\boldsymbol{I},\quad n_*\otimes n_*,\quad \hat{x}\otimes\hat{x},\quad n_*\otimes\hat{x},\quad \hat{x}\otimes n_*, \tag{B54}$$

https://doi.org/10.1017/jfm.2025.10821 Published online by Cambridge University Press

with coefficients given by $\langle n, \hat{x}\rangle^k$ for $k = 0, 1, 2, 3$. Concisely, we can write

$$\begin{aligned}&\mathcal{M}_\gamma : D^2\boldsymbol{E}(x)\\ &= \frac{1}{r^3}\big[f_1(\langle n_*, \hat{x}\rangle)\boldsymbol{I} + f_2(\langle n_*, \hat{x}\rangle)n_* \otimes n_* + f_3(\langle n_*, \hat{x}\rangle)\hat{x} \otimes \hat{x} + f_4(\langle n_*, \hat{x}\rangle)n_* \otimes \hat{x},\\ &\quad + f_5(\langle n_*, \hat{x}\rangle)\hat{x} \otimes n_*\big]\end{aligned} \tag{B55}$$

and

$$\begin{aligned}&\mathcal{M}_\gamma : D^2\boldsymbol{F}(x)\\ &= \frac{1}{r^5}\big[g_1(\langle n_*, \hat{x}\rangle)\boldsymbol{I} + g_2(\langle n_*, \hat{x}\rangle)n_* \otimes n_* + g_3(\langle n_*, \hat{x}\rangle)\hat{x} \otimes \hat{x} + g_4(\langle n_*, \hat{x}\rangle)n_* \otimes \hat{x},\\ &+ g_5(\langle n_*, \hat{x}\rangle)\hat{x} \otimes n_*\big]\end{aligned} \tag{B56}$$

where the f_i and g_i's are polynomials of degree at most three.

B.4 *Formula for $\mathcal{C}_\gamma$ and $\mathcal{D}_\gamma$*

Here we express $\mathcal{C}_\gamma$ and $\mathcal{D}_\gamma$ in more transparent forms.

(a) For $\mathcal{C}_\gamma$, from (4.21), we compute

$$\begin{aligned}\mathcal{C}_\gamma &= \boldsymbol{T}^v_{SV} - \boldsymbol{A} - \mathcal{B}_\gamma[\nabla \boldsymbol{v}]] - \mathcal{A}_\gamma(x)\\ &= \gamma_1\Big[\big(\boldsymbol{Q}\,(\boldsymbol{v}\cdot\nabla\boldsymbol{Q}) - (\boldsymbol{v}\cdot\nabla\boldsymbol{Q})\,\boldsymbol{Q}\big) + \big(\boldsymbol{Q}^2\boldsymbol{W} - 2\boldsymbol{Q}\boldsymbol{W}\boldsymbol{Q} + \boldsymbol{W}\boldsymbol{Q}^2\big)\\ &\qquad - \big(\boldsymbol{Q}_*(\boldsymbol{v}_*\cdot\nabla\boldsymbol{Q}) - (\boldsymbol{v}_*\cdot\nabla\boldsymbol{Q})\boldsymbol{Q}_*\big) - \big(\boldsymbol{Q}_*^2\boldsymbol{W} - 2\boldsymbol{Q}_*\boldsymbol{W}\boldsymbol{Q}_* + \boldsymbol{W}\boldsymbol{Q}_*^2\big)\Big]\\ &\quad + \gamma_2\Big[\big(\boldsymbol{v} - \boldsymbol{v}_*\big)\cdot\nabla\boldsymbol{Q} + \big(\boldsymbol{Q} - \boldsymbol{Q}_*\big)\nabla\boldsymbol{v} - (\nabla\boldsymbol{v})\big(\boldsymbol{Q} - \boldsymbol{Q}_*\big)\Big]\\ &\quad + \frac{\gamma_3}{2}\Big[\Big(\boldsymbol{Q}(\boldsymbol{v}\cdot\nabla\boldsymbol{Q}) + (\boldsymbol{v}\cdot\nabla\boldsymbol{Q})\boldsymbol{Q} + \boldsymbol{Q}^2\nabla\boldsymbol{v} - (\nabla\boldsymbol{v})\boldsymbol{Q}^2\Big)\\ &\qquad - \big(\boldsymbol{Q}_*(\boldsymbol{v}_*\cdot\nabla\boldsymbol{Q}) + (\boldsymbol{v}_*\cdot\nabla\boldsymbol{Q})\boldsymbol{Q}_*\big) - \Big(\boldsymbol{Q}_*^2(\nabla\boldsymbol{v}) - (\nabla\boldsymbol{v})\boldsymbol{Q}_*^2\Big)\Big]\\ &\quad + \gamma_4\Big[(\boldsymbol{Q} - \boldsymbol{Q}_*)\boldsymbol{A} + \boldsymbol{A}(\boldsymbol{Q} - \boldsymbol{Q}_*)\Big]\\ &\quad + \gamma_5\Big[(\boldsymbol{Q}^2 - \boldsymbol{Q}_*^2)\boldsymbol{A} + \boldsymbol{A}(\boldsymbol{Q}^2 - \boldsymbol{Q}_*^2)\Big]\\ &\quad + \gamma_6\Big[(\boldsymbol{A}\cdot\boldsymbol{Q})\boldsymbol{Q} - (\boldsymbol{A}\cdot\boldsymbol{Q}_*)\boldsymbol{Q}_*\Big]\\ &\quad + \gamma_7\Big[\Big(|\boldsymbol{Q}^2| - |\boldsymbol{Q}_*^2|\Big)\boldsymbol{A}\Big]\\ &\quad + \gamma_9\Big[\big((\boldsymbol{v}\cdot\nabla\boldsymbol{Q})\cdot\boldsymbol{Q}\big)\boldsymbol{Q} - \Big((\boldsymbol{v}_*\cdot\nabla\boldsymbol{Q})\cdot\boldsymbol{Q}_*\Big)\boldsymbol{Q}_*\Big]\\ &\quad + \gamma_{10}\Big[\big(\boldsymbol{Q}^2\cdot\boldsymbol{A}\big)\boldsymbol{Q} + (\boldsymbol{Q}\cdot\boldsymbol{A})\boldsymbol{Q}^2 - (\boldsymbol{Q}_*^2\cdot\boldsymbol{A})\boldsymbol{Q}_* - (\boldsymbol{Q}_*\cdot\boldsymbol{A})\boldsymbol{Q}_*^2\Big]\\ &\quad + \gamma_{11}\big[|\boldsymbol{Q}|^2(\boldsymbol{A}\cdot\boldsymbol{Q})\boldsymbol{Q} - |\boldsymbol{Q}_*|^2(\boldsymbol{A}\cdot\boldsymbol{Q}_*)\boldsymbol{Q}_*\big]\\ &\sim O\left(\frac{1}{r^3}\right).\end{aligned} \tag{B57}$$

https://doi.org/10.1017/jfm.2025.10821 Published online by Cambridge University Press

(*b*) For $\mathcal{D}_\gamma$, from (4.2), we have

$$\begin{aligned}\mathcal{D}_\gamma = -\Big[&\gamma_1\big(\boldsymbol{v}_*\cdot\nabla\boldsymbol{Q}+\boldsymbol{Q}_*\boldsymbol{W}-\boldsymbol{W}\boldsymbol{Q}_*+(\boldsymbol{v}-\boldsymbol{v}_*)\cdot\nabla\boldsymbol{Q}+(\boldsymbol{Q}-\boldsymbol{Q}_*)\boldsymbol{W}-\boldsymbol{W}(\boldsymbol{Q}-\boldsymbol{Q}_*)\big)\\ &+\gamma_2\boldsymbol{A}+\frac{\gamma_3}{2}\big(\boldsymbol{A}\boldsymbol{Q}_*+\boldsymbol{Q}_*\boldsymbol{A}+\boldsymbol{A}(\boldsymbol{Q}-\boldsymbol{Q}_*)+(\boldsymbol{Q}-\boldsymbol{Q}_*)\boldsymbol{A}\big)\\ &+\gamma_9\big((\boldsymbol{A}\cdot\boldsymbol{Q}_*+\boldsymbol{A}\cdot(\boldsymbol{Q}-\boldsymbol{Q}_*))\boldsymbol{Q}_*+(\boldsymbol{A}\cdot\boldsymbol{Q}_*+\boldsymbol{A}\cdot(\boldsymbol{Q}-\boldsymbol{Q}_*))(\boldsymbol{Q}-\boldsymbol{Q}_*)\big)\Big]\cdot\partial_i\boldsymbol{Q}\mathbf{e}_i\\ &\sim O\left(\frac{1}{r^4}\right).\end{aligned} \tag{B58}$$

Note that given $\boldsymbol{Q}$, both $\mathcal{C}_\gamma$ and $\mathcal{D}_\gamma$ are linear in $\boldsymbol{v}$.

From the form of $\mathcal{C}_\gamma$ and $\mathcal{D}_\gamma$, it can be seen that they involve multiplications between the following matrices:

$$\boldsymbol{A},\quad \boldsymbol{W},\quad \boldsymbol{Q}_*,\quad \boldsymbol{Q},\quad \boldsymbol{v}_*\cdot\nabla\boldsymbol{Q},\quad \boldsymbol{v}\cdot\nabla\boldsymbol{Q}. \tag{B59}$$

(i) For $\boldsymbol{A}$, $\boldsymbol{W}$, note that $\boldsymbol{v}=\boldsymbol{E}_S\boldsymbol{v}_*$ so that $\partial_j\boldsymbol{v}_i=\partial_j(\boldsymbol{E}_{Sil}\boldsymbol{v}_{*l})$ and $\partial_i\boldsymbol{v}_j=\partial_i(\boldsymbol{E}_{Sjl}\boldsymbol{v}_{*l})$. From (3.38), we have

$$\boldsymbol{E}_{Sil}\in\left[1,\frac{1}{r},\frac{1}{r^3}\right]\left\{\delta_{il},\hat{x}_i\hat{x}_l\right\} \tag{B60}$$

$$\partial_j\boldsymbol{E}_{Sil},\quad \partial_i\boldsymbol{E}_{Sjl}\in\left[\frac{1}{r^2},\frac{1}{r^4}\right]\left\{\delta_{il}\hat{x}_j,\quad \delta_{ij}\hat{x}_l,\quad \delta_{jl}\hat{x}_i,\quad \hat{x}_i\hat{x}_j\hat{x}_l\right\}. \tag{B61}$$

Thus,

$$\begin{aligned}\boldsymbol{A},\quad \boldsymbol{W}&\in\left\{\partial_j\boldsymbol{E}_{Sil}\boldsymbol{v}_{*l},\quad \partial_i\boldsymbol{E}_{Sjl}\boldsymbol{v}_{*l}\right\}\\ &=\left[\frac{1}{r^2},\frac{1}{r^4}\right]\left\{\delta_{il}\hat{x}_j\boldsymbol{v}_{*l},\quad \delta_{ij}\hat{x}_l\boldsymbol{v}_{*l},\quad \delta_{jl}\hat{x}_i\boldsymbol{v}_{*l},\quad \hat{x}_i\hat{x}_j\hat{x}_l\boldsymbol{v}_{*l}\right\}\\ &=\left[\frac{1}{r^2},\frac{1}{r^4}\right]\left[1,\quad\langle\hat{x},\boldsymbol{v}_*\rangle\right]\left\{\boldsymbol{I},\quad \boldsymbol{v}_*\otimes\hat{x},\quad \hat{x}\otimes\boldsymbol{v}_*,\quad \hat{x}\otimes\hat{x}\right\}.\end{aligned} \tag{B62}$$

(ii) For $\boldsymbol{Q}$, from (3.4)–(3.6), we have $\boldsymbol{Q}_*,\boldsymbol{Q}\in[1,\frac{1}{r},\frac{1}{r^3}]\left\{\boldsymbol{I},\quad n_*\otimes n_*,\quad \hat{x}\otimes\hat{x}\right\}$. Hence,

$$\boldsymbol{Q}_*,\boldsymbol{Q}_*^2,\boldsymbol{Q},\boldsymbol{Q}^2\in\left[1,\frac{1}{r},\ldots,\frac{1}{r^6}\right]\left[1,\langle\hat{x},n_*\rangle\right]\left\{\boldsymbol{I},\quad n_*\otimes n_*,\quad n_*\otimes\hat{x},\quad \hat{x}\otimes n_*,\quad \hat{x}\otimes\hat{x}\right\}. \tag{B63}$$

Furthermore, as $\partial_l\boldsymbol{Q}_{ij}=[(1/r^2),(1/r^4)]\{n_{*i}n_{*j}x_l,\quad \delta_{ij}x_l,\quad x_ix_jx_l,\quad \delta_{il}x_j,\quad \delta_{jl}x_i\}$, $(\boldsymbol{v}_*\cdot\nabla\boldsymbol{Q})_{ij}=\partial_l\boldsymbol{Q}_{ij}\boldsymbol{v}_{*l}$, and $(\boldsymbol{v}\cdot\nabla\boldsymbol{Q})_{ij}=\partial_l\boldsymbol{Q}_{ij}\boldsymbol{v}_l$, we have

$$\begin{aligned}&\boldsymbol{v}_*\cdot\nabla\boldsymbol{Q},\quad \boldsymbol{v}\cdot\nabla\boldsymbol{Q}\\ &\in\left[\frac{1}{r^2},\frac{1}{r^4}\right]\left\{n_{*i}n_{*j}x_l,\quad \delta_{ij}x_l,\quad x_ix_jx_l,\quad \delta_{il}x_j,\quad \delta_{jl}x_i\right\}\left\{\boldsymbol{v}_{*l},\boldsymbol{v}_l\right\}\\ &\in\left[\frac{1}{r^2},\frac{1}{r^4}\right]\left[1,\langle\hat{x},\boldsymbol{v}_*\rangle\right]\left\{\boldsymbol{I},\quad n_*\otimes n_*,\quad \boldsymbol{v}_*\otimes\hat{x},\quad \hat{x}\otimes\boldsymbol{v}_*,\quad \hat{x}\otimes\hat{x}\right\}.\end{aligned} \tag{B64}$$

(iii) From the above, we have

$$\begin{aligned}&\boldsymbol{A}\cdot\boldsymbol{Q}_*,\quad \boldsymbol{A}\cdot\boldsymbol{Q}_*^2,\quad \boldsymbol{A}\cdot\boldsymbol{Q},\quad \boldsymbol{A}\cdot\boldsymbol{Q}^2,\quad |\boldsymbol{Q}_*|^2,\quad |\boldsymbol{Q}|^2,\quad \boldsymbol{Q}_*\cdot(\boldsymbol{v}_*\cdot\nabla\boldsymbol{Q}),\quad \boldsymbol{Q}\cdot(\boldsymbol{v}\cdot\nabla\boldsymbol{Q})\\ &\in\left[1,\frac{1}{r^2},\ldots\frac{1}{r^6}\right]\left[1,\quad\langle x,\boldsymbol{v}_*\rangle,\quad \langle x,n_*\rangle,\quad \langle\boldsymbol{v}_*,n_*\rangle\right].\end{aligned} \tag{B65}$$

https://doi.org/10.1017/jfm.2025.10821 Published online by Cambridge University Press

Hence, taking appropriate products of all the above, we have

$$\mathcal{C}_\gamma \in \left[\frac{1}{r^3}, \ldots, \frac{1}{r^6}\right]\left[1,\ \langle \hat{x}, n_*\rangle,\ \langle \hat{x}, \boldsymbol{v}_*\rangle,\ \langle n_*, \boldsymbol{v}_*\rangle\right]\times \left\{\boldsymbol{I},\ n_*\otimes n_*,\ n_*\otimes \boldsymbol{v}_*,\ \boldsymbol{v}_*\otimes n_*,\ n_*\otimes \hat{x},\ \hat{x}\otimes n_*,\ \boldsymbol{v}_*\otimes \hat{x},\ \hat{x}\otimes \boldsymbol{v}_*,\ \hat{x}\otimes \hat{x}\right\}. \tag{B66}$$

For $\mathcal{D}_\gamma$, note that $\boldsymbol{Q}_{ij} \in [1, (1/r), (1/r^3)]\{\delta_{ij}, n_{*i}n_{*j}, \hat{x}_i\hat{x}_j\}$, we have

$$\partial_k \boldsymbol{Q}_{ij} \in \left[\frac{1}{r^2}, \frac{1}{r^4}\right]\left\{\delta_{ij}x_k,\ n_{*i}n_{*j}x_k,\ \delta_{ik}\hat{x}_j,\ \delta_{jk}\hat{x}_i,\ \hat{x}_i\hat{x}_j\hat{x}_k\right\}. \tag{B67}$$

Hence

$$\mathcal{D}_\gamma \in \left[\frac{1}{r^4}, \ldots, \frac{1}{r^9}\right]\left[1,\ \langle \hat{x}, n_*\rangle,\ \langle \hat{x}, \boldsymbol{v}_*\rangle,\ \langle n_*, \boldsymbol{v}_*\rangle\right]\left\{\hat{x},\ n_*,\ \boldsymbol{v}_*\right\}. \tag{B68}$$

Appendix C. Solution of isotropic Stokes flow in bounded domain

Even though our analysis is in the exterior domain $\mathbb{R}^3\backslash \boldsymbol{B}_a(0)$, the simulation domain is assumed to be an annulus with the inner and outer radii a and R, respectively, with $a \ll R$. As a validation of our numerical code, we verify that our simulations for the standard isotropic Stokes flow match with the analytical solution in this finite domain. We also establish that the solution in the bounded domain retains the same decay properties as that in an infinite domain as long as we stay away from the outer boundary.

We first compute the analytical solution to the Stokes flow in an annular domain $\Omega_{a,R} := \boldsymbol{B}_R(0)\backslash \boldsymbol{B}_a(0)$. In this case, we still have (3.29) and the first part of (3.30). Now the boundary conditions for u_r, u_θ become

$$\begin{aligned} &\text{at } r = a: && u_r = u_\theta = 0;\\ &\text{at } r = R: && u_r = V\cos\theta,\ \ u_\theta = -V\sin\theta \end{aligned} \tag{C1}$$

which are translated to

$$f(a) = 0,\ \ f'(a) = 0,\ \ f(R) = \frac{VR^2}{2},\ \ f'(R) = VR. \tag{C2}$$

The Stokes equation ($-\Delta \boldsymbol{u} + \nabla p = 0$) leads to following form of f:

$$f(r) = \frac{A}{r} + Br + Cr^2 + Dr^4 \tag{C3}$$

where the coefficients are determined by the boundary conditions (C2). We then have the following system of linear equations:

$$\begin{aligned} A + a^2B + a^3C + a^5D &= 0,\\ -A + a^2B + 2a^3C + 4a^5D &= 0,\\ 2A + 2R^2B + 2R^3C + 2R^5D &= VR^3,\\ -A + R^2B + 2R^3C + 4R^5D &= VR^3. \end{aligned} \tag{C4}$$

Upon introducing $\lambda = \dfrac{a}{R}$, the solution to above system is given by,

$$A = \frac{\lambda^3\left(1+\lambda+\lambda^2\right)}{(1-\lambda)^3\left(4+7\lambda+4\lambda^2\right)}R^3V =: \eta_A(\lambda)R^3V, \tag{C5}$$

https://doi.org/10.1017/jfm.2025.10821 Published online by Cambridge University Press

$$B = -\frac{3\lambda\left(1+\lambda+\lambda^2+\lambda^3+\lambda^4\right)}{(1-\lambda)^3\left(4+7\lambda+4\lambda^2\right)}RV =: \eta_B(\lambda)RV, \tag{C6}$$

$$C = \frac{\left(4+\lambda(1+\lambda)\left(4+9\lambda^2\right)\right)}{2(1-\lambda)^3\left(4+7\lambda+4\lambda^2\right)}V =: \eta_C(\lambda)V, \tag{C7}$$

$$D = -\frac{3\lambda\,(1+\lambda)}{2(1-\lambda)^3\left(4+7\lambda+4\lambda^2\right)}\frac{V}{R^2} =: \eta_D(\lambda)\frac{V}{R^2}. \tag{C8}$$

Then we have

$$\begin{aligned} u_r &= \frac{1}{r^2\sin\theta}\frac{\partial\Psi}{\partial\theta} = \frac{2f(r)}{r^2}\cos\theta \\ &= 2V\left(\eta_A(\lambda)\left(\frac{R}{r}\right)^3 + \eta_B(\lambda)\left(\frac{R}{r}\right) + \eta_C(\lambda) + \eta_D(\lambda)\left(\frac{r}{R}\right)^2\right)\cos\theta, \end{aligned} \tag{C9}$$

$$\begin{aligned} u_\theta &= \frac{-1}{r\sin\theta}\frac{\partial\Psi}{\partial r} = -\frac{f'(r)}{r}\sin\theta \\ &= V\left(\eta_A(\lambda)\left(\frac{R}{r}\right)^3 - \eta_B(\lambda)\left(\frac{R}{r}\right) - 2\eta_C(\lambda) - 4\eta_D(\lambda)\left(\frac{r}{R}\right)^2\right)\sin\theta. \end{aligned} \tag{C10}$$

We note the self-similarity or decay structures of the solution. These can be used to benchmark the numerical solution. In particular, if $a \ll R$ so that $\lambda \ll 1$, we have

$$\begin{aligned} &\eta_A(\lambda) = \frac{\lambda^3}{4} + O\left(\lambda^4\right), \quad \eta_B(\lambda) = -\frac{3\lambda}{4} + O\left(\lambda^2\right), \quad \eta_C(\lambda) = \frac{1}{2} + \frac{9\lambda}{8} + O\left(\lambda^2\right), \\ &\eta_D(\lambda) = -\frac{3\lambda}{8} + O\left(\lambda^2\right). \end{aligned} \tag{C11}$$

One can identify three distinct parameter regimes (a) $r \sim a$, (b) $a \ll r \ll R$ and (c) $r \sim R$. We will mostly interested in regime (b) as it corresponds to the flow far away from the particle, yet it is unaffected by the boundary of the computational domain. From (C9) and (C10), we have the following asymptotics:

(a) If $r \sim a$, then $r/R \sim \lambda$, then

$$u_r \sim V\left(1 - \frac{3}{2}\left(\frac{a}{r}\right) + \frac{1}{2}\left(\frac{a}{r}\right)^3\right)\cos\theta \tag{C12}$$

and

$$u_\theta \sim V\left(-1 + \frac{3}{4}\left(\frac{a}{r}\right) + \frac{1}{4}\left(\frac{a}{r}\right)^3\right)\sin\theta. \tag{C13}$$

(b) If $a \ll r \ll R$, then $\lambda \ll r/R \ll 1$, then

$$u_r \sim V\left(1 - \frac{3}{2}\left(\frac{a}{r}\right)\right)\cos\theta \tag{C14}$$

and

$$u_\theta \sim V\left(-1 + \frac{3}{4}\left(\frac{a}{r}\right)\right)\sin\theta. \tag{C15}$$

https://doi.org/10.1017/jfm.2025.10821 Published online by Cambridge University Press

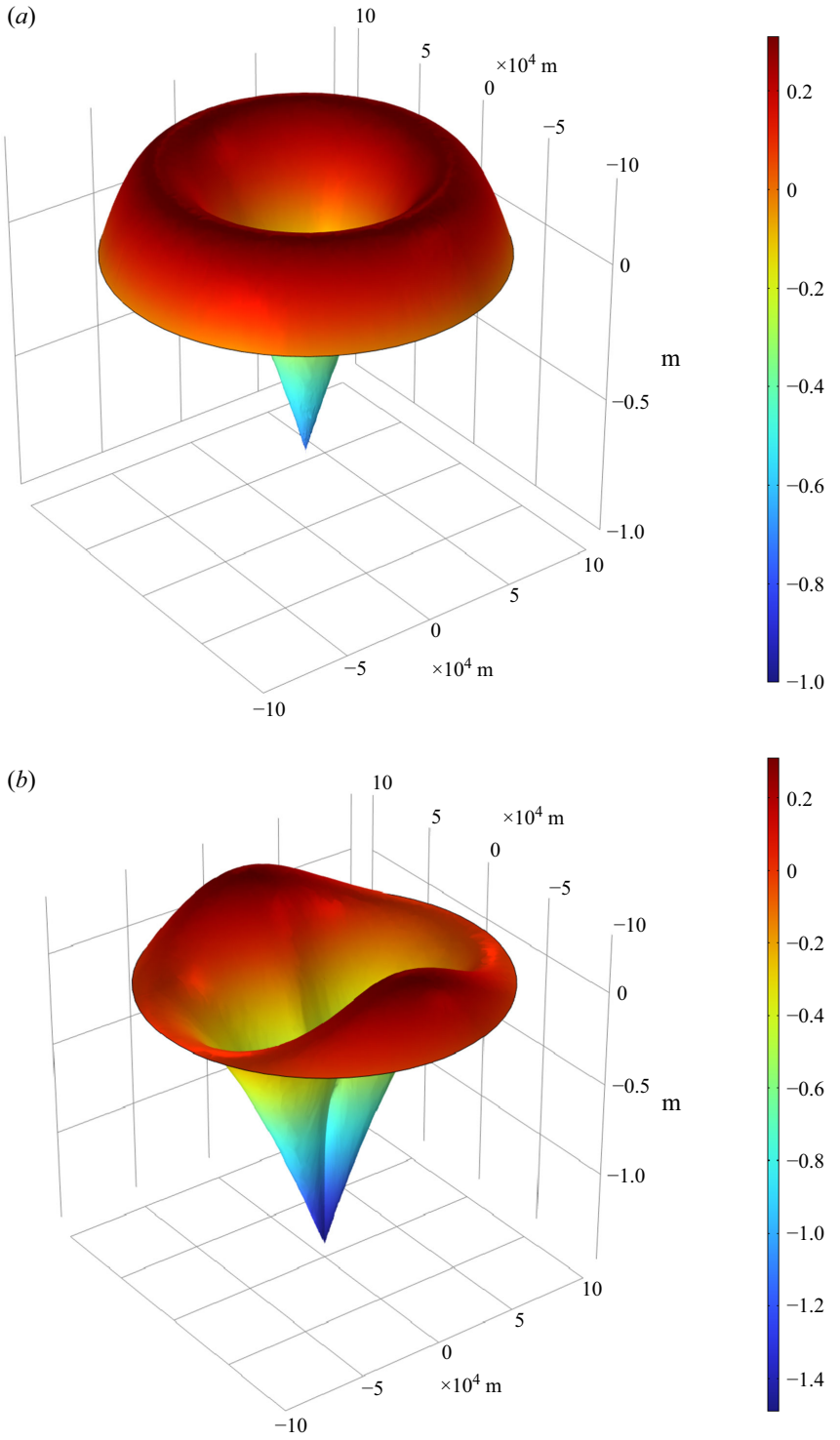

Figure 13. Here $g(r) = r((\boldsymbol{v}_1/V) - 1)$ for classical Stokes flow on $1 < r < 10^5$: (*a*) in yz-plane; (*b*) in xy-plane.

https://doi.org/10.1017/jfm.2025.10821 Published online by Cambridge University Press

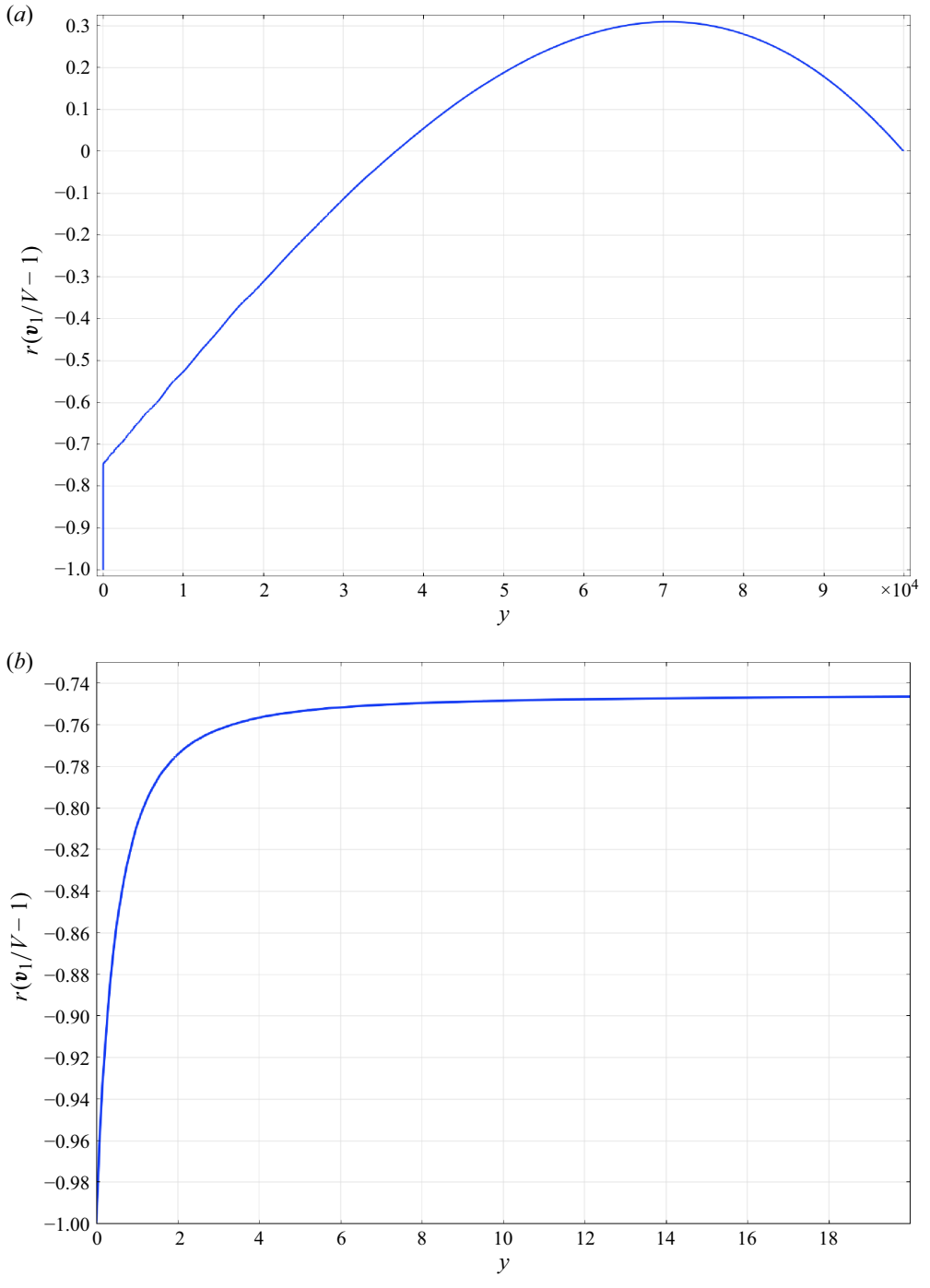

Figure 14. Radial profile (rescaled) $\boldsymbol{v}_1$ for classical Stokes flow (in the yz-plane) $1 < r < 10^5$: (*a*) $g(r) = r((\boldsymbol{v}_1/V) - 1)$; (*b*) zoomed-in version of (*a*).

https://doi.org/10.1017/jfm.2025.10821 Published online by Cambridge University Press

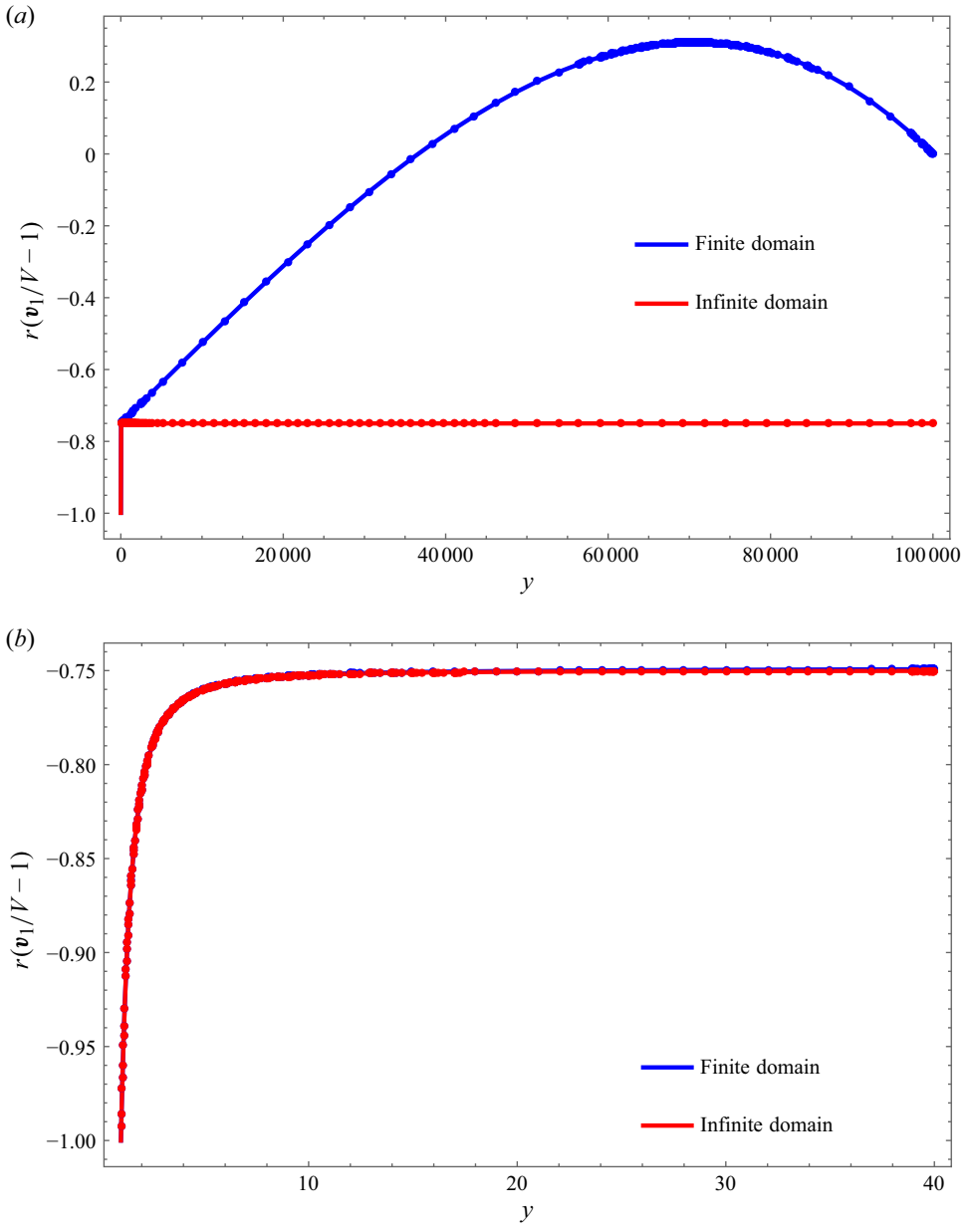

Figure 15. Comparison between the exact analytical rescaled radial profiles (along the y-axis) of $\boldsymbol{v}_1$ for classical Stokes flows, $g(r) = r((\boldsymbol{v}_1/V) - 1)$: (*a*) blue, finite domain ($1 < r < 10^5$); red, infinite domain ($1 < r < \infty$); (*b*) zoomed-in version of (*a*).

(*c*) If $r \sim R$, then

$$u_r \sim V\left(1 + \frac{3}{4}\left(\frac{a}{r}\right)\left(-2 + 3\left(\frac{r}{R}\right) - \left(\frac{r}{R}\right)^3\right)\right)\cos\theta \tag{C16}$$

https://doi.org/10.1017/jfm.2025.10821 Published online by Cambridge University Press

and

$$u_\theta \sim V\left(-1+\frac{3}{4}\left(\frac{a}{r}\right)\left(1-3\left(\frac{r}{R}\right)+2\left(\frac{r}{R}\right)^3\right)\right)\sin\theta. \tag{C17}$$

Note that due to the boundary of the computational domain, as expected, only regimes (a) and (b) are consistent with the exact solution (3.31) and (3.32) in the exterior domain.

In the following, we compute classical Stokes' flow on the domain $1 < r < 10^5$ with $\boldsymbol{v}_* = Ve_1$. We will plot $\boldsymbol{v}_1$ on the yz-plane demonstrating its radially symmetric behaviour. To this end, note that $\boldsymbol{v}_1 = u_r\cos\theta - u_\theta\sin\theta$. On the yz-plane, $\sin\theta = 1$ and hence by (C10) we have

$$\boldsymbol{v}_1 = -u_\theta\Big|_{\sin\theta=1} = -V\left(\eta_A(\lambda)\left(\frac{R}{r}\right)^3 - \eta_B(\lambda)\left(\frac{R}{r}\right) - 2\eta_C(\lambda) - 4\eta_D(\lambda)\left(\frac{r}{R}\right)^2\right). \tag{C18}$$

Our numerical results recover the above three asymptotics (a), (b) and (c). To illustrate this, we plot the rescaled radial profile of $\boldsymbol{v}_1$ for $a \le r \le R$,

$$g(r) := r\left(\frac{\boldsymbol{v}_1}{V} - 1\right) = -r\left(\eta_A(\lambda)\left(\frac{R}{r}\right)^3 - \eta_B(\lambda)\left(\frac{R}{r}\right) - 2\eta_C(\lambda) - 4\eta_D(\lambda)\left(\frac{r}{R}\right)^2 + 1\right). \tag{C19}$$

The results are depicted in figures 13 and 14.

As a further demonstration, in figure 15, we compare the radial behaviour along the y-axis between the analytical solution of $\boldsymbol{v}_1$ in the finite and infinite domain calculations. Although the overall profiles differ, due to the finite size effect, they do coincide very well near the particle, i.e. in regimes $r \sim a$ and $a \ll r \ll R$ indicating the accuracy of our numerical scheme.

References

Abels, H., Dolzmann, G. & Liu, Y.N. 2016 Strong solutions for the Beris-Edwards model for nematic liquid crystals with homogeneous Dirichlet boundary conditions. *Adv. Differential Equations* **21** (1–2), 109–152.

Acheson, D.J. 1990 *Elementary Fluid Dynamics*. Oxford University Press.

Alama, S., Bronsard, L. & Lamy, X. 2016 Minimizers of the Landau–de Gennes energy around a spherical colloid particle. *Arch. Ratl. Mech. Anal.* **222**, 427–450.

Alama, S., Bronsard, L., Lamy, X. & Venkatraman, R. 2023 Far-field expansions for harmonic maps and the electrostatics analogy in nematic suspensions. *J. Nonlinear Sci.* **33** (3), 39.

Alouges, F., Chambolle, A. & Stantejsky, D. 2021 The saturn ring effect in nematic liquid crystals with external field: effective energy and hysteresis. *Arch. Ratl. Mech. Anal.* **241** (3), 1403–1457.

Ball, J.M. 2017*a* Liquid crystals and their defects. In *Mathematical Thermodynamics of Complex Fluids: Cetraro, Italy 2015*, pp. 1–46.

Ball, J.M. 2017*b* Mathematics and liquid crystals. *Mol. Cryst. Liq. Cryst.* **647** (1), 1–27.

Batchelor, G. K. & Green, J.-T. 1972 The hydrodynamic interaction of two small freely-moving spheres in a linear flow field. *J. Fluid Mech.* **56** (2), 375–400.

Beris, A.N. & Edwards, B.J. 1994 Thermodynamics of flowing systems with internal microstructure. In *Oxford Engineering Science Series*, vol. 36. The Clarendon Press, Oxford University Press, New York, Oxford Science Publications.

Blinov, L.M., Kabayenkov, A.Y. & Sonin, A.A. 1989 Invited Lecture. Experimental studies of the anchoring energy of nematic liquid crystals. *Liq. Cryst.* **5** (2), 645–661.

Borthagaray, J.P. & Walker, S.W. 2021 The Q-tensor model with uniaxial constraint. In *Handbook of Numerical Analysis*, vol. **22**, pp. 313–382. Elsevier.

Chandler, T.G.J. & Spagnolie, S.E. 2023 A nematic liquid crystal with an immersed body: equilibrium, stress and paradox. *J. Fluid Mech.* **967**, A19.

https://doi.org/10.1017/jfm.2025.10821 Published online by Cambridge University Press

CHANDLER, T.G.J. & SPAGNOLIE, S.E. 2024*a* Exact and approximate solutions for elastic interactions in a nematic liquid crystal. *Siam J. Appl. Math.* **84** (6), 2476–2501.
CHANDLER, T.G.J. & SPAGNOLIE, S.E. 2024*b* Rigid and deformable bodies in nematic liquid crystals. *Physical Review Fluids* **9** (11), 110511.
CHANG, I.-D. & FINN, R. 1961 On the solutions of a class of equations occurring in continuum mechanics, with application to the stokes paradox. *Arch. Ratl. Mech. Anal.* **7** (1), 388–401.
CHWANG, A.T. & WU, T.Y.-T. 1975 Hydromechanics of low-Reynolds-number flow. Part 2. Singularity method for Stokes flows. *J. Fluid Mech.* **67** (4), 787–815.
COMSOL Multiphysics® v. 5.3. http://www.comsol.com/, COMSOL AB, Stockholm, Sweden.
DE GENNES, P.-G. & PROST, J. 1993 *The Physics of Liquid Crystals*. Oxford University Press.
DIOGO, A.C. 1983 Friction drag on a sphere moving in a nematic liquid crystal. *Mol. Cryst. Liq. Cryst.* **100** (1-2), 153–165.
DU, H., HU, X. & WANG, C. 2020 Suitable weak solutions for the co-rotational beris–edwards system in dimension three. *Arch. Ratl. Mech. Anal.* **238** (2), 749–803.
DU, Q., GUO, B. & SHEN, J. 2001 Fourier spectral approximation to a dissipative system modeling the flow of liquid crystals. *SIAM J. Numer. Anal.* **39** (3), 735–762.
ERICKSEN, J. L. 1987 Continuum theory of nematic liquid crystals. *Res Mech.* **21** (4), 381–392.
ERICKSEN, J.L. 1961 Conservation laws for liquid crystals. *T. Soc. Rheol.* **5** (1), 23–34.
ERICKSEN, J.L. 1991 Liquid crystals with variable degree of orientation. *Arch. Ratl. Mech. Anal.* **113** (2), 97–120.
FUKUDA, J.-I., STARK, H., YONEYA, M. & YOKOYAMA, H. 2004 Dynamics of a nematic liquid crystal around a spherical particle. *J. Phys.: Condens. Matter* **16** (19), S1957.
GALDI, G. 2011 *An Introduction to the Mathematical Theory of the Navier–Stokes Equations: Steady-State Problems*. Springer Science & Business Media.
GALDI, G.P. 1999 On the steady self-propelled motion of a body in a viscous incompressible fluid. *Arch. Ratl. Mech. Anal.* **148** (1), 53–88.
GALDI, G.P. 2002 On the motion of a rigid body in a viscous liquid: a mathematical analysis with applications. In *Handbook of Mathematical Fluid Dynamics*, vol. 1, pp. 653–791. Elsevier.
GÓMEZ-GONZÁLEZ, M. & DEL ÁLAMO, J.C. 2013 Flow of a viscous nematic fluid around a sphere. *J. Fluid Mech.* **725**, 299–331.
GUAZZELLI, E. & MORRIS, J.F. 2012 *A Physical Introduction to Suspension Dynamics*, vol. 45. Cambridge University Press.
HEUER, H., KNEPPE, H. & SCHNEIDER, F. 1992 Flow of a nematic liquid crystal around a sphere. *Mol. Cryst. Liq. Cryst. A* **214** (1), 43–61.
IZAKI, K. & KIMURA, Y. 2013 Interparticle force between different types of nematic colloids. *Phys. Rev. E* **87** (6), 062507.
KISHITA, T., KONDO, N., TAKAHASHI, K., ICHIKAWA, M., FUKUDA, J.-ICHI & KIMURA, Y. 2011 Interparticle force in nematic colloids: comparison between experiment and theory. *Physical Review E—Statistical, Nonlinear, and Soft Matter Physics* **84** (2), 021704.
KISHITA, T., TAKAHASHI, K., ICHIKAWA, M., FUKUDA, J.-ICHI & KIMURA, Y. 2010 Arrangement dependence of interparticle force in nematic colloids. *Physical Review E—Statistical, Nonlinear, and Soft Matter Physics* **81** (1), 010701.
KNEPPE, H., SCHNEIDER, F. & SCHWESINGER, B. 1991 Axisymmetrical flow of a nematic liquid crystal around a sphere. *Mol. Cryst. Liq. Cryst.* **205** (1), 9–28.
KOS, Ž. & RAVNIK, M. 2018 Elementary flow field profiles of micro-swimmers in weakly anisotropic nematic fluids: stokeslet, stresslet, rotlet and source flows. *Fluids* **3** (1), 15.
LADYZHENSKAYA, O.A. 1969 *The Mathematical Theory of Viscous Incompressible Flow*. Gordon & Breach Science Publishers.
LAVRENTOVICH, O. D. 1998 Topological defects in dispersed words and worlds around liquid crystals, or liquid crystal drops. *Liq. Cryst.* **24** (1), 117–126.
LESLIE, F.M. 1979 Theory of flow phenomena in liquid crystals. *Adv. Liq. Cryst.* **4**, 1–81.
LESLIE, F.M. 1992 Continuum theory for nematic liquid crystals. *Continuum Mech. Therm.* **4** (3), 167–175.
LIGHTHILL, M.J. 1952 On the squirming motion of nearly spherical deformable bodies through liquids at very small reynolds numbers. *Commun. Pur. Appl. Math.* **5** (2), 109–118.
LIN, F.-H. & LIU, C. 1995 Nonparabolic dissipative systems modeling the flow of liquid crystals. *Comm. Pure Appl. Math.* **48** (5), 501–537.
LIN, F.-H. & LIU, C. 2000 Existence of solutions for the Ericksen-leslie system. *Arch. Ration. Mech. Anal.* **154** (2), 135–156.

https://doi.org/10.1017/jfm.2025.10821 Published online by Cambridge University Press

LIU, C. & WALKINGTON, N.J. 2000 Approximation of liquid crystal flows. *SIAM J. Numer. Anal.* **37** (3), 725–741.

MUŠEVIČ, I. 2017 *Liquid Crystal Colloids*, vol. 10. Springer Cham.

PENG, C., TURIV, T., GUO, Y., WEI, Q.-H. & LAVRENTOVICH, O.D. 2016 Command of active matter by topological defects and patterns. *Science* **354** (6314), 882–885.

QIAN, T. & SHENG, P. 1998 Generalized hydrodynamic equations for nematic liquid crystals. *Phys. Rev. E* **58**, 7475–7485.

RAVNIK, M. & ŽUMER, S. 2009 Landau–de gennes modelling of nematic liquid crystal colloids. *Liq. Cryst.* **36** (10–11), 1201–1214.

RUHWANDL, R. W. & TERENTJEV, E. M. 1995 Friction drag on a cylinder moving in a nematic liquid crystal. *Zeitschrift für Naturforschung A* **50** (11), 1023–1030.

RUHWANDL, R. W. & TERENTJEV, E. M. 1996 Friction drag on a particle moving in a nematic liquid crystal. *Phys. Rev. E* **54** (5), 5204.

RUSSEL, W.B., SAVILLE, D.A. & SCHOWALTER, W.R. 1992 *Colloidal Dispersions*. Cambridge University Press.

SELINGER, J.V. 2018 Interpretation of saddle-splay and the oseen-frank free energy in liquid crystals. *Liq. Cryst. Rev.* **6** (2), 129–142.

SMALYUKH, I.I. 2018 Liquid crystal colloids. *Annu. Rev. Conden. Ma. P.* **9** (1), 207–226.

SONNET, A. M., MAFFETTONE, P. L. & VIRGA, E. G. 2004 Continuum theory for nematic liquid crystals with tensorial order. *J. Non-NEWTON. Fluid* **119** (1), 51–59.

SONNET, A.M. & VIRGA, E.G. 2001 Dynamics of dissipative ordered fluids. *Phys. Rev. E* **64** (3), 031705.

SONNET, A.M. & VIRGA, E.G. 2012 *Dissipative Ordered Fluids: Theories for Liquid Crystals*. Springer Science & Business Media.

SPAGNOLIE, S.E. 2015 *Complex Fluids in Biological Systems*. Biological and Medical Physics, Biomedical Engineering. Springer New York.

STARK, H. 1999 Director field configurations around a spherical particle in a nematic liquid crystal. *The European Physical Journal B-Condensed Matter and Complex Systems* **10**, 311–321.

STARK, H. 2001 Physics of colloidal dispersions in nematic liquid crystals. *Physics Reports* **351** (6), 387–474.

STARK, H. & VENTZKI, D. 2001 Stokes drag of spherical particles in a nematic environment at low ericksen numbers. *Phys. Rev. E* **64** (3), 031711.

WALKINGTON, N.J. 2011 Numerical approximation of nematic liquid crystal flows governed by the Ericksen-leslie equations. *ESAIM: Mathematical Modelling and Numerical Analysis* **45** (03), 523–540.

WANG, W., ZHANG, L. & ZHANG, P. 2021 Modelling and computation of liquid crystals. *Acta Numer.* **30**, 765–851.

WILLMAN, E., FERNÁNDEZ, F.A., JAMES, R. & DAY, S.E. 2007 Modeling of weak anisotropic anchoring of nematic liquid crystals in the landau–de gennes theory. *Ieee T. Electron Dev.* **54** (10), 2630–2637.

WU, H., XU, X. & ZARNESCU, A. 2019 Dynamics and flow effects in the beris-edwards system modeling nematic liquid crystals. *Arch. Ratl. Mech. Anal.* **231**, 1217–1267.

ZHOU, S., SOKOLOV, A., LAVRENTOVICH, O.D. & ARANSON, I.S. 2014 Living liquid crystals. *Biophys. J.* **106** (2), 420a.

ZHOU, S., TOVKACH, O., GOLOVATY, D., SOKOLOV, A., ARANSON, I.S. & LAVRENTOVICH, O.D. 2017 Dynamic states of swimming bacteria in a nematic liquid crystal cell with homeotropic alignment. *New J. Phys.* **19** (5), 055006.

https://doi.org/10.1017/jfm.2025.10821 Published online by Cambridge University Press